2027

Effects of polymerization on mechanical properties and wear of printed materials

BOSTON UNIVERSITY

HENRY M. GOLDMAN SCHOOL OF DENTAL MEDICINE

Thesis

EFFECTS OF POLYMERIZATION ON MECHANICAL PROPERTIES AND WEAR OF PRINTED MATERIALS

by

NAVIKA GUPTA

BDS, Maharashtra University of Health Sciences, 2018

Submitted in partial fulfillment of the requirements for the degree of

Master of Science in Dentistry
in the Department of Restorative Science and Biomaterials

2027

Approved by:

First Reader _____

Dr. Russell Giordano II, D.MD, D.M.Sc. FADM, FADI, CAGS
Assistant Dean of Biomaterials and Biomaterials Research
Professor and Director of Biomaterials

Second Reader

_____

Dr. Yuwei Fan, MSc, PhD
Research Associate Professor of Biomaterials

Third Reader _____

John Ictech-Cassis D.M.D., D.D.S., C.A.G.S., FICD., FACD.
Clinical Professor
Program Director of Operative and Esthetic and Digital Dentistry
Director of Dental Health Center.

Chairman’s Approval

Signature: _____

Konstantinos Michalakis, D.D.S, C.A.G.S., M.Sc., Ph.D., F.A.C.P Professor and Chair, Department of Restorative Sciences and Biomaterials Boston University Henry M. Goldman School of Dental Medicine Professor, Center for Multiscale and Translational Mechanobiology Boston University College of Engineering

DEDICATION

This thesis is dedicated to the individuals whose unwavering support, belief, and encouragement have carried me through this challenging and rewarding journey.

First and foremost, I extend my deepest gratitude to my husband, whose faith in my abilities never wavered, even during times when I struggled to believe in myself. His constant motivation and emotional strength were instrumental in helping me persevere through moments of doubt and self-questioning.

To my in-laws, whose kindness and encouragement created a space in which I could pursue this path with focus and determination. Their support has been deeply felt and genuinely appreciated.

To my parents, I owe everything. Their lifelong support, unconditional love, and belief in my dreams have been the foundation of all my accomplishments. They instilled in me the values of hard work and perseverance, and their pride in my progress continues to inspire me every day.

Lastly, I dedicate this work to my sister, whose emotional support and constant encouragement have been a source of great comfort. Her presence, even from afar, has helped me stay grounded and resilient throughout this journey.

To all my close family and friends, thank you for believing in me.

ACKNOWLEDGMENTS

I would like to express my sincere gratitude to my advisor, Dr. Yuwei Fan, for his invaluable advice, mentorship, and unwavering support throughout the course of my thesis. His expertise, patience, and commitment to excellence have been instrumental in guiding my research and helping me grow both academically and professionally. Dr. Fan was always available, at all hours of the day, to answer my questions, offer feedback, assist with statistical analysis, and promptly provide thoughtful solutions whenever challenges arose. His generous availability and dedication were central to the progress and success of this work.

I am also deeply thankful to Dr. Russell Giordano for his insightful guidance, generous time, and steadfast encouragement. His contributions have significantly enriched the quality and direction of my research, and I am grateful for the opportunity to gain experience from him.

I am also grateful to Dr. Michalakis for introducing me to a new dimension of research and for broadening my academic perspective by encouraging me to transcend the boundaries of what I had previously considered within my capabilities.

I would also like to extend my gratitude to Dr. John Ictech-Cassis for guiding me in correlating my research findings with clinical practice and for fostering the further development of my clinical skills.

I would like to extend my heartfelt thanks to Dr. Jacob Miszuk, Research Assistant Professor, whose technical support and guidance in the laboratory were vital to the successful completion of my experiments. His readiness to assist, particularly during equipment issues and unexpected setbacks, ensured the continuity and integrity of the experimental process.

In addition, I am grateful to my colleagues, especially Daniel Monteros and Harshal Modh, for their camaraderie, thoughtful discussions, and continuous support, which have been an integral part of this journey. Their encouragement helped create a collaborative and motivating research environment for which I am truly appreciative.

This thesis would not have been possible without the support and contributions of all those mentioned above.

EFFECTS OF POLYMERIZATION ON MECHANICAL PROPERTIES AND WEAR OF PRINTED MATERIALS

NAVIKA GUPTA

Boston University, Henry M. Goldman School of Dental Medicine, 2027

Major Professor: Russell Giordano II, D.M.D, D.M.Sc, C.A.G.S.
Associate Professor of Restorative Sciences & Biomaterials

ABSTRACT

Objective:

This study aimed to evaluate the effects of different post-polymerization methods on the mechanical properties, surface hardness, degree of conversion (DC), and wear resistance of various 3D-printed (3DP) dental materials. The goal was to determine optimal polymerization protocols that enhance performance and longevity of 3DP restorations.

Materials and Methods:

Five commercially available 3DP resins, both filled and unfilled, including 1) Sprintray Ceramic Crown, 2) Rodin Sculpture 2.0, 3) Rodin Titan, 4) Rodin Denture base 2.0, and 5) Sprintray High impact Denture Base were tested following five post-polymerization methods: 1)Sprintray Nanocure, 2) Otoflash with nitrogen, 3) Otoflash without nitrogen, 4) Oven, and 5)Sprintray Procure 2. Standardized bar-shaped, discs and pins specimens were fabricated using Sprintray Pro S and Asiga printers. Flexural strength was measured using a three-point bending test on an Instron 5566A machine; Vickers hardness values were recorded using a Buehler Wilson VH1202 Microhardness tester; DC was analyzed using Fourier-transform infrared spectroscopy (FTIR). Wear resistance was assessed by

measuring height and weight loss after one million wear cycles on a pin on plate linear wear tester under simulated loading conditions.

Results:

Post-polymerization method significantly influenced mechanical properties and wear performance. For filled resins, Otoflash with Nitrogen and Oven yielded the highest flexural strength and surface hardness. In unfilled resins, Otoflash with nitrogen and Nanocure methods showed comparatively better results. Degree of conversion was positively correlated with hardness and strength. Post-polymerization method significantly influenced mechanical properties and wear performance. For filled resins, Otoflash with nitrogen and Oven demonstrated the best wear resistance. In unfilled resins, the Oven and Otoflash with nitrogen methods exhibited the lowest wear loss, whereas Procure showed the highest wear.

Conclusion:

Post-polymerization protocols play a critical role in defining the final properties of 3D-printed dental resins. Selection of polymerization conditions tailored to material type can significantly improve structural integrity and wear behavior, thereby enhancing the clinical reliability of 3DP dental restorations.

TABLE OF CONTENTS

LIST OF TABLES

LIST OF FIGURES

LIST OF ABBREVIATIONS

ADA..... American Dental Association

ANOVA .....Analysis of Variance

BU ..... Boston University

CAD.....Computer-Aided Design

CAM .....Computer-Aided Manufacturing

CV.....Coefficient of Variance

DLP..... Digital Light Processing

EDS..... Energy Dispersive Spectrometry

FDA..... Food and Drug Administration

IPA ..... Isopropyl Alcohol

ISO ..... International Standards Organization

LCD.....Liquid Crystal Display

LED.....Light Emitting Diode

MMA.....Methyl Methacrylate

PAC..... PacDent Ceramic Nanohybrid

PMMA .....Poly Methyl Methacrylate

RDB2..... Rodin Denture Base 2.0

RT..... Rodin Titan

RTN2..... Rodin Titan with Nitrogen

SHIDB.....SprintRay High Impact Denture Base

SDNC.....Sprintray High Impact Denture Base polymerized with Nanocure

SCC.....SprintRay Ceramic Crown

SC2.....Rodin Sculpture 2

SDS .....Safety Data Sheet

SEM ..... Scanning Electron Microscope

SLA.....Stereolithography

CHAPTER 1. INTRODUCTION

1.1 Digital Dentistry and the Rise of Additive Manufacturing

The evolution of digital technology has significantly transformed modern dental practice, streamlining workflows and enhancing the quality and efficiency of restorative procedures. Digital dentistry encompasses a wide range of innovations, including intraoral scanners, CAD/CAM systems, and 3D printers, all of which enable clinicians to fabricate custom dental restorations with greater accuracy, reduced turnaround time, and improved patient outcomes (Davidowitz & Kotick, 2011).

Traditional subtractive methods, such as milling, have long been integrated into CAD/CAM workflows for producing crowns, inlays, onlays, and dentures. Milling eliminates several steps from conventional techniques, including physical impressions, wax-ups, and casting (Turkyilmaz, 2021). Moreover, multi-axis milling machines improve precision and allow for same-day restorations. However, limitations such as tool wear, restricted geometries due to bur size, and significant material waste have led to the increasing interest in additive manufacturing.

3D printing, or additive manufacturing, constructs objects layer-by-layer based on digital models, offering benefits such as greater material efficiency, faster production for batch processing, reduced dependency on bur diameters, and the ability to print complex geometries (Strub et al., 2006; Huang et al., 2013). In dentistry, 3D printing facilitates rapid prototyping and manufacturing of crowns, dentures, surgical guides, splints, and orthodontic appliances, with increasing adoption driven by affordability and customization potential (Çakmak et al., 2022; Nulty et al., 2022).

1.2 Clinical Relevance and Material Development

Recent advancements in printable resin formulations, particularly those incorporating filler particles or hybrid ceramic compositions, have enabled their use for definitive restorations. These developments coincide with policy changes, such as the ADA's 2023 revision of the CDT definition for ceramics, which now encompasses 3D-printed materials previously excluded from coverage (ADA, 2023). This regulatory shift underscores the need for robust mechanical performance data to ensure the reliability of printed restorations in long-term clinical use.

The clinical success of 3D-printed restorations depend heavily on their mechanical properties, including flexural strength, hardness, wear resistance, and degree of polymerization. These properties are influenced by multiple factors, such as printer type, material formulation, filler content, and critically, the post-polymerization process. Post-polymerization enhances the degree of conversion (DC), crosslinking, and surface characteristics of printed resins, directly impacting their performance in the oral environment (Stansbury & Idacavage, 2016; Ko et al., 2021).

1.3 Advantages and Disadvantages of 3D Printing

The primary advantages of 3D printing in dentistry include rapid and customizable fabrication, minimal material waste, and the ability to produce intricate geometries not feasible with milling. This is especially beneficial in producing provisional restorations, aligners, splints, and surgical guides (Tian et al., 2021). The reduced need for mechanical instrumentation allows for the preservation of material integrity and lower cost per unit. However, 3D printing also presents certain drawbacks. Post-processing steps such as

cleaning, support removal, and polymerization can be labor-intensive and impact dimensional accuracy. The mechanical properties of printed restorations can be inferior to those of milled counterparts, particularly if post- polymerization is suboptimal. Variability in printer technologies (SLA, DLP, LCD) further affects standardization, as does the lack of consensus on optimal polymerization protocols (Ko et al., 2021; Chen et al., 2021).

1.4 Composition and Polymerization Dynamics of 3D-Printed Dental Resins

3D-printed dental resins, whether filled or unfilled, are complex photopolymer formulations comprising a reactive monomer matrix, photoinitiators, stabilizers, and in some cases, inorganic fillers. The monomeric backbone typically consists of dimethacrylate compounds such as Bis-GMA, UDMA, or TEGDMA, which undergo free-radical polymerization when activated by specific wavelengths of light (Bagheri and Jin, 2019). Photoinitiators, commonly camphorquinone or Type I acylphosphine oxides, are responsible for initiating this polymerization process under light in the 385–405 nm range, often influenced by the spectral output of the curing unit used (Stansbury and Idacavage, 2016). Unfilled resins rely solely on the degree of monomer conversion and network formation for mechanical integrity, making them suitable for flexible or high-impact applications such as denture bases. Conversely, filled resins incorporate inorganic or ceramic particles, such as silica (SiO_2), zirconia (ZrO_2), or alumina (Al_2O_3), which contribute to improved wear resistance, dimensional stability, and mechanical strength (Alshamrani et al., 2016).

While the elemental composition remains constant before and after polymerization, the post-polymerization process profoundly influences the resin's microstructural integration and functional performance. The energy output, exposure time, wavelength specificity, and atmospheric conditions such as polymerization under nitrogen, can significantly affect the degree of conversion (DC), surface morphology, and filler-matrix interaction (Chrószcz et al., 2021). Insufficient polymerization may leave residual monomers that compromise both mechanical properties and biocompatibility. Thus, optimal polymerization conditions are essential not only to achieve high DC values but also to enhance filler incorporation, reduce porosities, and ensure the clinical reliability of 3D-printed restorations.

1.5 Mechanical Properties and Role of Polymerization

Dental restorations must withstand various stresses and functional loads, necessitating a thorough understanding of mechanical properties. Key metrics include:

Flexural Strength: Resistance to deformation under bending forces, commonly measured using a three-point bend test.

Surface Hardness: Assessed via Vickers microhardness testing to determine a material's resistance to indentation and abrasiveness.

Wear Resistance: Indicates a material's durability under repetitive contact, simulating long-term mastication.

Degree of Conversion (DC): Refers to the percentage of monomers converted into polymer, a critical factor influenced by polymerization time, light intensity, wavelength, and polymerization atmosphere.

Post-polymerization plays a pivotal role in optimizing these properties. Incomplete polymerization results in reduced crosslinking density, inferior wear resistance, lower hardness, and inadequate flexural strength. The use of nitrogen environments, higher light intensities, or extended polymerization durations can significantly improve polymerization efficiency and material performance (Hartley et al., 2022; Stansbury & Idacavage, 2016).

1.6 Post-Polymerization Techniques in 3D Printing

Post-polymerization is a crucial step in the additive manufacturing workflow that ensures complete polymerization of printed resins. Several methods are employed to improve the degree of conversion and enhance mechanical properties:

1.6.1 Standard Light Polymerization (Procure):

This technique employs a UVA light engine, primarily emitting light at a peak wavelength of 385 nm, to initiate and advance polymer crosslinking. While this method is convenient and widely accessible, it may present limitations in polymerization of thicker, pigmented, or highly filled resins due to suboptimal light penetration. The resulting degree of polymerization can vary significantly based on material translucency and specimen geometry.

1.6.2 High-Intensity Flash Polymerization (e.g., Otoflash):

Otoflash systems utilize stroboscopic xenon flash lamps to deliver high-intensity light pulses across a broad spectral range (250–950 nm). A key distinction was made between polymerization with and without a nitrogen atmosphere. The nitrogen environment

eliminates oxygen inhibition at the resin surface, which significantly enhances the degree of conversion and mechanical surface properties, particularly in filled resins, to promote deeper and more uniform polymerization (Wada et al., 2023). When used with or without an inert nitrogen atmosphere, Otoflash can significantly enhance hardness and wear resistance, although its performance varies depending on the material.

1.6.3 Inert Atmosphere Polymerization (e.g., Nitrogen-flushed chambers):

Polymerization in a nitrogen environment reduces oxygen inhibition at the surface layer, promoting better crosslinking. This technique is particularly effective in improving surface hardness and is often used in conjunction with flash polymerization systems (Wada et al., 2023).

1.6.4 Nanocure Systems:

Nanocure units are advanced light-polymerization devices that employ calibrated combinations of light and heat to promote polymerization. These systems provide programmable polymerization profiles tailored to material-specific requirements, enabling enhanced polymer network formation. Their ability to deliver high-throughput, precision-controlled polymerization has demonstrated efficacy in both surface and bulk property improvement. However, their adoption is currently limited by high equipment costs and restricted clinical availability.

1.6.5 Oven Polymerization:

This method combines initial photopolymerization with a subsequent thermal post-cure phase to promote further crosslinking and increase thermal stability. In the present study,

specimens underwent preliminary polymerization using Otoflash (without nitrogen), followed by thermal treatment at 100°C for 15 minutes in a gravity convection oven. This dual-phase protocol was designed to optimize the resin's degree of conversion and improve the mechanical robustness of the printed material (Bayarsaikha n et al., 2021; Lim et al., 2021).

The selection of an appropriate post-polymerization protocol should be guided by the clinical application, resin composition, restoration thickness, and mechanical performance objectives. This study systematically compares these five methods to elucidate their impact on key material properties, thereby providing evidence-based recommendations for optimizing 3D printing workflows in restorative dentistry.

1.7 Need for Standardized Evaluation of Printed Materials

Despite the rapid commercialization of printable dental materials, there is a lack of standardized, peer-reviewed data comparing their mechanical properties across different polymerization protocols and printer technologies. Manufacturer claims are often unsubstantiated by independent research, perpetuating a knowledge gap that could compromise clinical outcomes. Moreover, the specific impact of post-polymerization methods on the mechanical performance of newly introduced materials remains underexplored.

Studies have indicated that increased filler content and improved filler-matrix integration are positively correlated with mechanical strength and wear resistance (Ilie & Hickel, 2009; Garoushi et al., 2013). However, filler characteristics alone are insufficient; polymerization protocols—including light wavelength, exposure time, and presence of

inert gas—also critically affect the polymerization efficiency and long-term durability of printed restorations (Tian et al., 2021; Hartley et al., 2022).

1.8 Statement of the Problem

The recent ADA update broadening the CDT definition of ceramics to include 3D-printed materials has opened new opportunities for permanent dental restorations fabricated using additive manufacturing. However, the clinical viability of these materials hinges on their mechanical properties, many of which remain unverified by independent research. Key attributes such as flexural strength, wear resistance, hardness, and degree of conversion are influenced by multiple factors, particularly post-polymerization protocols. In the absence of standardized testing and performance data, clinicians risk adopting suboptimal materials or polymerization techniques, potentially compromising restoration longevity and patient outcomes.

1.8.1 Purpose of the Study

This in-vitro study aims to evaluate and compare the effects of various post-polymerization methods on the mechanical properties of 3D-printed dental resin materials. By investigating flexural strength, surface hardness, wear resistance, and degree of conversion, the study seeks to determine optimal post-polymerization protocols that enhance material performance and durability.

1.8.2 Study Objectives

- To evaluate flexural strength of different 3D-printed resin materials using a three-point bend test.

- To assess surface hardness using the Vickers microhardness test.
- To evaluate wear resistance after various post-polymerization protocols.
- To measure the degree of conversion (DC) of printed resins and correlate with mechanical performance.
- To investigate the microstructure and elemental composition of resin materials using SEM and EDS

1.8.3 Research Hypotheses

- There are no differences in flexural strength among the tested 3D-printed resin materials.
- There is no difference in surface hardness among 3D-printed resin materials.
- There is no difference in wear properties among 3D-printed resin materials.
- The post-polymerization process does not significantly affect the mechanical properties, surface hardness, Degree of Conversion, or wear resistance of 3DP dental materials.
- Degree of conversion is not significantly associated with mechanical properties.

Chapter 2. MATERIAL & METHODS

2.1 Materials

This in-vitro investigation assessed the mechanical and chemical performance of five commercially available 3D-printed dental resins as seen in Figure 1. These materials were selected based on their clinical applicability, FDA clearance, and variability in filler content and photopolymer composition. The selected resins encompass both tooth- and tissue-colored formulations designed for definitive intraoral prostheses. Table 1 lists the material's shade, reference code, lot number and expiration date.

2.1.1 SprintRay Ceramic Crown (SCC) –

SprintRay Ceramic Crown is a hybrid nanoceramic resin indicated for the fabrication of permanent crowns, inlays, onlays, and veneers. Manufactured by SprintRay (USA), its formulation comprises multifunctional oligomers (20–60%), monomers (20–50%), photoinitiators (0.1–10%), various functional additives (10–60%), and a ceramic filler content exceeding 50% by weight (SprintRay, 2024)).

2.1.2 Rodin Titan (RT) –

Rodin Titan, developed by Pac-Dent, is a high-strength resin optimized for full-contour prosthetic restorations offering a balance between esthetics and durability. Its composition includes methacrylic esters and photoinitiators. It is indicated for a broad range of applications including single-unit crowns, inlays, onlays, veneers, provisional restorations, and denture tooth arches (Pac-Dent, 2023a).

2.1.3 Rodin Sculpture 2.0 (RS2) –

Rodin Sculpture 2.0 is a nanohybrid ceramic-filled resin engineered for the fabrication of permanent restorations using open-system 3D printers. It is suitable for crowns, inlays, onlays, veneers, and denture teeth. The resin contains a high load of ceramic fillers exceeding 60% to enhance mechanical stability. Its matrix consists of methacrylic esters and proprietary photoinitiator systems (Pac-Dent, 2023b).

2.1.4 Rodin Denture Base 2.0 (RDB2) –

Rodin Denture Base 2.0 is a biocompatible, pink-tinted resin specifically designed for the fabrication of complete and partial removable denture bases. It features a matrix of high-molecular-weight methacrylate oligomers and cross-linking agents to impart fracture resistance and dimensional stability for long-term intraoral use.

2.1.5 SprintRay High Impact Denture Base (SHIDB) –

SprintRay High Impact Denture Base is a high-performance denture base resin developed to provide enhanced strength, impact resistance, and long-term wear durability. The formulation is primarily based on polymethyl methacrylate (PMMA) derivatives with the addition of proprietary impact modifiers. This resin is FDA-cleared for definitive denture fabrication.

Each material's chemical composition, filler loading, and manufacturer-recommended printing and post-polymerization parameters were documented. Only FDA-cleared, Class II dental materials indicated for definitive restorations or long-term denture base

fabrication were included in this study to ensure clinical relevance and regulatory compliance.

Figure 1. Resin materials in this study. Sprintray Ceramic Crown, Rodin Sculpture 2, Rodin Titan, Rodin Denture Base 2.0, Sprintray High Impact Denture Base.

Table 1. List of material's shade, reference code, lot number and expiration date.

	Abr.	Shade	REF	LOT	EXP

Sprintray Ceramic Crown	SCC	A2	SRI-0202086	S23K28CA22	4/28/25
Rodin Titan	RT	OM1	3DR-TITAN	404025	5/2025
Rodin Sculpture 2	RS2	A3	23877	312065	12/2024
Rodin Denture Base 2.0	RDB2	MEHARRY	23861	404142	04/2026
Sprintray High Impact Denture Base	SHIDB	Original Pink	SRI-0202039	S23128HDB0P1	2/28/25

Two 3D-printers were used in this in-vitro study; printers were chosen owing to their availability in the Boston University Dental Biomaterial Laboratory at the Department of Restorative Science and Biomaterials, Henry M. Goldman School of Dental Medicine. Asiga MAX and Sprintray Pro 95S printer were used in this study as shown in Figure 2 and listed in Table 2.

Table 2. List of 3D printers used in the study.

Printer	**Asiga Max**	**SprintRay Pro 95S**
Build Volumes X, Y, Z	119 x 67 x 75 mm	192 × 120 × 210 mm
Pixel Resolution	62 µm	95 µm

Technology	DLP	DLP
LED Wavelenth	385–405 nm	405 nm
Material Compatibilty	> 500 open-system materials	SprintRay proprietary materials
Software	Asiga Composer 1.3.3	RayWare

Figure 2. 3D printer used in this in-vitro study, Asiga Max, Sprintray Pro 95S.

2.2 Study Design

The primary objective of this study was to assess the impact of various post-polymerization protocols on the mechanical performance of selected 3D-printed dental resin materials. The experimental framework encompassed four key evaluations:

1. Flexural Strength (Three-point bending)
2. Vickers Microhardness
3. Wear Resistance (Pin-on-plate)
4. Degree of Conversion (FTIR analysis)

Each resin was processed using five different post-polymerization protocols:

- Sprintray Nanocure

The SprintRay Nanocure unit utilizes a narrow-spectrum LED light source, with a peak wavelength at approximately 405 nm and a spectral width of about 10–20 nm. The polymerization cycle lasts 2.5-12 minutes. The chamber incorporates an integrated 180 W heater with active thermal control up to 100 °C. The device preheats automatically and maintains an optimal curing temperature of reportedly around 60–80 °C during curing, to maximize cross-linking. This "controlled heat" accelerates polymerization and improves mechanical properties, eliminating the need for nitrogen purging. The system uses a silent fan and vents to regulate temperature without noise. It is equipped with 34 high-power LED emitters distributing substantial optical power. Nanocure's limited spectral range and moderate energy output may restrict its effectiveness in polymerization filled or highly pigmented resins with variable photoinitiator systems.

Designed for SprintRay's entire dental resin library, including biocompatible Class II materials such as splints, surgical guides, denture base and teeth, and crowns, it supports over-the-air resin profile updates, including user-defined curing profiles for third-party resins. The dual UV wavelengths target common dental photoinitiators to ensure full cure in a wide range of light-curable dental polymers.

- Otoflash with nitrogen gas (99.998% purity from Linde Gas)

The Otoflash G171 is a high-intensity, xenon flash-based curing unit that delivers energy in the form of broad-spectrum light pulses ranging from 280 to 700 nm. Two xenon flashbulbs of 100 W each fire bursts of high-intensity light at a frequency of about 10

flashes per second, the unit capably delivers a highly efficient, rapid cure. In-chamber irradiance has been measured around 50 mW/cm² (UVA range) under standard conditions. In this study, specimens were subjected to 2,000-5,000 flashes. The chamber was flushed with Nitrogen gas.

- Otoflash without nitrogen gas
- Oven (Incubated in the Oven at 100°C for 15 minutes after Otoflash without nitrogen)

Oven polymerization involves an additional thermal treatment step following light exposure. In this study, the oven-polymerization method utilized an incubator in which specimens were heated at 100°C for 15 minutes after being pre-polymerized using Otoflash without nitrogen.

- Sprintray Procure 2

Procure 2 utilizes a UV-A LED light engine with a peak emission at ≈385 nm. The Procure 2 employs 42 LED emitters at this wavelength, providing a narrow spectral output centered in the 385 nm UV range. It was used for a 9-25-minute cycle at a temperature range between 60 and 80°C. It delivers high-intensity UV illumination with near-uniform distribution across the curing chamber. The Procure 2's patented light motion system scans 360° to ensure every surface is evenly cured. Essentially, the UV light source (or reflector mechanism) moves or "scans" around the chamber, so that the models receive uniform illumination from all angles. This prevents any shadowed areas or under-cured spots on the printed models, an important factor for consistent mechanical properties and biocompatibility in applications like dental devices. The irradiance is rated

>50 mW/cm² (UV-A) under its default settings. Due to its high irradiance, the Procure 2 is capable of delivering a substantial energy dose within a relatively short duration.

Each group included:

n= 25 specimens for flexural strength

n=25 specimens for wear resistance

n=25 specimens for Vickers hardness and DC

Table 3 elaborates the sample size and specimen design used for each tested dental resin material across four different mechanical and chemical characterization tests.

STL files were exported and prepared using either Asiga Composer or SprintRay RayWare software. Support structures and spacing were optimized for building stability and uniformity. The designs ensured minimal warpage and uniform light exposure during printing.

Table 3. Specimen numbers for the study.

Material	Flexural Strength (3-pt bend test)	Vickers microhardness	Wear test	Degree of Conversion
	Bars (25mm x 2mm x 2mm)	Discs (14mm diameter and 2mm thickness)	Cylindrical pins (3.5mm	Discs (14mm diameter and 2mm thickness)

			diameter × 9mm	
SCC	25	25 (5 indentations)	25	25
RT	25	25 (5 indentations)	25	25
SC2	25	25 (5 indentations)	25	25
RDB2	25	25 (5 indentations)	25	25
SHIDB	25	25 (5 indentations)	25	25
Asiga	75	75 (375)	75	75
Sprintray	50	50 (250)	50	50
Total	125	125 (625)	125	125

2.3 Specimen Design and Fabrication

All test specimens were digitally modeled using *Blender 3.2* (The Blender Foundation, Netherlands), a versatile open-source 3D design platform, to ensure standardized dimensions and reproducibility across all experimental groups. Geometries were specifically tailored to align with the dimensional requirements of each mechanical test. Rectangular bars measuring 25 mm × 2 mm × 2 mm as seen in Figure 3, were designed for flexural strength testing in accordance with ISO 6872-2015 Ceramic materials (ISO 6872:2015 Dentistry Ceramic materials, 2023) specifications for three-point bending. For

Vickers microhardness and degree of conversion (DC) assessments, disc-shaped specimens with a 14 mm diameter and 2 mm thickness as seen in Figure 3, were fabricated to provide flat, homogenous surfaces suitable for indentation and spectroscopic analysis. Cylindrical pins, 3.5 mm in diameter and 9 mm in height as seen in Figure 3, were designed for wear resistance testing to ensure compatibility with the pin-on-plate setup.

All designs were exported in Standard Tessellation Language (STL) format and processed using either *Asiga Composer 1.3.3* or *SprintRay RayWare* software for slicing and print preparation. Specimens were uniformly spaced at 2 mm intervals and optimally oriented to reduce support-induced deformation and enhance exposure uniformity during photopolymerization. Custom support structures were configured in accordance with each resin's specific requirements and the respective printer's capabilities, balancing mechanical stability with ease of removal post-printing.

This fabrication protocol was developed to minimize warpage, ensure dimensional accuracy, and promote consistent light penetration, thereby facilitating homogeneous polymerization throughout each specimen. All STL models and slicing parameters were archived for traceability and reproducibility.

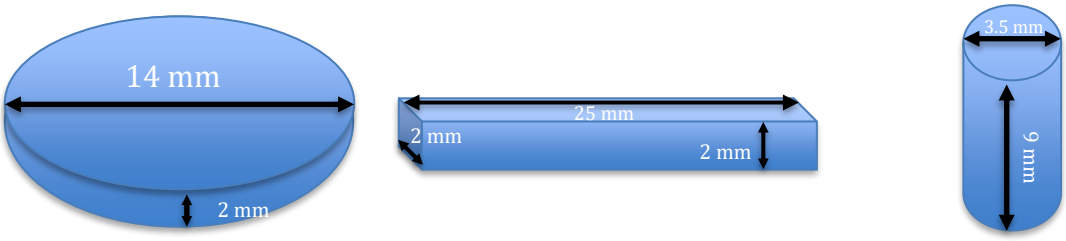

Figure 3. Vickers Hardness disc design, three-point Flexural Strength bar, Wear test pin design

2.3.1 Printing Protocols

Prior to printing, all resin bottles were removed from cold storage (maintained at 15°C) and equilibrated to room temperature. The contents were then homogenized by rolling each bottle in a jar milling machine (*U.S. Stoneware, Ohio, USA*) for an additional 20 minutes to ensure uniform dispersion of fillers and photoinitiators.

Specimens fabricated from Rodin resins were printed using the *Asiga Max* 3D printer in conjunction with *Asiga Composer* software, applying the validated *Pac-Dent Rodin 002* profile. A print temperature of 30 °C and a layer thickness of 50 µm were employed. STL files were spaced with a 3.00 mm inter-object clearance to avoid cross-interference during printing and to ensure even exposure.

SprintRay materials were processed on the *SprintRay Pro 95S* printer using *SprintRay RayWare* software. Validated manufacturer-specific print profiles were applied, utilizing a consistent slice thickness of 50 µm and a polymerization wavelength of 405 nm. As with Rodin resins, a 3.00 mm spacing between printed objects was maintained.

Upon completion of the printing cycle, the build platform was allowed to rest momentarily to permit excess unpolymerized resin to drain back into the resin vat. The build platform was then detached, and residual unpolymerized resin on the platform and specimens was dislodged using high-pressure compressed air. Each specimen was gently sprayed with 99% isopropyl alcohol (IPA), prepared from *Fisher A416-4* and reverse osmosis (RO) water. To prevent overexposure to solvent, the specimens were not

immersed in IPA; instead, they were swiftly wiped multiple times with IPA-saturated lint-free paper towels until a chalk-free, matte finish was achieved. A fine blade was carefully inserted beneath the base of each specimen to separate it from the build platform without damaging the geometry.

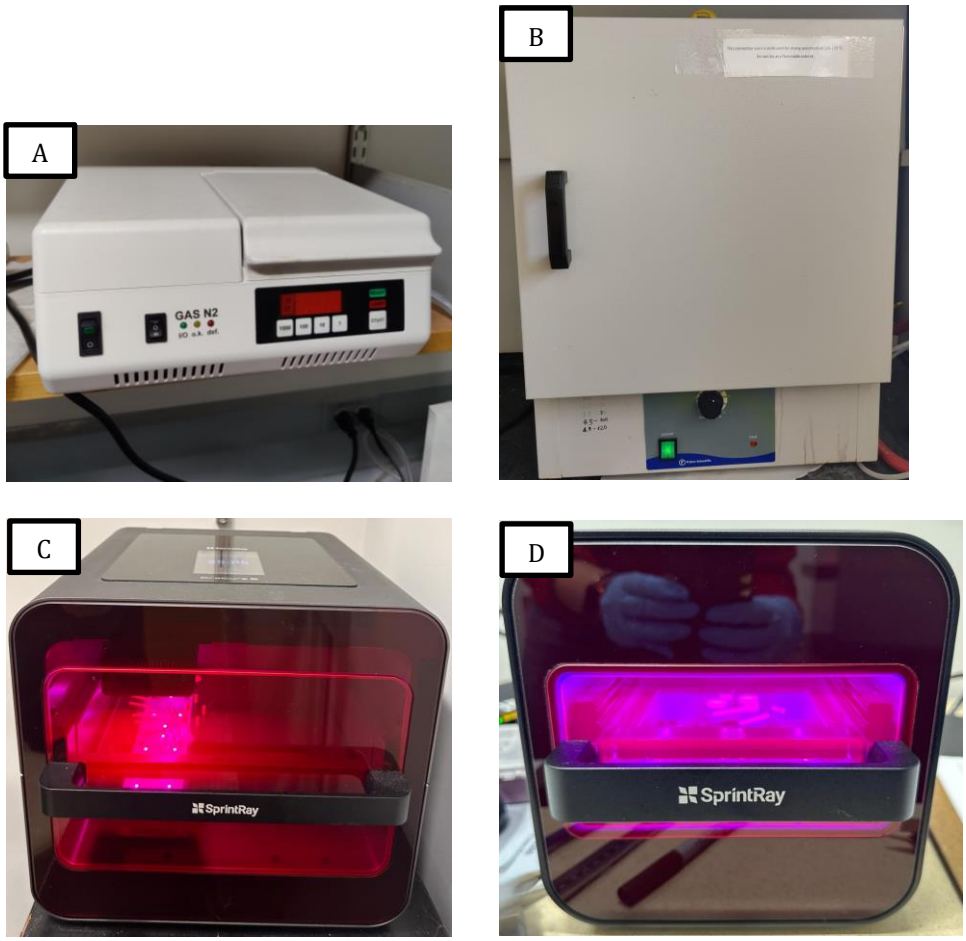

Figure 4. Curing Units: Otoflash G171 (A), Isotemp Gravity Convection Oven Model 664 (B), Procure 2 (C), Nanocure (D).

2.3.2 Polymerization Protocol

Following the initial cleaning and drying with lint-free paper towels, all specimens underwent post-polymerization using five distinct polymerization protocols to evaluate their impact on the material properties. The post-polymerization methods included:

1. Otoflash G171 (NK-optik GmbH, Baierbrunn, Germany) as seen in Figure 4 (A) —specimens were exposed to 2000–5000 xenon light flashes within a chamber actively purged with high-purity nitrogen gas (99.998% purity, Linde Gas Nitrogen), ensuring an oxygen-reduced environment to minimize inhibition of the polymerization process.
2. Otoflash G171 without Nitrogen—specimens were subjected to the same light exposure (2000–5000 flashes) without nitrogen purging, representing polymerization under ambient atmospheric conditions.
3. SprintRay ProCure 2 as seen in Figure 4 (C) —specimens were placed in Zone A of the chamber and polymerized for durations ranging from 9 to 25 minutes, based on the manufacturer's validated protocol and material-specific guidelines.
4. SprintRay NanoCure as seen in Figure 4 (D) —a proprietary chamber delivering controlled light exposure, used to post-cure specimens for durations ranging from 90 seconds to 13 minutes, depending on the resin formulation.
5. Isotemp Gravity Convection Oven (Model 664, Thermo Fisher Scientific, Ohio, USA) as seen in Figure 4 (B) specimens were pre-polymerized using the Otoflash G171 without nitrogen and then thermally post-polymerized at 100°C for 15 minutes in the convection oven, simulating a dual-mode polymerization enhancement protocol.

Upon completion of post-polymerization, all specimens were immediately transferred to a sealed plastic container and stored in a dark, dry environment at ambient room temperature (~22°C) for 24 hours prior to any mechanical testing. This standardized

aging process ensured polymer network stabilization and equilibration of residual stresses, thereby promoting consistency in mechanical property evaluation across all experimental groups.

2.3.3 Polishing Protocol

Prior to mechanical testing, all specimens underwent standardized surface preparation to ensure a consistent finish and to minimize surface irregularities that could influence test outcomes. Specimens designated for flexural strength and Vickers microhardness or degree of conversion (DC) analysis were initially polished by hand using P-600 grit aluminum oxide abrasive paper (*Norton Abrasives, Saint-Gobain, USA*), which has an approximate particle size of 35 µm. This initial abrasion step was employed to remove surface artifacts resulting from the printing process and residual support structure markings.

For wear resistance testing, cylindrical pin specimens were subjected to further refinement using a 15 µm diamond polishing disc on the *EcoMet 250 Grinder-Polisher* (*Buehler, IL, USA*). The polishing procedure was conducted at a rotational speed of 60 rpm for 2 minutes to achieve a planar, uniform surface, thereby ensuring consistent contact with the antagonist ceramic plates during the pin-on-plate wear test.

Specimens prepared for Vickers hardness and DC testing, as well as those intended for three-point flexural testing, underwent a sequential two-step polishing regimen. The first step involved mechanical polishing using a 15 µm diamond disc for 2 minutes, followed by a final fine polishing stage using a 1 µm Hi-Purity Alumina Suspension (*Precision*

Surfaces International, TX, USA) for 3 minutes. The polishing process was continued until a scratch-free, highly reflective surface was obtained, which is critical for precise microindentation and spectroscopic evaluation.

2.4 Experimental Procedures

This investigation comprehensively examined the mechanical performance and polymerization efficacy of five commercially available 3D-printed dental resin materials subjected to distinct post-polymerization protocols. The primary objective was to elucidate the effect of polymerization conditions on four critical material properties: flexural strength (assessed via three-point bending), Vickers microhardness, wear resistance (evaluated using a pin-on-plate apparatus), and degree of conversion (DC), quantified through Fourier-transform infrared (FTIR) spectroscopy. Each experimental procedure was conducted in accordance with the relevant ISO standards or rigorously validated laboratory methodologies. The findings aimed to establish a clearer understanding of how various post-polymerization strategies influence the structural integrity and long-term functional performance of 3D-printed dental restorations.

2.4.1 Three-point bend Flexural Strength Testing

For each 3D-printed resin group and the control group, twenty-five rectangular bar specimens were subjected to three-point bending tests in accordance with (ISO 6872:2015 DentistryCeramic materials, 2023) (ISO 6872:2015 Dentistry- Ceramic materials, 2023), the international standard for evaluating the flexural properties of dental ceramics. Mechanical testing was conducted using an Instron 5566A universal testing

machine (Instron Corp., Norwood, MA, USA), as illustrated in Figure 5. Each specimen was positioned horizontally with the printed layers aligned perpendicular to the loading direction and supported across a 20 mm span, as shown in Figure 5.

A stainless-steel-loading roller, connected to a calibrated 10 kN load cell, applied a compressive force at the specimen's midpoint at a crosshead speed of 0.5 mm/min until fracture occurred. Prior to testing, precise specimen dimensions (width and thickness) were recorded using a high-accuracy digital caliper (Absolute AOS, Mitutoyo Corporation, Japan) to ensure accuracy in stress calculations. Bluehill Universal software was employed to control the machine parameters and capture the force-extension data in real time.

Flexural strength was defined as the maximum stress value recorded at the point of fracture. After failure, the broken fragments were carefully retrieved, labeled, and stored for subsequent analysis. The flexural strength (FS) for each specimen was calculated using the following equation for three-point bending:

$$FS = \frac{3F\ L}{2\ w\ h^2}$$

FS = Flexural strength (MPa)

F = Maximum force at break or yield (N)

L = Support span length (mm)

w = Specimen's width (mm) h = Specimen's thickness (mm)

Figure 5. 5566A electromechanical Universal Tester. 20mm support jig with stainless steel rollers.

2.4.*2* Vickers Microhardness Test

Vickers microhardness evaluation was conducted on twenty-five disc-shaped specimens (14 mm in diameter and 2 mm in thickness) for each resin group. Five indentations were performed per specimen, with a minimum spacing of 400 µm between each to mitigate

the risk of stress field interference. Testing was carried out using the Wilson 1202 Vickers/Knoop microhardness tester (Buehler, Illinois, USA) as seen in Figure 6, employing a precision diamond Vickers indenter. A constant load of 10 grams was applied with a dwell time of 15 seconds for each indentation. Indentation diagonals were measured at 50× magnification, and the Vickers Hardness Number (VHN) was calculated in accordance with standardized procedures. All data were meticulously recorded in laboratory logbooks, and specimens were cataloged and preserved for potential future analyses.

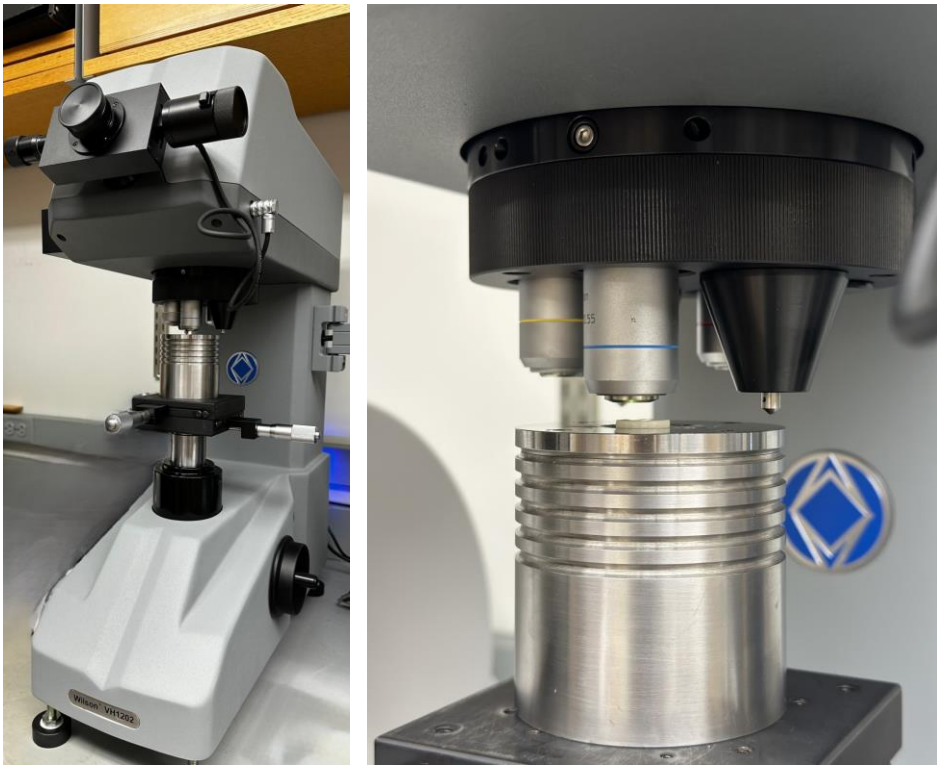

Figure 6. Wilson VH1202 Vickers/Knoop microhardness tester. A specimen's testing in progress.

2.4.3 Wear Resistance Test

The wear resistance of the 3D-printed dental resins was assessed using a standardized pin-on-plate wear testing configuration, wherein cylindrical resin specimens were articulated against feldspathic ceramic reference plates as seen in Figure 7. The antagonist plates were fabricated from Vita Mark II, a machinable ceramic material widely recognized for its enamel-analogous wear properties (Al-Hiyasat et al., 1999). Vita Mark II blocks were sectioned into uniform 3 mm-thick slices using an Isomet 5000 Linear Precision Saw (Buehler, IL, USA) equipped with a diamond wafering blade. Four slices were subsequently affixed using sticky wax to create a stable, continuous test surface.

To ensure a consistent and level contact interface, the ceramic plates underwent sequential polishing with the EcoMet 250 Grinder/Polisher (Buehler, IL, USA), progressing through 125 µm, 70 µm, 45 µm, and 15 µm resin-bonded diamond grinding discs. Marker ink was intermittently applied to verify surface flatness throughout the polishing process. Each material group contributed twenty-five cylindrical resin pins (3.5 mm diameter × 9 mm height), which were securely bonded to stainless steel rods using a light-cured adhesive resin. The rods were equipped with metal bushings and subjected to a constant vertical load of 341 grams, then mounted onto a dual-station, reciprocating wear-testing apparatus. The resin pins reciprocated across the ceramic plates with a 10

mm stroke length at a frequency of 100 cycles per minute. A continuous water drip system was employed to flush out wear debris and mitigate thermal accumulation. The test was conducted over 200,000 cycles, with intermediate assessments performed at 100,000 cycles. Height loss of the resin pins was measured using a high-precision Mitutoyo Absolute electronic indicator (Mitutoyo Corp., Japan), while weight loss was determined using a calibrated XS204 analytical balance (Mettler Toledo, Columbus, OH, USA). Prior to weighing, all specimens were stored in a vacuum desiccator as seen in Figure 8 for 3–4 days to eliminate residual moisture and ensure accurate mass readings.

Following the completion of testing, specimens were carefully detached from their mounts, cataloged, and reserved for subsequent documentation and analysis.

Figure 7. Pin-on-plate Wear Test Machine. Automatic Timer.

Figure 8. Metal rods glued with resin pins. Vacuum Desiccator.

2.4.4 Degree of Conversion (DC)

The degree of conversion (DC) of each resin was determined using a Bruker Fourier Transform Infrared (FTIR) Spectrometer integrated with an Attenuated Total Reflectance (ATR) accessory, enabling direct surface analysis of both unpolymerized and polymerized resin samples. For each material, two sample types were analyzed: unpolymerized liquid resin and post-polymerized disc specimens (14 mm in diameter × 2 mm in thickness), with only one side polished according to protocol. Prior to each measurement, the ATR crystal was meticulously cleaned using 99% isopropyl alcohol (IPA) and lint-free laboratory wipes to prevent contamination and spectral interference. A volume of 2–3 µL of liquid resin was dispensed onto the ATR crystal using a precision micropipette, whereas solid disc specimens were gently clamped onto the ATR platform

to ensure optimal surface contact. Spectral acquisition was configured over the range of 4000–400 cm^{-1} with a resolution of 4 cm^{-1} and 24 co-added scans per sample. Background spectra were collected at the beginning of the experiment to calibrate the instrument and eliminate environmental noise.

The degree of conversion was quantified by comparing the absorbance of the acrylate carbon-carbon double bond (C=C) at 1637 cm^{-1}, which decreases upon polymerization, against an internal reference peak that remains stable during polymerization. For aromatic resins, the reference peak was centered at 1608 cm^{-1}, while for amide-containing matrices, the amide II peak at 1537 cm^{-1} was used (Chrószcz et al., 2021). The DC was calculated using the following formulas:

For aromatic-based matrices:

$$\mathrm{DC}(\%) = \left(1 - \frac{\left(\frac{A_{C=C}}{A_{C=Ar}}\right)\mathrm{polymer}}{\left(\frac{A_{C=C}}{A_{C=Ar}}\right)\mathrm{monomer}}\right) \times 100$$

Where $A_{c=c}$ is the absorption intensity of the band resulting from the carbon-carbon double bond stretching vibrations, located at 1637 cm^{-1} and A_{Ar} is the absorption intensity of the internal standard- the band resulting from the skeletal stretching vibrations of the carbon-carbon bonds in the aromatic rings located at 1608 cm^{-1}.

For amide-containing matrices:

$$\mathrm{DC}(\%) = \left(1 - \frac{\left(\frac{A_{C=C}}{A_{C=Am}}\right)\mathrm{polymer}}{\left(\frac{A_{C=C}}{A_{C=Am}}\right)monomer}\right) \times 100$$

Where $A_{c=c}$ is the absorption intensity of the band resulting from the carbon-carbon double bond stretching vibrations, located at 1637 cm^{-1} and A_{am} is the absorption intensity of the internal standard- the band resulting from the skeletal stretching vibrations of the carbon-carbon bonds in the amide II band located at 1537 cm^{-1} (Wang et al., 2018).

All samples were analyzed in duplicates to ensure statistical reliability. A reduction in the aliphatic C=C peak intensity relative to the reference peak was interpreted as indicative of a higher degree of polymer conversion. Throughout the procedure, appropriate personal protective equipment (PPE) was worn, and all chemical waste was disposed of in compliance with institutional safety and hazardous waste protocols.

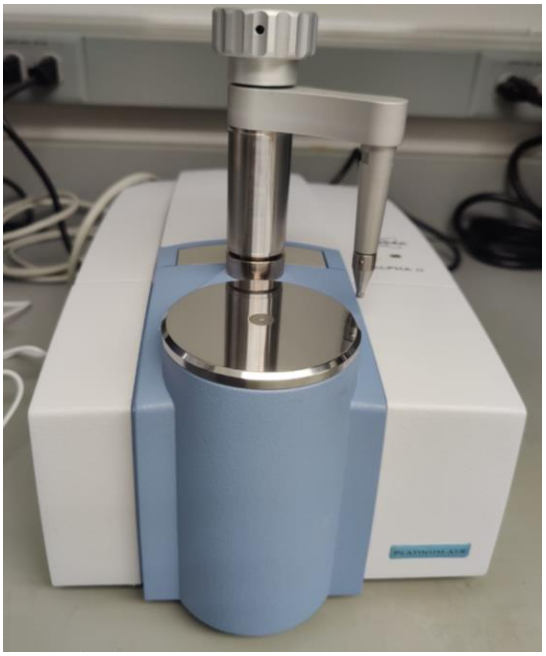

Figure 9. Bruker Fourier Transform Infrared (FTIR) Spectrometer.

2.4.5 Microstructural and Elemental Analysis

Microstructural evaluation and elemental characterization of the tested resin materials were performed using Scanning Electron Microscopy (SEM) and Energy Dispersive X-ray Spectroscopy (EDS), respectively. The primary objective was to investigate filler morphology, dispersion, and the fracture characteristics of specimens—particularly those demonstrating inferior mechanical performance in flexural testing. SEM analysis was conducted using the Hitachi SU5600 field emission scanning electron microscope (Hitachi High-Technology, Japan) operated at an accelerating voltage of 15 kV. High-resolution imaging was performed at magnifications of 100×, 200×, 500×, 1000×, 2000×, and 5000× to enable detailed assessment of filler particle geometry, interfacial integration within the polymer matrix, and the presence of structural anomalies such as voids, microcracks, or phase separations.

Complementary EDS analysis was carried out using an Oxford Instruments X-Max 50 mm^2 Silicon Drift Detector (Oxford Instruments, Bristol, UK), integrated with the Aztec software platform. Spectral acquisition was executed at the same accelerating voltage and a fixed working distance of 10 mm. Two representative regions per specimen, one on the surface and one at the fractured cross-section, were selected for elemental mapping and semi-quantitative compositional analysis as seen in Figure9. The integration of SEM and EDS provided a comprehensive understanding of the inorganic filler composition and its distribution, offering critical insights into how microstructural features influence the observed mechanical behavior of the tested materials.

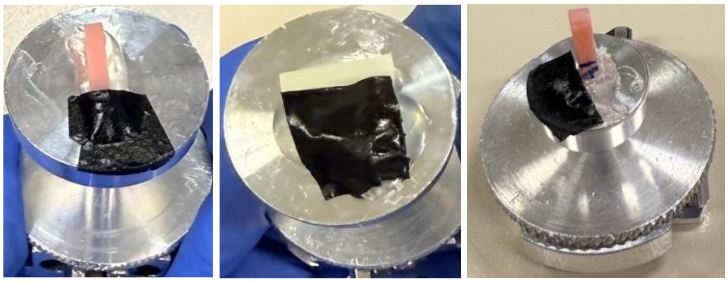

Figure 10. Flexural Strength bar attached to specimen mount.

2.4.6 Statistical Analysis

All mechanical performance data were subjected to statistical analysis using JMP Pro 18.0.2 (SAS Institute Inc., Cary, NC, USA). Descriptive statistics, including means and standard deviations, were computed for each experimental group. One-way analysis of variance (ANOVA) followed by Tukey's Honest Significant Difference (HSD) post hoc test was employed to identify statistically significant differences among groups. For pairwise comparisons, independent sample t-tests were utilized. In addition, Pearson correlation coefficients were calculated to evaluate the strength and direction of linear relationships between the degree of conversion (DC) and mechanical properties. A significance level of $\alpha = 0.05$ was adopted for all statistical procedures.

This rigorous analytical framework enabled standardized and reproducible comparisons of material performance across diverse post-polymerization protocols, offering valuable insights to inform evidence-based best practices in clinical 3D printing workflows.

Chapter 3. RESULTS

This section delineates the outcomes of the mechanical and chemical characterization of the selected 3D-printed dental resin materials. To facilitate clarity and enable meaningful comparison, the findings are organized into two primary categories based on material composition: **filled resins** and **unfilled resins**. The filled resin group comprises SprintRay Ceramic Crown (SCC), Rodin Titan (RT), and Rodin Sculpture 2.0 (RS2)—materials formulated with ceramic or inorganic filler phases to augment mechanical performance. In contrast, the unfilled resin group includes Rodin Denture Base 2.0 (RDB2) and SprintRay High Impact Denture Base (SHIDB), which are predominantly composed of polymeric matrices without a discrete filler phase.

Within each category, the data are reported for four critical performance metrics:

- Flexural strength (MPa)
- Vickers microhardness (VHN)
- Wear resistance (height and weight loss)
- Degree of Conversion (DC%)

Each specimen group underwent five distinct post-polymerization protocols: Nanocure, Otoflash with nitrogen, Otoflash without nitrogen, conventional oven polymerization, and Procure 2, to assess the influence of polymerization strategy on material behavior. Statistical analyses, including analysis of variance and post hoc comparisons, were performed to evaluate the significance of intergroup differences across polymerization methods and resin types.

3.1. Three-point Flexural Strength

3.1.1 Filled Resins

Table 4 presents the mean, standard deviation (SD), and coefficient of variation (CV) of flexural strength (MPa) for each filled resin processed under different polymerization methods. As depicted in Figure 10, SC2 demonstrated the highest mean flexural strength of 179.10 MPA when polymerized using the oven method, followed by the Otoflash with nitrogen group at 160.62 MPa. The lowest mean value was Procure at 133.32 MPa.

RT displayed a narrower range across polymerization methods. The highest flexural strength of 156.26 MPa was observed in both Otoflash with nitrogen while the lowest was seen in the Nanocure at 134.30 MPa.

SCC showed its highest strength in the Otoflash with nitrogen at 150.10 MPa and the lowest in the Otoflash without nitrogen at 134.53 MPa and oven groups at 134.44 MPa.

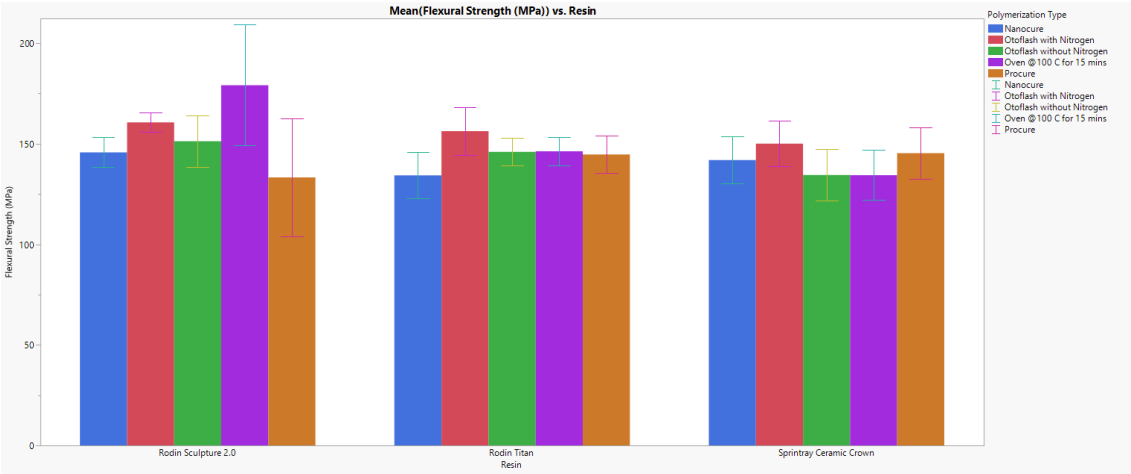

Figure 11. Bar chart of three-point flexural strength for tested filled materials.

Table 4. Summary of three-point flexural strength (MPa) for tested filled materials.

		Flexural Strength			
Resin	Polymerization Type	N	Mean (MPa)	Std Dev (MPa)	CV (%)
Rodin Sculpture 2.0	Nanocure	5	145.69	7.43	5.10
	Otoflash with Nitrogen	5	160.62	4.90	3.05
	Otoflash without Nitrogen	5	151.24	12.72	8.41
	Oven @100 C for 15 mins	5	179.10	30.04	16.78
	Procure	5	133.32	29.31	21.98
Rodin Titan	Nanocure	5	134.30	11.44	8.52
	Otoflash with Nitrogen	5	156.26	12.04	7.71
	Otoflash without Nitrogen	5	145.99	6.92	4.74
	Oven @100 C for 15 mins	5	146.25	6.97	4.76
	Procure	5	144.68	9.26	6.40
Sprintray Ceramic Crown	Nanocure	5	141.93	11.57	8.15
	Otoflash with Nitrogen	5	150.10	11.20	7.46
	Otoflash without Nitrogen	5	134.53	12.71	9.44
	Oven @100 C for 15 mins	5	134.44	12.48	9.29
	Procure	5	145.36	12.73	8.76

The least squares means (LSMeans), and ANOVA analyses collectively revealed statistically significant differences among both resins and polymerization methods ($p=0.0002$) as shown in Table 5. The analysis in Table 6 revealed statistically significant effects for all examined factors. Specifically, the type of resin ($p = 0.0093$), polymerization method ($p = 0.0079$), and the interaction between resin type and polymerization method ($p = 0.0059$) all demonstrated significance at the $\alpha = 0.05$ level. These findings underscore that both the material composition and the selected post-polymerization protocol independently influence the flexural strength of the printed specimens. Among the polymerization protocols, as depicted in Table 7 and Figure 11, Otoflash with nitrogen showed the highest LSMean flexural strength at 155.66 MPa,

followed closely by oven polymerization at 100°C for 15 minutes at 153.26 MPa, both statistically significant, whereas Nanocure at 140.64 MPa and Procure at 141.12 MPa had the lowest performance. The interaction effect revealed that RS2 polymerized with oven at 100°C demonstrated the highest flexural strength overall at 179.10 MPa as shown in Table 8, significantly greater than other combinations. This emphasizes that both resin composition and post-polymerization method independently and interactively influence mechanical performance.

Table 5. Analysis of Variance of flexural strength (MPa) for tested filled materials.

Source	DF	Sum of Squares	Mean Square	F Ratio
Model	14	10469.86	747.85	3.58
Error	64	13377.32	209.02	**Prob > F**
C. Total	78	23847.18		0.0002*

Table 6. Effect Tests of flexural strength (MPa) for tested filled materials.

Source	Nparm	DF	Sum of Squares	F Ratio	Prob > F
Resin	2	2	2104.3	5.03	0.0093*
Polymerization Type	4	4	3172.08	3.79	0.0079*
Resin* Polymerization Type	8	8	5071.53	3.03	0.0059*

Table 7. LSMeans Differences Tukey HSD Polymerization Type of flexural strength (MPa) for filled materials.

Level	Least Sq Mean (Flexural Strength (MPa))	Std Error	Mean (Flexural Strength (MPa))	Std Dev (Flexural Strength (MPa))	Tukey Test Connective Letter
Otoflash with Nitrogen	155.66	3.45	140.15	25.66	A
Oven @100 C for 15 mins	153.26	3.73	133.17	33.11	A B
Otoflash without Nitrogen	143.92	3.73	127.79	24.93	A B
Procure	141.12	3.73	124.09	27.57	B
Nanocure	140.64	3.73	126.53	18.89	B

*Levels not connected by the same letter are significantly different.
α=0.050 Q=2.80707

Table 8. LSMeans Differences Tukey HSD Material*Polymerization type of flexural strength (MPa) for tested filled materials.

Level	Significance	Least Sq Mean	Std Error
Rodin Sculpture 2.0, Oven @100 C for 15 mins	A	179.10	6.47
Rodin Sculpture 2.0, Otoflash with Nitrogen	A B	160.62	6.47
Rodin Titan, Otoflash with Nitrogen	A B	156.26	4.82
Rodin Sculpture 2.0, Otoflash without Nitrogen	A B	151.24	6.47
Sprintray Ceramic Crown, Otoflash with Nitrogen	A B	150.10	6.47
Rodin Titan, Oven @100 C for 15 mins	B	146.25	6.47
Rodin Titan, Otoflash without Nitrogen	B	145.99	6.47
Rodin Sculpture 2.0, Nanocure	B	145.69	6.47
Sprintray Ceramic Crown, Procure	B	145.36	6.47
Rodin Titan, Procure	B	144.68	6.47
Sprintray Ceramic Crown, Nanocure	B	141.93	6.47
Sprintray Ceramic Crown, Otoflash without Nitrogen	B	134.53	6.47
Sprintray Ceramic Crown, Oven @100 C for 15 mins	B	134.44	6.47
Rodin Titan, Nanocure	B	134.30	6.47
Rodin Sculpture 2.0, Procure	B	133.32	6.47

*Levels not connected by same letter are significantly different.
α=0.050 Q=3.52715

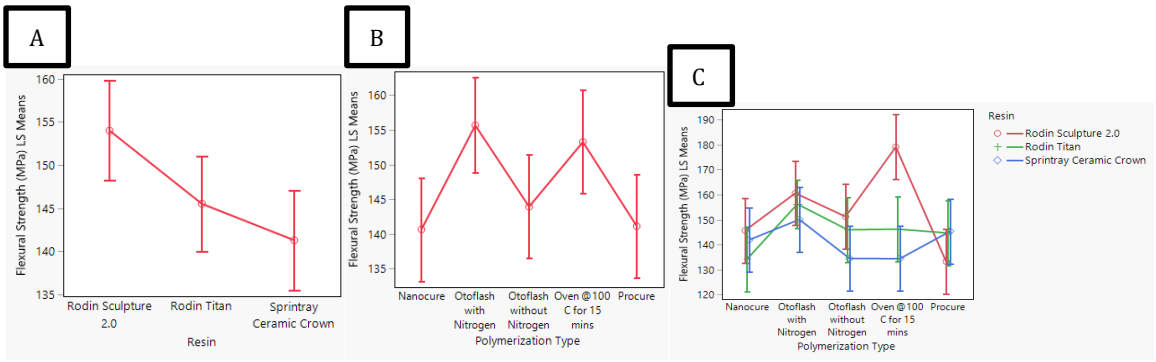

Figure 12. Least Squares means Plot of Flexural Strength (MPa) by Resin (A), Polymerization Type (B), Resin*Polymerization Type (C) of filled materials.

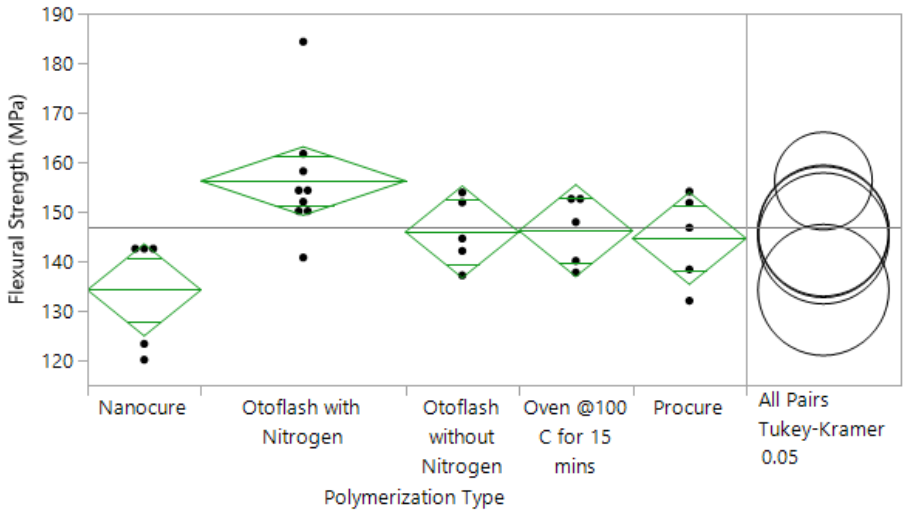

Figure 13. Oneway Analysis of Flexural Strength (MPa) By Polymerization Type for RT.

Table 9. Analysis of Variance of flexural strength (MPa) for RT.

Source	DF	Sum of Squares	Mean Square	F Ratio	Prob > F
Polymerization Type	4	1612.53	403.13	4.01	0.0125*
Error	24	2412.58	100.52		
C. Total	28	4025.11			

Table 10. Connecting Letters Report on flexural strength (MPa) for RT.

Level	Mean Flexural Strength (MPa)	Std Error	Std Dev Flexural Strength (MPa)	Significance
Otoflash with Nitrogen	156.26	3.34	12.04	A
Oven @100 C for 15 mins	146.25	4.48	6.97	A B
Otoflash without Nitrogen	145.99	4.48	6.92	A B
Procure	144.68	4.48	9.26	A B
Nanocure	134.30	4.48	11.44	B

*Levels not connected by the same letter are significantly different.

The one-way ANOVA results for Rodin Titan indicate that polymerization type significantly influences flexural strength (p = 0.0125) as seen in Table 9. Table 10 and Figure 12 presents that among the five polymerization methods, Otoflash with nitrogen produced the highest mean flexural strength of 156.26 MPa, which was statistically significantly greater than Nanocure at 134.30 MPa, as shown in the Tukey-Kramer HSD

post hoc test (p = 0.0052) as depicted in Table 11. While oven-polymerization at 146.25 MPa, Otoflash without nitrogen at 145.99 MPa, and Procure at 144.68 MPa groups also showed higher mean values than Nanocure, these differences were not statistically significant. The connecting letters report confirms that Otoflash with nitrogen stands out as the only polymerization protocol statistically significant to Nanocure in enhancing the mechanical performance of Rodin Titan.

Table 11. Tukey-Kramer HSD Ordered Differences Report of flexural strength (MPa) for RT.

Level	- Level	Difference	Std Err Dif	Lower CL	Upper CL	p-Value
Otoflash with Nitrogen	Nanocure	21.95755	5.592335	5.4824	38.43274	0.0052*
Oven @100 C for 15 mins	Nanocure	11.94954	6.341112	-6.7316	30.63065	0.3521
Otoflash without Nitrogen	Nanocure	11.68930	6.341112	-6.9918	30.37041	0.3734
Otoflash with Nitrogen	Procure	11.57467	5.592335	-4.9005	28.04986	0.2653
Procure	Nanocure	10.38288	6.341112	-8.2982	29.06399	0.4893
Otoflash with Nitrogen	Otoflash without Nitrogen	10.26825	5.592335	-6.2069	26.74344	0.3772
Otoflash with Nitrogen	Oven @100 C for 15 mins	10.00801	5.592335	-6.4672	26.48320	0.4023
Oven @100 C for 15 mins	Procure	1.56666	6.341112	-17.1145	20.24777	0.9991
Otoflash without Nitrogen	Procure	1.30642	6.341112	-17.3747	19.98753	0.9996
Oven @100 C for 15 mins	Otoflash without Nitrogen	0.26024	6.341112	-18.4209	18.94135	1.0000

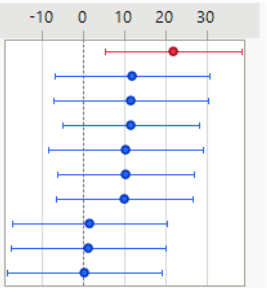

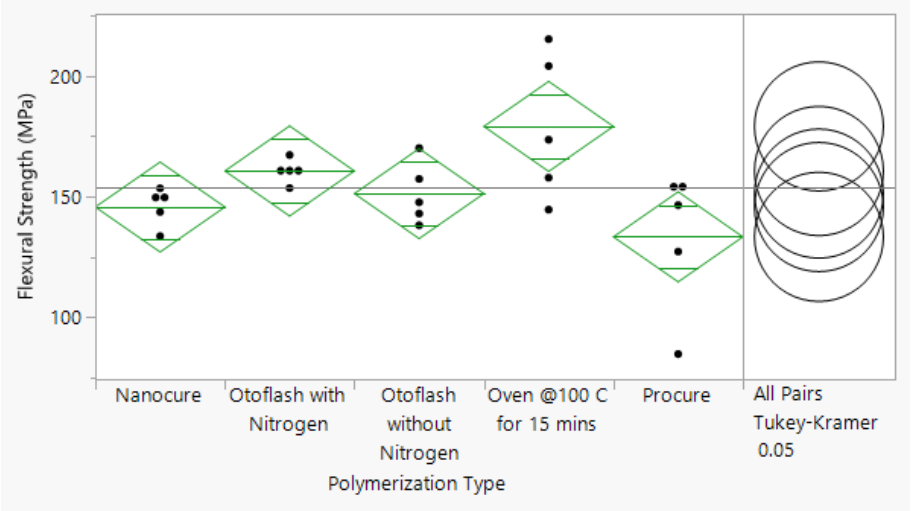

Figure 14. Oneway Analysis of Flexural Strength (MPa) By Polymerization Type for SC2.

Table 12. Analysis of Variance of flexural strength (MPa) for SC2.

Source	DF	Sum of Squares	Mean Square	F Ratio	Prob > F
Polymerization Type	4	5890.02	1472.51	3.67	0.0211*
Error	20	8009.99	400.50		
C. Total	24	13900.01			

Table 13. Connecting Letters Report on flexural strength (MPa) for SC2.

Level	Mean (Flexural Strength (MPa))	Std Error	Std Dev (Flexural Strength (MPa))	Significance
Oven @100 C for 15 mins	179.10	8.95	30.04	A
Otoflash with Nitrogen	160.62	8.95	4.9	A B
Otoflash without Nitrogen	151.24	8.95	12.72	A B
Nanocure	145.69	8.95	7.43	A B
Procure	133.32	8.95	29.31	B

*Levels not connected by the same letter are significantly different.

For Rodin Sculpture 2.0, the one-way ANOVA revealed a statistically significant effect of polymerization method on flexural strength (p = 0.021) as seen in Table 12. Table 13 and Figure13 depict that among the different techniques tested, oven polymerization at 100 °C for 15 minutes produced the highest mean flexural strength of 179.10 MPa, followed by Otoflash with nitrogen at 160.62 MPa. The lowest value was seen with the Procure at 33.32 MPa, which was significantly lower than oven polymerization (p = 0.0132) as indicated in the Tukey HSD post hoc analysis as seen in Table 14. The connecting letters report shows Oven @100°C as significantly different from Procure.

Table 14. Tukey-Kramer HSD Ordered Differences Report of flexural strength (MPa) for SC2.

Level	- Level	Difference	Std Err Dif	Lower CL	Upper CL	p-Value
Oven @100 C for 15 mins	Procure	45.77734	12.65701	7.9028	83.65186	0.0132*
Oven @100 C for 15 mins	Nanocure	33.40588	12.65701	-4.4686	71.28040	0.1005
Oven @100 C for 15 mins	Otoflash without Nitrogen	27.85056	12.65701	-10.0240	65.72508	0.2198
Otoflash with Nitrogen	Procure	27.30218	12.65701	-10.5723	65.17670	0.2360
Oven @100 C for 15 mins	Otoflash with Nitrogen	18.47516	12.65701	-19.3994	56.34968	0.5986
Otoflash without Nitrogen	Procure	17.92678	12.65701	-19.9477	55.80130	0.6248
Otoflash with Nitrogen	Nanocure	14.93072	12.65701	-22.9438	52.80524	0.7625
Nanocure	Procure	12.37146	12.65701	-25.5031	50.24598	0.8622
Otoflash with Nitrogen	Otoflash without Nitrogen	9.37540	12.65701	-28.4991	47.24992	0.9442
Otoflash without Nitrogen	Nanocure	5.55532	12.65701	-32.3192	43.42984	0.9917

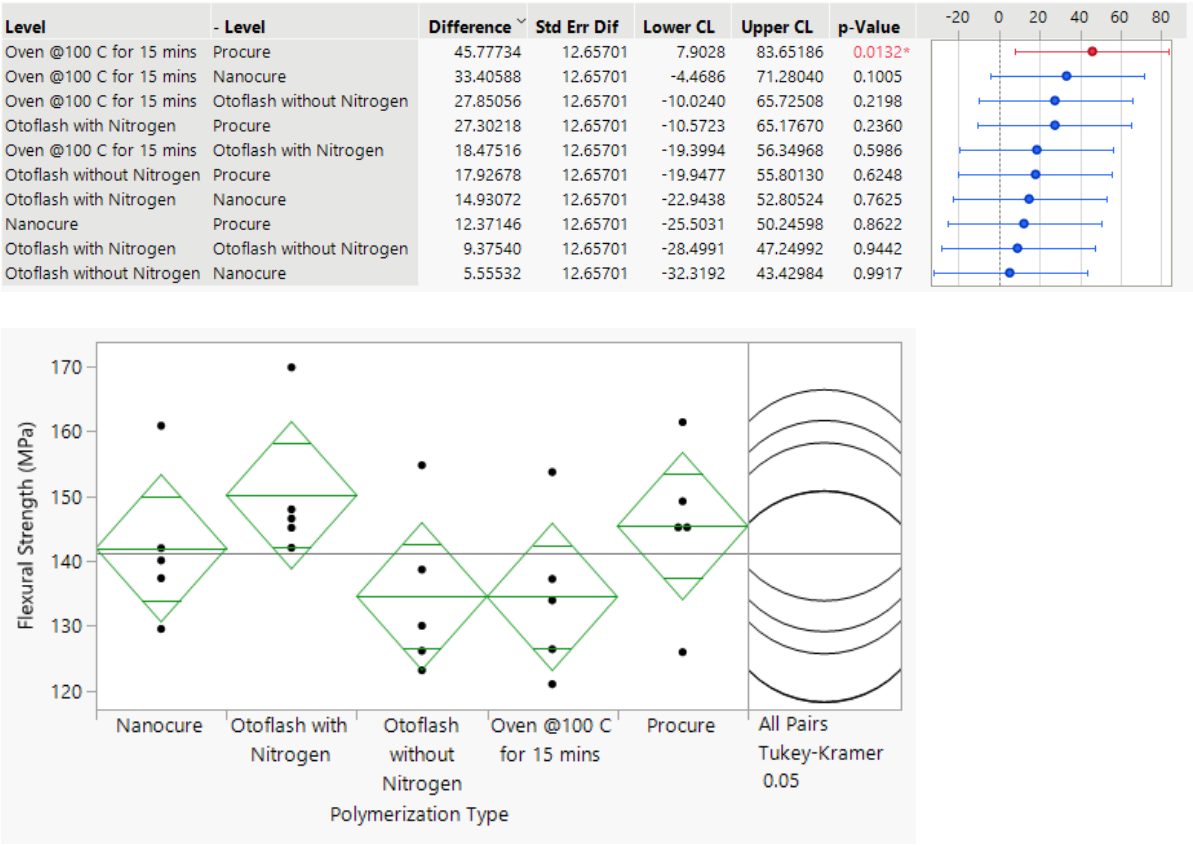

Figure 15. Oneway Analysis of Flexural Strength (MPa) By Polymerization Type for SCC.

Table 15. Analysis of Varience of flexural strength (MPa) for SCC.

Source	DF	Sum of Squares	Mean Square	F Ratio	Prob > F
Polymerization Type	4	936	234	1.58	0.2173
Error	20	2954.75	147.74		
C. Total	24	3890.75			

Table 16. Connecting Letters Report on flexural strength (MPa) for SCC.

Level	Mean (Flexural Strength (MPa))	Std Error	Std Dev (Flexural Strength (MPa))	Significance
Otoflash with Nitrogen	150.10	5.44	11.2	A

Level	Mean (Flexural Strength (MPa))	Std Error	Std Dev (Flexural Strength (MPa))	Significance
Procure	145.36	5.44	5.69	A
Nanocure	141.93	5.44	11.571925	A
Otoflash without Nitrogen	134.53	5.44	12.71	A
Oven @100 C for 15 mins	134.44	5.44	12.48	A

*Levels not connected by same letter are significantly different.

For SprintRay Ceramic Crown (SCC), the one-way ANOVA revealed no statistically significant difference in flexural strength among the five polymerization methods (p = 0.2173) as seen in Table 15. Table 16 and Figure 14 indicate that while Otoflash with nitrogen yielded the highest mean flexural strength at 150.10 MPa, followed by Procure at 145.36 MPa and Nanocure at 141.93 MPa, the differences among these polymerization methods and the lowest-performing groups such as Oven at 100 °C for 15 minutes at 134.44 MPa and Otoflash without nitrogen at 134.53 MPa, were not statistically significant. This conclusion is supported by the Tukey HSD post hoc analysis presented in Table 17, which shows overlapping groupings with no pairwise comparisons exceeding the threshold for significance at $\alpha = 0.05$.

Table 17. Tukey-Kramer HSD Ordered Differences Report of flexural strength (MPa) for SCC.

Level	- Level	Difference	Std Err Dif	Lower CL	Upper CL	p-Value
Otoflash with Nitrogen	Oven @100 C for 15 mins	15.66186	7.687329	-7.3415	38.66524	0.2850
Otoflash with Nitrogen	Otoflash without Nitrogen	15.56782	7.687329	-7.4356	38.57120	0.2904
Procure	Oven @100 C for 15 mins	10.92056	7.687329	-12.0828	33.92394	0.6222
Procure	Otoflash without Nitrogen	10.82652	7.687329	-12.1769	33.82990	0.6296
Otoflash with Nitrogen	Nanocure	8.16656	7.687329	-14.8368	31.16994	0.8232
Nanocure	Oven @100 C for 15 mins	7.49530	7.687329	-15.5081	30.49868	0.8632
Nanocure	Otoflash without Nitrogen	7.40126	7.687329	-15.6021	30.40464	0.8684
Otoflash with Nitrogen	Procure	4.74130	7.687329	-18.2621	27.74468	0.9707
Procure	Nanocure	3.42526	7.687329	-19.5781	26.42864	0.9912
Otoflash without Nitrogen	Oven @100 C for 15 mins	0.09404	7.687329	-22.9093	23.09742	1.0000

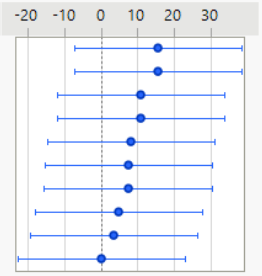

3.1.2 Unfilled Resins

Table 18 and Figure 15 summarize the flexural strength values of the two unfilled denture base resins: Rodin Denture Base 2.0 and SprintRay High Impact Denture Base. RDB2 showed consistent performance across all polymerization methods, with values ranging from 102.58 MPa for Procure to 104.98 MPa for Nanocure. These results indicate a relatively stable behavior irrespective of the polymerization approach, with minimal deviation and a coefficient of variation (CV) under 8% in all groups.

On the other hand, SHIDB demonstrated greater variability. The highest flexural strength was recorded in the Otoflash with nitrogen group at 117.17 MPa, while the lowest was noted in the Procure group at 94.52 MPa. High standard deviations and CVs above 24% in Procure and Otoflash without nitrogen groups highlight potential inconsistencies in polymer network formation for this material under certain polymerization conditions.

Overall, unfilled resins generally displayed lower flexural strength compared to filled resins. However, similar to filled resins, Otoflash with nitrogen yielded the highest strength values, especially in SprintRay High Impact Denture Base.

	Flexural Strength (MPa)				
Resin	**Polymerization Type**	**N**	**Mean**	**Std Dev**	**CV**
Rodin Denture Base 2.0	Nanocure	5	104.98	1.97	1.88
	Otoflash with Nitrogen	5	103.71	2.11	2.04
	Otoflash without Nitrogen	5	102.72	1.00	0.97
	Oven @100 C for 15 mins	5	103.20	3.88	3.76

	Procure	5	102.58	7.45	7.26
Sprintray High Impact Denture Base	Nanocure	5	111.69	11.49	10.29
	Otoflash with Nitrogen	5	117.17	24.80	21.16
	Otoflash without Nitrogen	5	104.45	27.05	25.90
	Oven @100 C for 15 mins	5	102.87	18.25	17.74
	Procure	5	94.52	22.91	24.24

Table 18. Summary of three-point flexural strength (MPa) for unfilled materials.

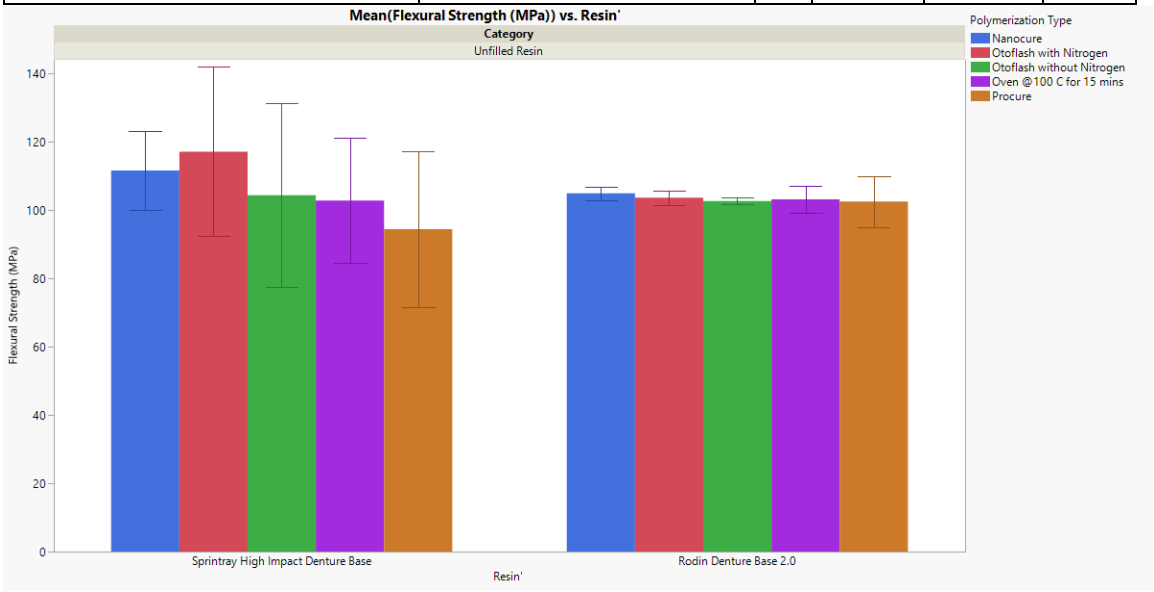

Figure 16. Bar chart of three-point flexural strength for tested unfilled materials.

The ANOVA and Least Squares Means (LSMeans) analyses performed on unfilled resins Rodin Denture Base 2.0 and SprintRay High Impact Denture Base revealed no statistically significant differences among either the resin types, the polymerization methods, or their interaction as seen in Table 19. The overall model demonstrated a low explanatory power, with an R^2 value of 0.1467 and an adjusted R^2 of -0.0362, indicating minimal variance accounted for by the independent variables. Specifically, p-values for the main effects of resin type ($p = 0.53$), polymerization method ($p = 0.44$), and the resin–polymerization method interaction ($p = 0.6$) were all above the conventional

threshold of 0.05 as seen in Table 20. **Table 21** presents the Least Squares Means (LSMeans) comparison of flexural strength among different post-polymerization methods for unfilled resin materials. Although Otoflash with nitrogen yielded the highest mean flexural strength (110.44 MPa), followed closely by Nanocure (108.33 MPa), Otoflash without nitrogen (103.59 MPa), Oven at 100 °C for 15 minutes (103.04 MPa), and Procure (98.55 MPa), all polymerization methods were grouped under the same statistical subset labeled "A." This indicates that the differences among these groups were not statistically significant based on Tukey's HSD post hoc test ($\alpha = 0.05$, $Q = 2.84981$). Figure 16 illustrated that the LSMeans plot showed numerically higher flexural strength for SprintRay High Impact Denture Base, particularly when polymerized with Otoflash using nitrogen at 117.17 MPa, compared to Rodin Denture Base 2.0. However, none of these differences reached statistical significance, as supported by overlapping confidence intervals and shared letter groupings in Tukey's HSD post-hoc test as seen in Table 22.

Table 19. Analysis of Variance of flexural strength for unfilled materials.

Source	**DF**	**Sum of Squares**	**Mean Square**	**F Ratio**
Model	9	1707	189.67	0.80
Error	42	9930.19	236.43	**Prob > F**
C. Total	51	11637.18		0.62

Table 20. Effect Tests of flexural strength for unfilled materials.

Source	**Nparm**	**DF**	**Sum of Squares**	**F Ratio**	**Prob > F**
Resin	1	1	93.92	0.40	0.53
Polymerization Type	4	4	900.31	0.95	0.44
Resin*Polymerization Type	4	4	650.66	0.69	0.60

Table 21. LSMeans Differences Tukey HSD Polymerization Type of flexural strength for unfilled materials.

Level	Least Sq Mean (Flexural Strength (MPa))	Std Error	Mean (Flexural Strength (MPa))	Std Dev (Flexural Strength (MPa))	Significance
Otoflash with N2	110.44	4.86	110.44	18.04	A
Nanocure	108.33	4.50	108.89	9.24	A
Otoflash w/o N2	103.59	4.86	103.59	18.07	A
Oven	103.04	4.86	106.14	15.67	A
Procure	98.55	4.86	98.55	16.61	A

*Levels not connected by the same letter are significantly different.

α=0.050 Q=2.84981

Table 22. LSMeans Differences Tukey HSD Material*Polymerization type of flexural strength for unfilled materials.

Level	Significance	Least Sq Mean	Std Error
Sprintray High Impact Denture Base, Otoflash with Nitrogen	A	117.17	6.88
Sprintray High Impact Denture Base, Nanocure	A	111.69	5.81
Rodin Denture Base 2.0, Nanocure	A	104.98	6.88
Sprintray High Impact Denture Base, Otoflash without Nitrogen	A	104.45	6.88
Rodin Denture Base 2.0, Otoflash with Nitrogen	A	103.71	6.88
Rodin Denture Base 2.0, Oven @100 C for 15 mins	A	103.20	6.88
Sprintray High Impact Denture Base, Oven @100 C for 15 mins	A	102.87	6.88
Rodin Denture Base 2.0, Otoflash without Nitrogen	A	102.72	6.88
Rodin Denture Base 2.0, Procure	A	102.58	6.88
Sprintray High Impact Denture Base, Procure	A	94.52	6.88

*Levels not connected by same letter are significantly different.

α=0.050 Q=3.33885

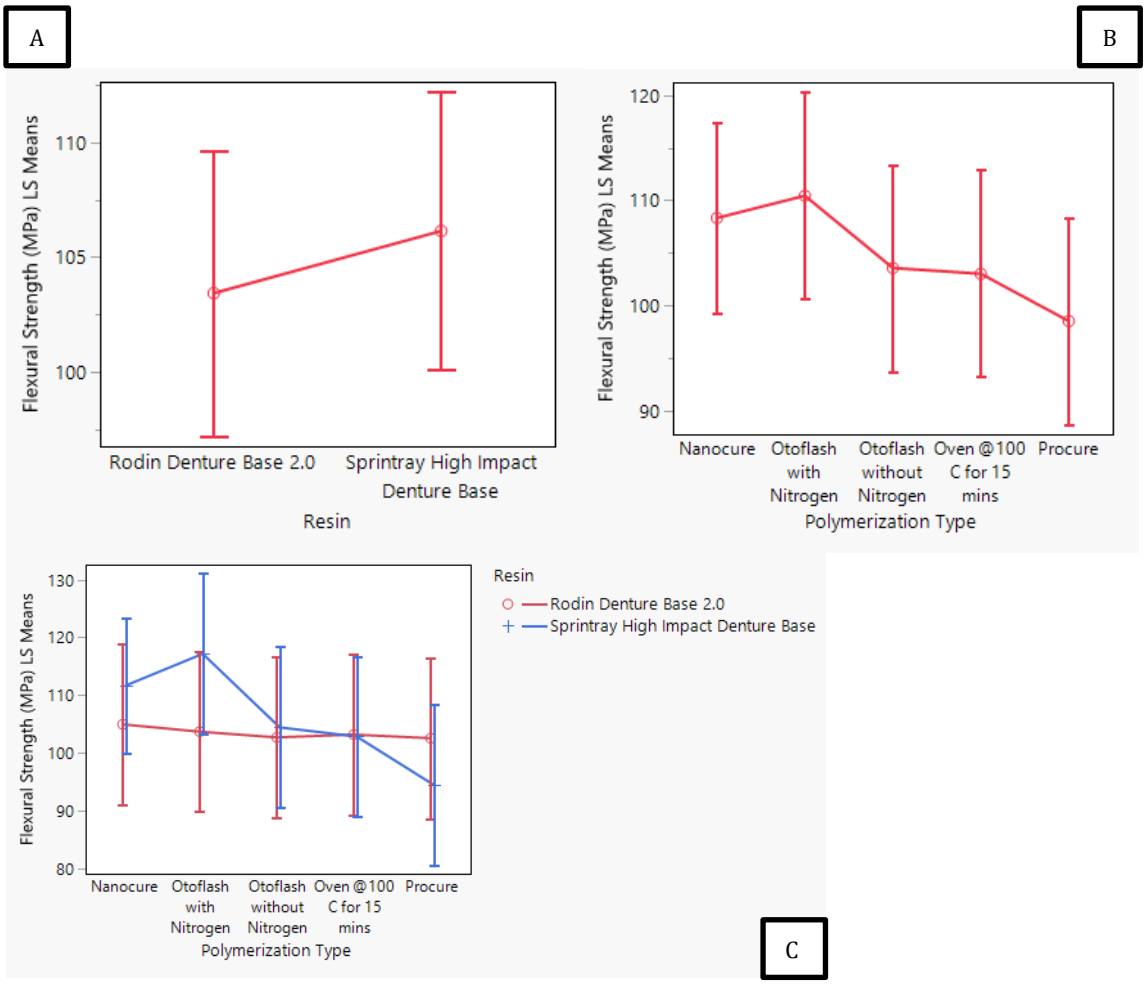

Figure 17. Least Squares means Plot of Flexural Strength (MPa) by Resin (A), Polymerization Type (B), Resin*Polymerization Type (C) for tested unfilled materials.

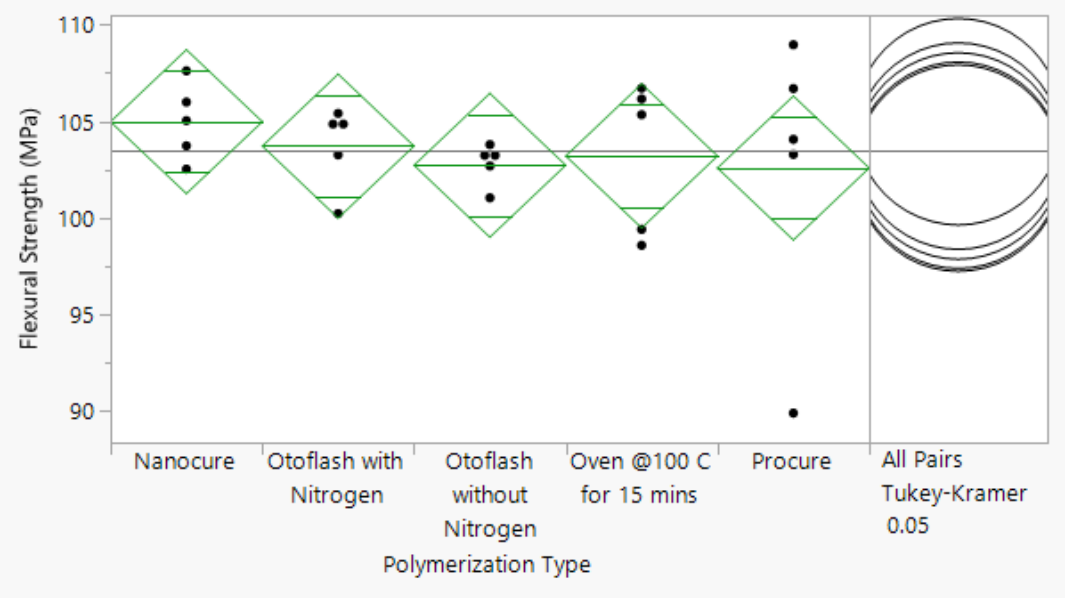

Figure 18. Oneway Analysis of Flexural Strength (MPa) By Polymerization Type for RDB2.

Table 23. Analysis of Variance of flexural strength for RDB2.

Source	DF	Sum of Squares	Mean Square	F Ratio	Prob > F
Polymerization Type	4	18.81	4.70	0.29	0.88
Error	20	319.60	15.98		
C. Total	24	338.41			

Table 24. Connecting Letters Report on flexural strength for RDB2.

Level	Mean (Flexural Strength (MPa))	Std Error	Std Dev (Flexural Strength (MPa))	Significance
Nanocure	104.98	1.79	1.97	A
Otoflash with Nitrogen	103.71	1.79	2.11	A
Oven @100 C for 15 mins	103.20	1.79	3.88	A
Otoflash without Nitrogen	102.72	1.79	1.001	A
Procure	102.58	1.79	7.45	A

*Levels not connected by same letter are significantly different.

The one-way ANOVA for RDB2 indicated no statistically significant difference in flexural strength across the five polymerization methods ($p = 0.88$), with an R^2 value of

just 0.0556 and a negative adjusted R^2 (–0.13), suggesting a very weak explanatory model as seen in Table 23. Mean flexural strength ranged narrowly from 102.58 MPa for Procure to 104.98 MPa for Nanocure, with overlapping confidence intervals and low standard deviations of ±1.79 MPa for all groups. Figure 17 illustrates the one-way analysis of flexural strength (MPa) across different polymerization types for the unfilled resin Rodin Denture Base 2.0 (RDB2). Although Otoflash with nitrogen and Nanocure exhibited slightly higher mean flexural strength values of 110.44 MPa and 108.33 MPa, respectively, all five polymerization protocols produced comparable results, with overlapping confidence intervals in the diamond plots. Notably, Procure demonstrated the lowest mean flexural strength of 98.55 MPa, with a wider spread of data points, including a visible outlier. Despite these numerical differences, Tukey-Kramer HSD analysis further confirmed this finding, as all groups belonged to the same statistical subset (group "A"), and no pairwise comparison between polymerization methods reached significance as seen in Table 24.

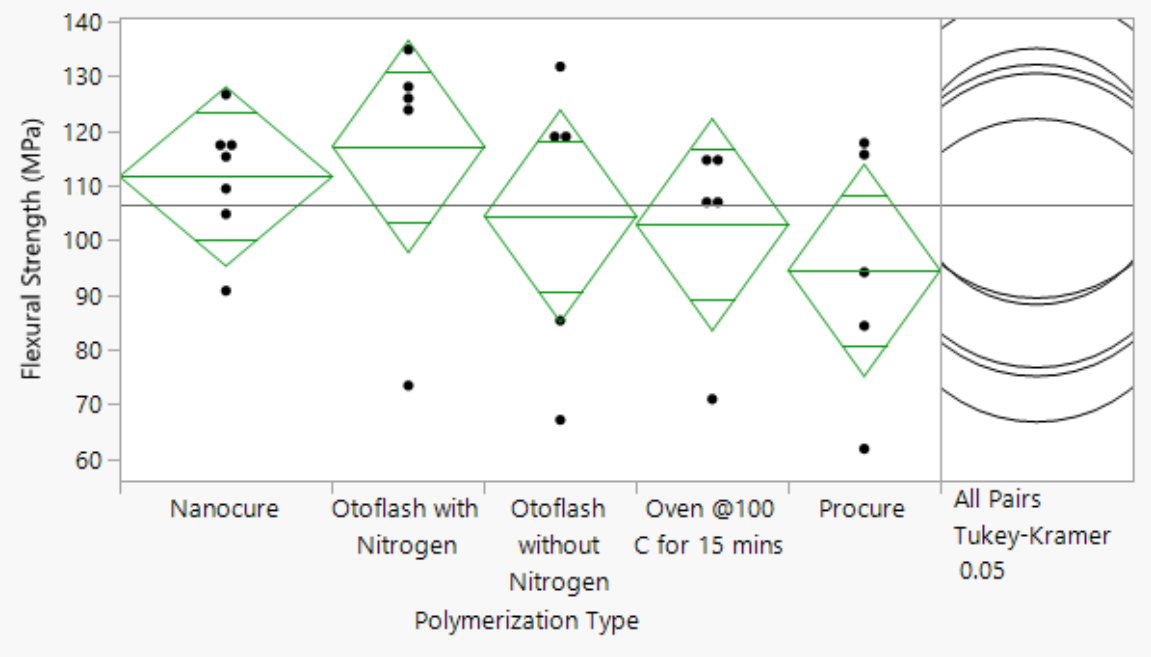

Figure 19. Oneway Analysis of Flexural Strength (MPa) By Polymerization Type for SHIDB.

Table 25. Analysis of Variance of flexural strength for SHIDB

Source	DF	Sum of Squares	Mean Square	F Ratio	Prob > F
Polymerization Type	4	1562.42	390.61	0.8942	0.4841
Error	22	9610.59	436.85		
C. Total	26	11173.01			

Table 26. Connecting Letters Report on flexural strength for SHIDB

Level	Mean (Flexural Strength (MPa))	Std Error	Std Dev (Flexural Strength (MPa))	Significance
Otoflash with Nitrogen	117.17	9.3471	24.8	A
Nanocure	111.69	7.8998	11.49	A
Otoflash without Nitrogen	104.45	9.3471	27.05	A
Oven @100 C for 15 mins	102.87	9.3471	18.25	A
Procure	94.52	9.3471	21.91	A

*Levels not connected by same letter are significantly different.

The one-way ANOVA results for SHIDB revealed no statistically significant differences among the five polymerization methods in terms of flexural strength ($p = 0.4841$) as seen

in Table 25. The R^2 value was 0.1398 with a negative adjusted R^2 of –0.0166, indicating that the polymerization method did not meaningfully explain the observed variance. Table 26 presents mean flexural strength that ranged from 94.52 MPa for Procure to 117.17 MPa for Otoflash with nitrogen, with large standard errors of 9.35 MPa reflecting high variability within each group. Figure 18 displays the one-way analysis of flexural strength (MPa) across five polymerization protocols for SprintRay High Impact Denture Base (SHIDB). Among all groups, Otoflash with nitrogen demonstrated the highest mean flexural strength of 130 MPa, followed by Nanocure at 115 MPa, while Procure exhibited the lowest mean value of 90 MPa, with notable variability and outliers observed in the dataset. Despite numerical differences, particularly the 22.65 MPa gap between the Otoflash with nitrogen and Procure groups, the Tukey-Kramer HSD analysis revealed no statistically significant pairwise comparisons (all p-values > 0.44). All polymerization techniques belonged to a single statistical group, indicating homogeneity.

3.2 Vickers Microhardness

3.2.1 Filled Resins

The Vickers microhardness test results for filled resins- Rodin Sculpture 2.0, Rodin Titan, and SprintRay Ceramic Crown, demonstrated a noticeable influence of polymerization method on the surface hardness values as seen in Table 27 and Figure 19. For RS2, the highest average hardness was observed with Otoflash with nitrogen at 38.49 and the lowest values were seen in the Oven-polymerized at 32.34 and Procure at 32.51 groups.

In RT, Otoflash with nitrogen again produced a significantly higher hardness of 66.20 compared to other methods. The Oven-polymerized group showed a much lower value of 22.49, with the highest variation (CV = 47.09%).

For SCC, the Otoflash with nitrogen method once again yielded the highest hardness value of 67.20, while the remaining groups: Nanocure at 43.15, Otoflash without nitrogen at 42.84, Oven 43.13, and Procure at 42.13, displayed consistent and comparable hardness values around 42–43 HV with low coefficients of variation (CV < 14%).

Overall, Otoflash with nitrogen consistently produced the highest Vickers hardness values across all filled resin types.

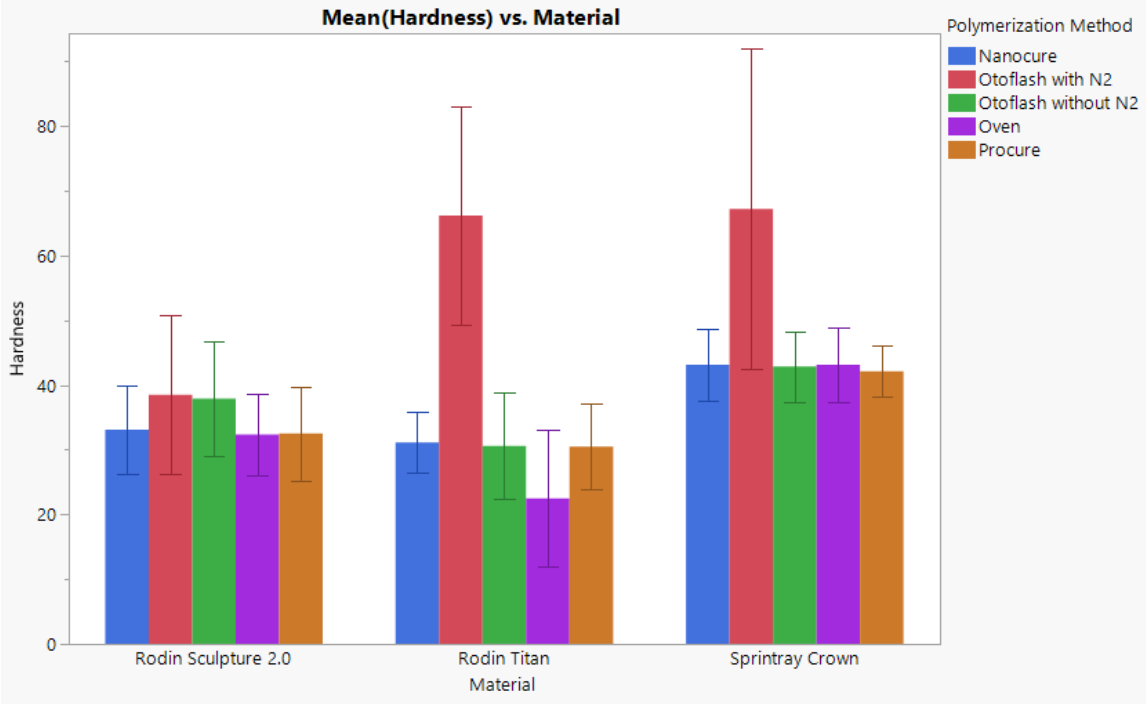

Figure 20. Bar chart of Vickers Microhardness for tested filled materials.

		Hardness (HV kgf/mm2)			
Material	**Polymerization Method**	**N**	**Mean**	**Std Dev**	**CV**
Rodin Sculpture 2.0	Nanocure	25	33.08	6.78	20.51
	Otoflash with N2	25	38.49	12.26	31.86
	Otoflash without N2	25	37.90	8.79	23.19
	Oven	25	32.34	6.35	19.63
	Procure	25	32.51	7.42	22.27
Rodin Titan	Nanocure	25	31.14	4.66	14.97
	Otoflash with N2	25	66.2	16.91	25.54
	Otoflash without N2	25	30.59	8.19	26.78
	Oven	29	22.49	10.59	47.09
	Procure	25	30.49	6.62	21.70
Sprintray Ceramic Crown	Nanocure	25	43.15	5.53	12.81
	Otoflash with N2	25	67.2	24.72	36.77
	Otoflash without N2	25	42.84	5.49	12.80
	Oven	25	43.13	5.70	13.21
	Procure	25	42.13	3.88	9.20

Table 27. Summary of Vickers Microhardness for filled materials.

The Least Squares Means analysis for Vickers hardness in filled resins showed statistically significant differences based on both the resin material and the polymerization method ($p < 0.0001$) as seen in Table 28. Table 29 presents the results of the effect tests assessing the impact of resin material, polymerization method, and their interaction on the Vickers microhardness of filled 3D-printed dental resins. All three sources of variation showed statistically significant effects on hardness values ($p < 0.0001$). Among the materials, SprintRay Ceramic Crown exhibited the highest average hardness with a value of 47.69, which was significantly greater than Rodin Titan at 36.18 and Rodin Sculpture 2.0 at 34.86. Regarding the polymerization protocols, as seen in Table 30, Otoflash with nitrogen produced the highest hardness overall at 57.30,

significantly outperforming Otoflash without nitrogen at 37.11, Nanocure at 35.79, Procure at 35.04, and Oven at 32.65, all of which were statistically similar but lower.

Table 31 depicts that the interaction analysis further emphasized this pattern, with Sprintray Ceramic Crown polymerized using Otoflash with nitrogen reaching the highest observed hardness at 67.20, followed closely by Rodin Titan under the same condition at 66.20. These two combinations formed the top statistical group. In contrast, the lowest hardness was seen in Rodin Titan polymerized in an oven, with a value of 22.49, indicating a significant reduction. Figure 20 illustrates the variation in Vickers microhardness (VHN) across filled resin materials and polymerization protocols. Among the materials tested, SprintRay Ceramic Crown demonstrated the highest hardness values, followed by Rodin Titan and Rodin Sculpture 2.0, as evident in the first plot.

In the second plot, Otoflash with nitrogen produced the highest microhardness across all polymerization methods, significantly outperforming oven polymerization and procure, which showed the lowest values.

The third interaction plot confirms that SprintRay Ceramic Crown benefited the most from Otoflash with nitrogen, reaching peak hardness above 60 VHN.

Overall, the results confirm that both material composition and post-polymerization methods significantly affect microhardness, with Otoflash with nitrogen consistently enhancing performance across all filled resins.

Table 28. Analysis of Variance of Vickers Microhardness for filled materials.

Source	DF	Sum of Squares	Mean Square	F Ratio
Model	14	55895.14	3992.51	37.04
Error	364	39233.48	107.78	**Prob > F**
C. Total	378	95128.62		<.0001*

Table 29. Effect Tests of Vickers Microhardness for filled materials.

Source	Nparm	DF	Sum of Squares	F Ratio	Prob > F
Material	2	2	12487.83	57.93	<.0001*
Polymerization Method	4	4	30392.8	70.49	<.0001*
Material*Polymerization Method	8	8	12241.1	14.2	<.0001*

Table 30. LSMeans Differences Tukey HSD Polymerization Type of Vickers Microhardness for filled materials.

Level	Least Sq Mean (HV)	Std Error	Mean (HV)	Std Dev (HV)	Significance
Otoflash with N2	57.23	1.2	57.3	22.78	A
Otoflash without N2	37.11	1.2	37.11	9.07	B
Nanocure	35.79	1.2	35.79	7.74	B
Procure	35.04	1.2	35.04	7.89	B
Oven	32.65	1.17	32.14	11.66	B

*Levels not connected by the same letter are significantly different.
α=0.050 Q=2.74151

Table 31. LSMeans Differences Tukey HSD Material*Polymerization type of Vickers Microhardness for tested filled materials.

Level	Significance	Least Sq Mean	Std Error
Sprintray Ceramic Crown, Otoflash with N2	A	67.2	2.08
Rodin Titan, Otoflash with N2	A	66.2	2.08
Sprintray Ceramic Crown, Nanocure	B	43.15	2.08
Sprintray Ceramic Crown, Oven	B	43.13	2.08
Sprintray Ceramic Crown, Otoflash without N2	B C	42.84	2.08
Sprintray Ceramic Crown, Procure	B C D	42.13	2.08
Rodin Sculpture 2.0, Otoflash with N2	B C D E	38.49	2.08
Rodin Sculpture 2.0, Otoflash without N2	B C D E	37.9	2.08
Rodin Sculpture 2.0, Nanocure	B C D E	33.08	2.08
Rodin Sculpture 2.0, Procure	E	32.52	2.08
Rodin Sculpture 2.0, Oven	E	32.34	2.08
Rodin Titan, Nanocure	E F	31.14	2.08
Rodin Titan, Otoflash without N2	E F	30.59	2.08
Rodin Titan, Procure	E F	30.49	2.08
Rodin Titan, Oven	F	22.49	1.93

*Levels not connected by the same letter are significantly different.
α=0.050 Q=3.41491

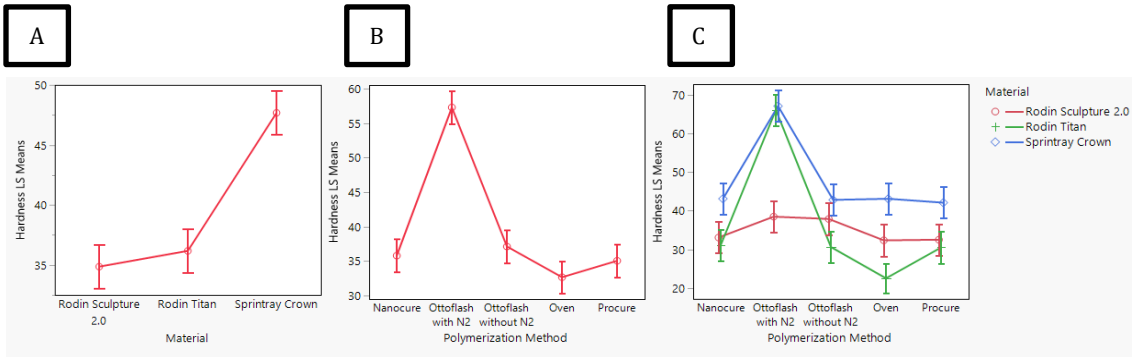

Figure 21. Least Squares means Plot of Flexural Strength (MPa) by Resin (A), Polymerization Type (B), Resin*Polymerization Type (C) for filled materials.

3.2.2 Unfilled Resins

Table 32 presents the Vickers microhardness values for the unfilled resins, Rodin Denture Base 2 and SprintRay High Impact Denture Base, which varied across polymerization methods but remained lower in magnitude compared to filled resins. RDB2 demonstrated the highest hardness with Otoflash with nitrogen at 18.04 and the lowest with Otoflash without nitrogen at 5.12. Despite this, RDB2 showed low standard deviations with Nanocure at 0.28 and Oven at 0.23, reflecting consistency in those groups.

In contrast, SHIDB exhibited consistently higher hardness values across all polymerization protocols. The highest hardness was recorded with Otoflash with nitrogen at 25.71 and the lowest with Nanocure at 21.54. The values were fairly uniform, indicating less sensitivity to polymerization variation. However, the CV was highest for Otoflash with nitrogen at 22.93 in this group, showing greater dispersion compared to other polymerization conditions.

Overall, SHIDB demonstrated superior hardness relative to RDB2, with Otoflash with nitrogen enhancing surface hardness most effectively in both unfilled resins as seen in Figure 21.

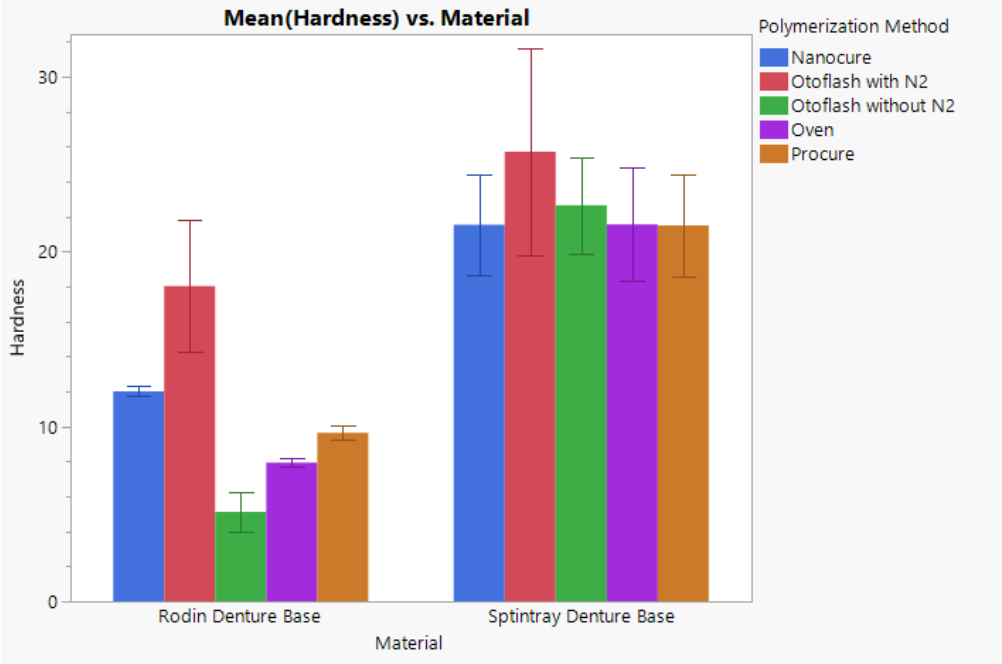

Figure 22. Bar chart of Vickers Microhardness for tested unfilled materials.

Table 32. Summary of Vickers Microhardness for unfilled materials.

		Hardness (HV kgf/mm2)			
Material	**Polymerization Method**	**N**	**Mean**	**Std Dev**	**CV**
Rodin Denture Base	Nanocure	25	12.01	0.28	2.33
	Otoflash with N2	25	18.04	3.75	20.77
	Otoflash without N2	25	5.12	1.14	22.25
	Oven	25	7.94	0.23	2.91
	Procure	25	9.64	0.39	4.06
Sprintray Denture Base	Nanocure	25	21.54	2.89	13.41
	Otoflash with N2	25	25.71	5.9	22.93
	Otoflash without N2	25	22.65	2.77	12.23
	Oven	25	21.56	3.26	15.12
	Procure	25	21.51	2.91	13.54

The least squares means analysis for unfilled resins revealed statistically significant effects of both material type and polymerization method on Vickers hardness ($p < 0.0001$) as seen in Table 33 and Table 34. SHIDB exhibited significantly higher mean hardness value of 22.59 compared to RDB2 at 10.55 as illustrated in Figure 22. Among polymerization methods, Otoflash with nitrogen produced the highest overall hardness value of 21.88, followed by Nanocure at 16.77, Procure at 15.57, Oven at 14.75, and Otoflash without nitrogen at 13.88 as seen in Table 35.

When evaluating the material–polymerization interaction, as depicted in Table 36 SHIDB polymerized with Otoflash with nitrogen achieved the highest mean hardness value of 25.71, significantly outperforming all other combinations. Other SprintRay groups showed similar hardness values around 21.5–22.7 regardless of polymerization type. In contrast, RDB2 exhibited substantial variability across polymerization protocols: the highest hardness was obtained with Otoflash with nitrogen at 18.04, followed by Nanocure at 12.01, Procure at 9.64, Oven at 7.94, and the lowest with Otoflash without nitrogen at 5.12.

Table 33. Analysis of Variance of Vickers Microhardness for tested unfilled materials.

Source	DF	Sum of Squares	Mean Square	F Ratio
Model	9	11779.60	1308.84	153.04
Error	240	2052.52	8.55	**Prob > F**
C. Total	249	13832.12		<.0001*

Table 34. Effect Tests of Vickers Microhardness for tested unfilled materials.

Source	Nparm	DF	Sum of Squares	F Ratio	Prob > F
Material	1	1	9067.33	1060.24	<.0001*

Source	Nparm	DF	Sum of Squares	F Ratio	Prob > F
Polymerization Method	4	4	1985.35	58.04	<.0001*
Material*Polymerization Method	4	4	726.93	21.25	<.0001*

Table 35. LSMeans Differences Tukey HSD Polymerization Type of Vickers Microhardness for tested unfilled materials.

Level	Least Sq Mean (HV)	Std Error	Mean (HV)	Std Dev (HV)	Significance
Otoflash with N2	21.88	0.41	21.88	6.24	A
Nanocure	16.77	0.41	16.77	5.22	B
Procure	15.57	0.41	15.57	6.34	B C
Oven	14.75	0.41	14.75	7.25	C D
Otoflash without N2	13.88	0.41	13.88	9.10	D

*Levels not connected by same letter are significantly different.
α=0.050 Q=2.74864.

Table 36. LSMeans Differences Tukey HSD Material*Polymerization type of Vickers Microhardness for tested unfilled materials.

Level	Significance	Least Sq Mean	Std Error
Sptintray Denture Base, Otoflash with N2	A	25.71	0.58
Sptintray Denture Base, Otoflash without N2	B	22.65	0.58
Sptintray Denture Base, Oven	B	21.56	0.58
Sptintray Denture Base, Nanocure	B	21.54	0.58
Sptintray Denture Base, Procure	B	21.51	0.58
Rodin Denture Base, Otoflash with N2	C	18.04	0.58
Rodin Denture Base, Nanocure	D	12.01	0.58
Rodin Denture Base, Procure	D E	9.64	0.58
Rodin Denture Base, Oven	E	7.94	0.58
Rodin Denture Base, Otoflash without N2	F	5.12	0.58

*Levels not connected by same letter are significantly different.
α=0.050 Q=3.19376

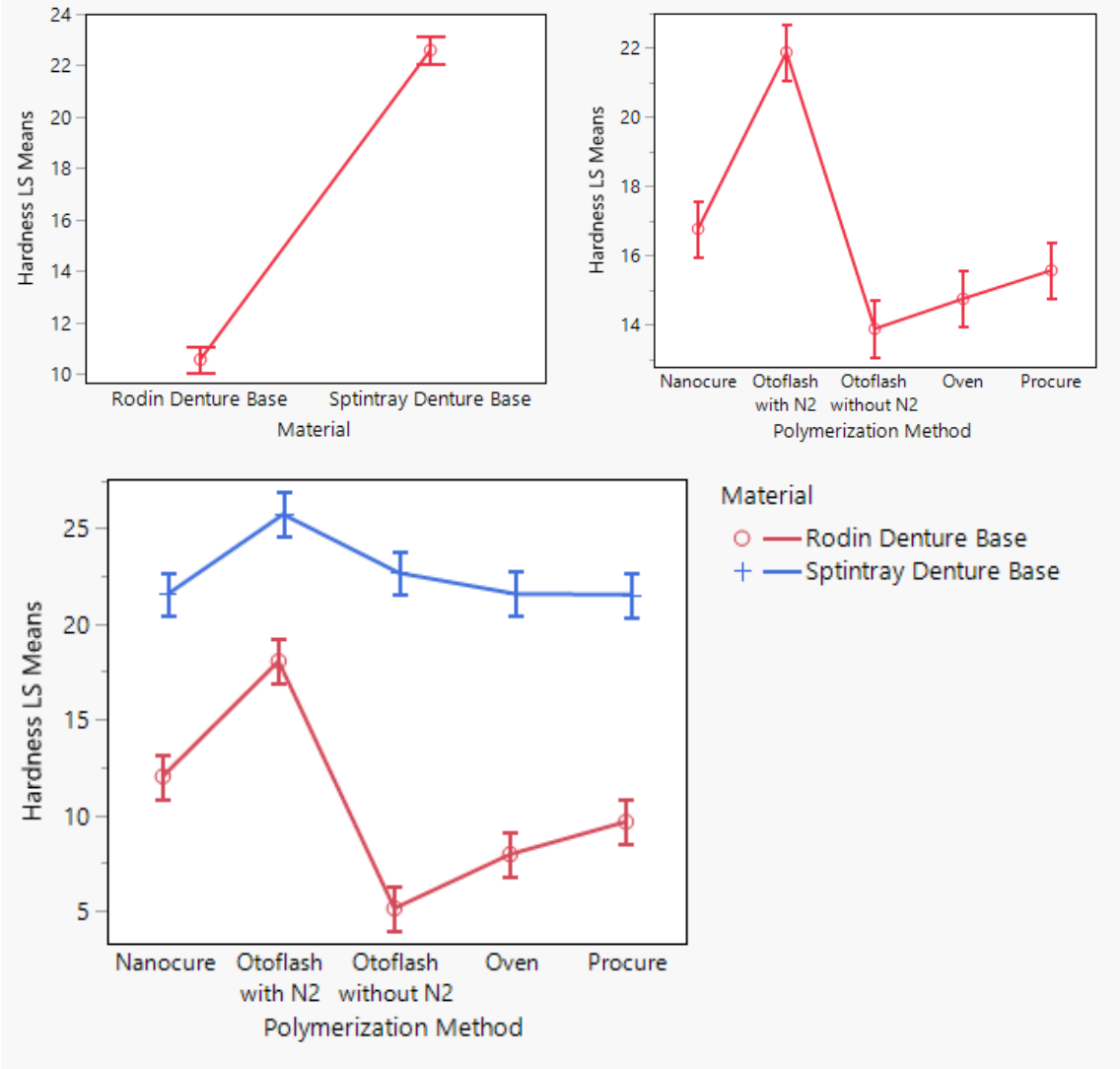

Figure 23. Least Squares means Plot of Vickers Hardness by Material, Polymerization Type, Material*Polymerization Type for unfilled materials.

3.3 Wear Resistance

Wear resistance was evaluated by measuring both vertical height loss and weight loss of specimens after 100,000 and 200,000 cycles. While both metrics provide insight into material degradation, weight loss measurements may be confounded by water sorption during prolonged cyclic loading in a moist environment. This water uptake can

artificially alter the weight of the specimen, leading to inaccurate estimations of true material loss. Therefore, to ensure the integrity of the data, only height loss values are considered reliable and are included in the final analysis of wear resistance.

3.3.1 Filled Resins

Table 37 presents the wear resistance for filled materials, RS2 exhibited the highest mean height loss when polymerized with Nanocure at 513.75 μm per million cycle wear, while the lowest wear was observed with Otoflash with nitrogen at 126.75 μm per million cycle wear.

For RT, the least height loss observed in the Procure group at 164.95 μm per million cycle wear and the greatest with Oven polymerization at 408.75 μm per million cycle wear.

In SCC, Otoflash with nitrogen again demonstrated the best wear resistance, with only 165.63 μm per million cycle wear of height loss. Procure exhibited the highest wear at 518.25 μm.

Overall, Otoflash with nitrogen consistently showed the lowest height wear across all filled resin types as seen in Figure 23.

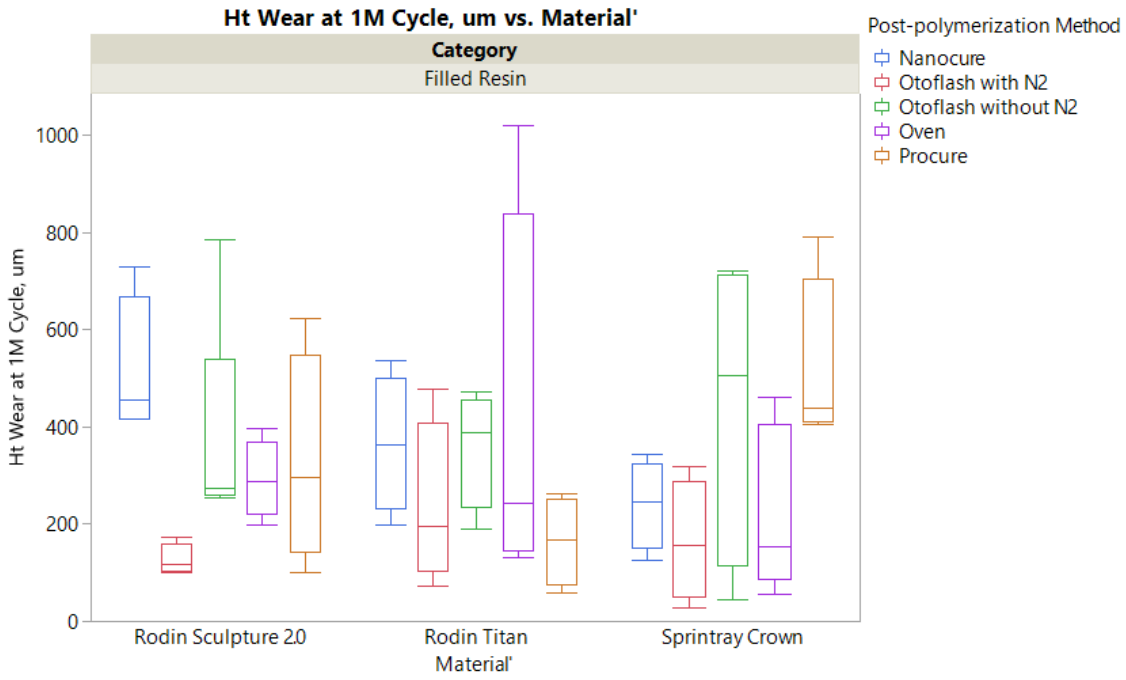

Figure 24. Bar chart of Height Wear for tested filled materials.

Table 37. Summary of Wear Resistance for filled materials.

			Ht Wear at 1M Cycle, µm			
Category	Material	Post-polymerization Method	N	Mean	Std Dev	CV
Filled Resin	Rodin Sculpture 2.0	Nanocure	4	513.75	147.45	28.70
		Otoflash with N2	4	126.75	32.28	25.47
		Otoflash without N2	5	375.00	229.67	61.24
		Oven	4	292.75	81.01	27.67
		Procure	4	328.33	218.38	66.51
	Rodin Titan	Nanocure	4	365.75	139.81	38.23
		Otoflash with N2	4	235.76	171.92	72.92
		Otoflash without N2	4	359.74	121.53	33.78
		Oven	4	408.75	412.75	100.98
		Procure	4	164.95	92.37	56.00
	Sprintray Ceramic Crown	Nanocure	4	240.50	90.76	37.74
		Otoflash with N2	4	165.63	122.84	74.17
		Otoflash without N2	4	443.75	322.11	72.59
		Oven	5	228.00	170.02	74.57
		Procure	4	518.25	182.10	35.14

The least squares means analysis for vertical height loss in unfilled resins revealed no statistically significant differences between materials or post-polymerization methods, as indicated by the p-values > 0.05 for all effects: post-polymerization method $p = 0.0662$, material $p = 0.9449$, and interaction $p = 0.12$ as seen in Table 38 and Table 39. Despite the lack of significance, numerical trends were observed. Table 40 presents that among the post-polymerization methods, Otoflash with nitrogen showed the lowest mean height loss at 176.04 µm per million cycle wear, while Otoflash without nitrogen showed the highest at 392.83 µm per million cycle wear, followed closely by Nanocure at 373.33 µm per million cycle wear. Intermediate values were seen with Procure at 337.18 µm per million cycle wear and Oven at 309.83 µm per million cycle wear. Table 41 illustrates the least squares means for height wear across various filled resin–polymerization combinations. Although no statistically significant differences were detected (all groups assigned the same significance letter), clear trends were observed. The highest wear was recorded for Sprintray Ceramic Crown with Procure at 518.25 µm per million cycle wear and Nanocure-treated Rodin Sculpture 2.0 at 513.75 µm per million cycle wear, while the lowest was seen in Rodin Sculpture 2.0 polymerized with Otoflash under nitrogen at 126.75 µm per million cycle wear.

Figure 24 displays the LSMeans of height wear (in µm) at 1 million cycles for filled resin materials subjected to various post-polymerization protocols.

The first graph demonstrates that Otoflash with nitrogen significantly reduced height wear compared to other methods, whereas Nanocure and Otoflash without nitrogen exhibited higher wear. The second graph shows minimal variation in wear among the

three tested resins—SC2, RT and SCC—indicating material type had a less pronounced effect. The interaction plot in Figure 24 (C) reveals that the combination of Sprintray Ceramic Crown with Otoflash with nitrogen yielded the least wear, while Procure-treated Sprintray Ceramic Crown and Nanocure-treated Rodin Sculpture 2.0 showed the highest wear values.

Table 38. Analysis of Variance of Wear Resistance for filled materials.

Source	DF	Sum of Squares	Mean Square	F Ratio
Model	14	869611.8	62115.1	1.65
Error	47	1766770.9	37590.9	**Prob > F**
C. Total	61	2636382.8		0.0998

Table 39. Effect Tests of Height Wear for filled materials.

Source	Nparm	DF	Sum of Squares	F Ratio	Prob > F
Post-polymerization Method	4	4	355793.57	2.37	0.07
Material	2	2	4264.61	0.06	0.94
Post-polymerization Method*Material	8	8	510059.36	1.70	0.12

Table 40. LSMeans Differences Tukey HSD Polymerization Type of Height Wear for filled materials.

Level	LSM (Ht wear at 1 M Cycle, µm)	Std Error	Mean (Ht wear at 1 M Cycle, µm)	Std Dev (Ht Wear at 1 M Cycle, µm)	Significance
Otoflash without N2	392.83	54.07	391.46	220.39	A
Nanocure	373.33	55.97	373.33	164.67	A
Procure	337.18	55.97	337.18	217.06	A
Oven	309.83	54.07	303.54	244.89	A
Otoflash with N2	176.04	55.97	17.04	121.16	A

*Levels not connected by same letter are significantly different.

α=0.050 Q=2.83649

Table 41. LSMeans Differences Tukey HSD Material*Polymerization type of Height Wear for filled materials.

Level	Least Sq Mean	Std Error	Significance
Procure, Sprintray Ceramic Crown	518.25	96.94	A
Nanocure, Rodin Sculpture 2.0	513.75	96.94	A

Level	Least Sq Mean	Std Error	Significance
Otoflash without N2, Sprintray Ceramic Crown	443.75	96.94	A
Oven, Rodin Titan	408.75	96.94	A
Otoflash without N2, Rodin Sculpture 2.0	375.00	86.71	A
Nanocure, Rodin Titan	365.75	96.94	A
Otoflash without N2, Rodin Titan	359.74	96.94	A
Procure, Rodin Sculpture 2.0	328.33	96.94	A
Oven, Rodin Sculpture 2.0	292.75	96.94	A
Nanocure, Sprintray Ceramic Crown	240.50	96.94	A
Otoflash with N2, Rodin Titan	235.76	96.94	A
Oven, Sprintray Ceramic Crown	228.00	86.71	A
Otoflash with N2, Sprintray Ceramic Crown	165.63	96.94	A
Procure, Rodin Titan	164.95	96.94	A
Otoflash with N2, Rodin Sculpture 2.0	126.75	96.94	A

*Levels not connected by the same letter are significantly different.

α=0.050 Q=3.57707

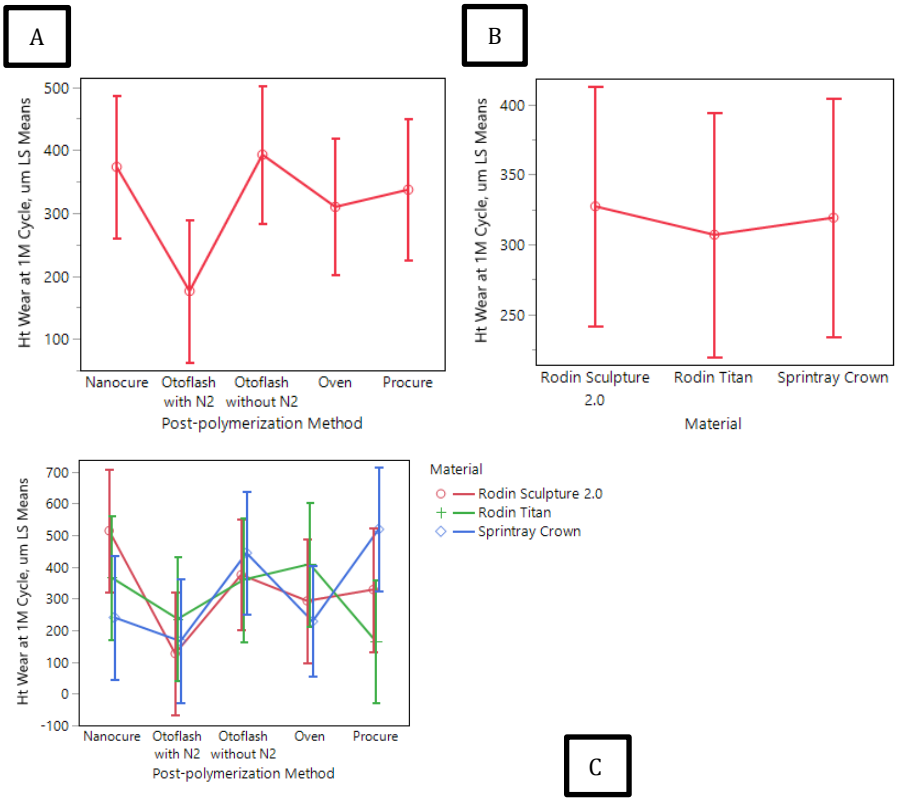

Figure 25. Least Squares means Plot of Height Wear at 1 million cycles by Resin (A), Polymerization Type (B), Resin*Polymerization Type (C) for filled materials.

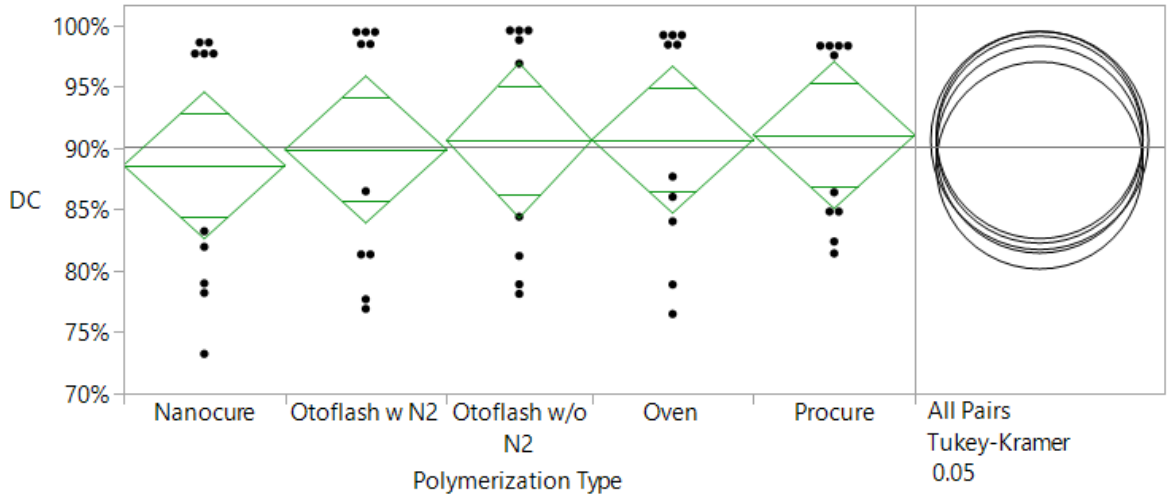

Figure 26. Oneway Analysis of Height Wear at 1 million cycles by Polymerization Type for RT.

Table 42. Analysis of Variance of Height Wear for RT.

Source	DF	Sum of Squares	Mean Square	F Ratio	Prob > F
Post-polymerization Method	4	167356.71	41839.2	0.86	0.5090
Error	15	728299.01	48553.3		
C. Total	19	895655.71			

Table 43. Connecting Letters Report on Height Wear for RT.

Level	Mean (Ht Wear at 1 M Cycle, µm)	Std Error	Std Dev (Ht Wear at 1 M Cycle, µm)	Significance
Oven	408.75	110.17	412.75	A
Nanocure	365.75	110.17	139.81	A
Otoflash without N2	359.74	110.17	121.53	A
Otoflash with N2	235.76	110.17	171.92	A
Procure	164.95	110.17	92.37	A

*Levels not connected by the same letter are significantly different.

Table 42 presents the one-way ANOVA for Rodin Titan, which revealed no statistically significant difference in mean height wear among the five post-polymerization methods ($p = 0.5090$). The method with the highest mean height loss was Oven at 408.75 µm per million cycle wear, followed closely by Nanocure at 365.75 µm per million cycle wear

and Otoflash without N_2 at 359.74 µm per million cycle wear. Lower wear values were observed for Otoflash with N_2 at 235.76 µm per million cycle wear and Procure at 164.95 µm per million cycle wear as seen in Table 43. Despite these numerical differences, the Tukey-Kramer HSD test confirmed that none of the group comparisons reached statistical significance, as all means shared the same connecting letter "A." The high standard error (110.17 µm) and overlapping confidence intervals across groups suggest substantial variability in wear measurements, reducing the statistical power to detect meaningful differences.

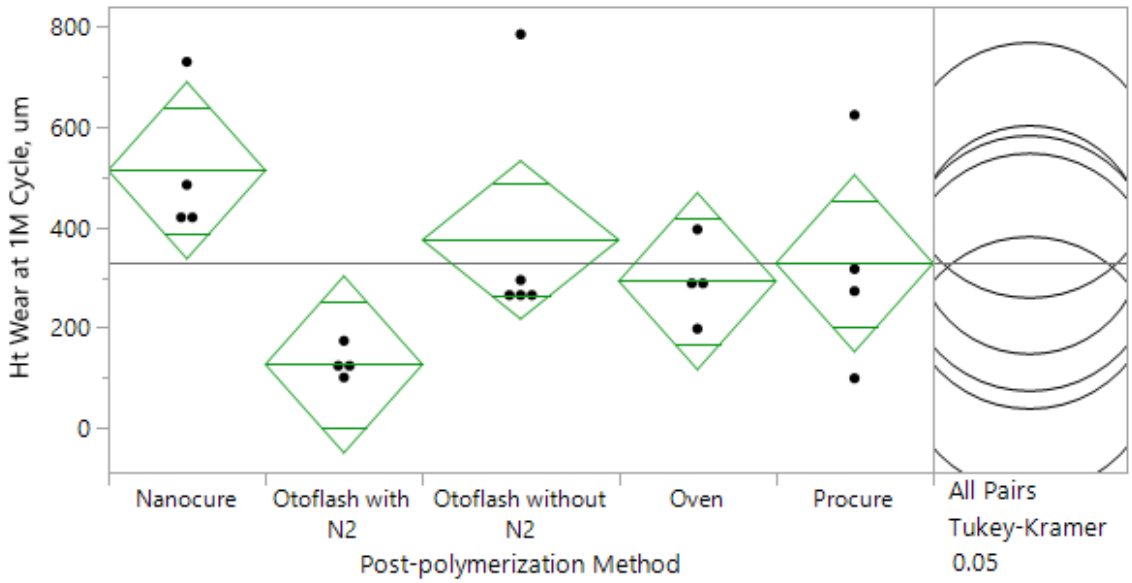

Figure 27. Oneway Analysis of Height Wear at 1 million Cycle by Polymerization Type for SC2.

Table 44. Analysis of Variance of Height Wear for SC2.

Source	DF	Sum of Squares	Mean Square	F Ratio	Prob > F
Post-polymerization Method	4	315988.55	78997.1	2.86	0.0580
Error	16	442103.69	27631.5		
C. Total	20	758092.24			

Table 45. Connecting Letters Report on Height Wear for SC2.

Level	Mean (Ht Wear at 1 M Cycle, µm)	Std Error	Std Dev (Ht Wear at 1 M Cycle, µm)	Significance
Nanocure	513.75	83.11	147.45	A
Otoflash without N2	375.00	74.34	229.67	A B
Procure	328.33	83.11	218.38	A B
Oven	292.75	83.11	81.01	A B
Otoflash with N2	126.75	83.11	32.28	B

*Levels not connected by the same letter are significantly different.

Table 45 presents the one-way ANOVA assessing the effect of post-polymerization method on height wear for Rodin Sculpture 2.0, which showed a trend toward significance ($p = 0.0580$), suggesting potential differences among groups. The highest mean height wear was observed for Nanocure at 513.75 µm, followed by Otoflash without N_2 at 375.00 µm per million cycle wear, Procure at 328.33 µm per million cycle wear, and Oven at 292.75 µm per million cycle wear, while Otoflash with N_2 exhibited the lowest wear at 126.75 µm per million cycle wear as seen in Table 46. According to the Tukey-Kramer HSD, only Nanocure and Otoflash with N_2 were significantly different (mean difference = 387 µm, $p = 0.0321$). The remaining methods exhibited overlapping confidence intervals and were not statistically distinguishable, although Nanocure consistently trended toward higher wear.

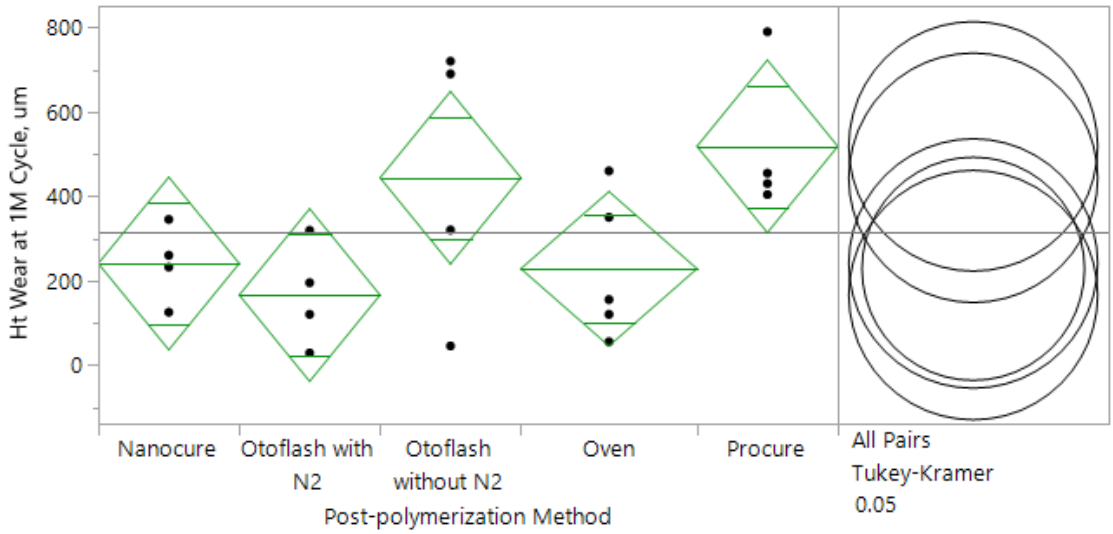

Figure 28. Oneway Analysis of Height Wear at 1 million cycles by Polymerization Type for SCC.

Table 46. Analysis of Variance of Height Wear for SCC.

Source	DF	Sum of Squares	Mean Square	F Ratio	Prob > F
Post-polymerization Method	4	380846.53	95211.6	2.55	0.08
Error	16	596368.23	37273.0		
C. Total	20	977214.76			

Table 47. Connecting Letters Report on Height Wear for SCC.

Level	Mean (Ht Wear at 1 M Cycle, µm)	Std Error	Std Dev (Ht Wear at 1 M Cycle, µm)	Significance
Procure	518.25	96.53	182.1	A
Otoflash without N2	443.75	96.53	322.11	A
Nanocure	240.50	96.53	90.76	A
Oven	228.00	86.34	170.02	A
Otoflash with N2	165.63	96.53	122.84	A

*Levels not connected by the same letter are significantly different.

Table 48 presents the one-way ANOVA investigating the effect of post-polymerization method on height wear for Sprintray Crown, which revealed no statistically significant differences between groups ($p = 0.0792$), though some trends were observed. Procure

exhibited the highest mean height wear at 518.25 μm per million cycle wear, followed by Otoflash without N_2 at 443.75 μm per million cycle wear, Nanocure at 240.50 μm per million cycle wear, Oven at 228.00 μm per million cycle wear, and the lowest was Otoflash with N_2 at 165.63 μm per million cycle wear as seen in Table 49. Despite these differences, Tukey-Kramer post-hoc analysis found that all pairwise comparisons were statistically non-significant, with overlapping confidence intervals and *p*-values well above 0.05.

3.3.2 Unfilled Resins

For unfilled resins, as illustrated in Figure 28 and Table 51, SHIDB Nanocure group had the lowest mean wear at 342.5 μm per million cycle wear, indicating the best wear resistance. The Procure method exhibited the highest height loss at 1346.00 μm per million cycle wear, with large standard deviations (±953.13 μm), reflecting substantial variability.

In contrast, RDB2 showed higher wear overall. Otoflash without N_2 resulted in the lowest height loss at 258.60 μm per million cycle wear, followed by Otoflash with N_2 at 331.42 μm per million cycle wear. Procure exhibited the highest wear at 671.20 μm per million cycle wear.

Overall, within unfilled resins, Otoflash without N_2 for RDB2 and Nanocure for SHIDB, demonstrated more favorable wear resistance. Conversely, Procure polymerization led to the highest wear in both materials.

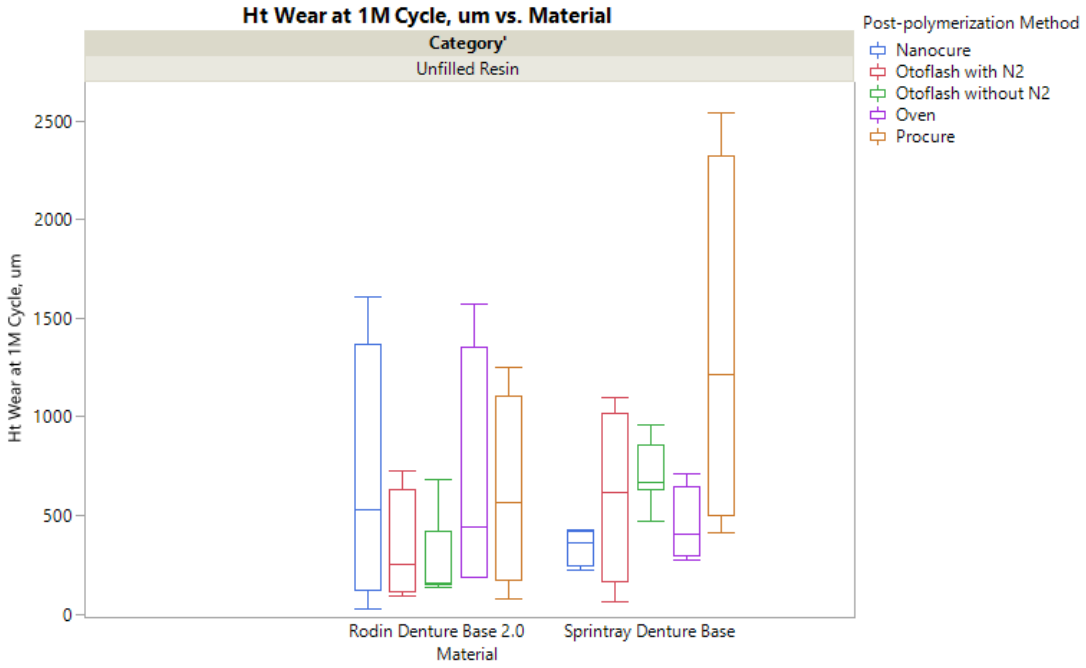

Figure 29. Bar chart of Wear Resistance for tested unfilled materials.

Table 48. Summary of Wear Resistance for tested unfilled materials.

			Ht Wear at 1M Cycle, um			
Category	**Material**	**Post-polymerization Method**	**N**	**Mean**	**Std Dev**	**CV**
Unfilled Resin	Rodin Denture Base 2.0	Nanocure	4	671.20	676.43	100.78
		Otoflash with N2	4	331.42	281.25	84.86
		Otoflash without N2	5	258.60	236.29	91.37
		Oven	4	658.99	653.09	99.11
		Procure	4	616.25	489.65	79.46
	Sprintray Denture Base	Nanocure	4	342.50	92.31	26.95
		Otoflash with N2	4	597.95	440.70	73.70
		Otoflash without N2	7	723.49	169.05	23.37
		Oven	4	447.25	189.64	42.40
		Procure	4	1346.00	953.13	70.81

The LSMeans analysis for height wear in unfilled resins revealed notable trends across different post-polymerization methods and materials, although most differences were not statistically significant at the 0.05 level as seen in Table 52. Table 54 presents that among

the post-polymerization methods, Procure exhibited the highest mean height loss at 981.13 μm per million cycle wear, indicating the poorest wear resistance, while Otoflash with N_2 showed the lowest at 464.69 μm per million cycle wear. However, all methods were grouped into the same Tukey HSD subset, suggesting that these differences were not statistically significant as seen in Table 55. When comparing materials, SDB showed a higher mean height wear at 691.44 μm per million cycle wear than RDB2 at 507.29 μm per million cycle wear, again without statistical significance. The interaction between material and polymerization method revealed more pronounced effects as seen in Table 53. The combination of Procure with SDB resulted in the highest wear at 1346.00 μm per million cycle wear and was the only group significantly different from others, as indicated by Tukey HSD grouping. In contrast, Otoflash without N_2 on RDB2 showed the lowest wear at 258.60 μm per million cycle wear, suggesting superior wear resistance. These findings emphasize that while individual material or polymerization method effects may not differ significantly, their combination can substantially influence the wear behavior of unfilled resins as seen in Figure 29.

Table 49. Analysis of Variance of Wear Resistance for tested unfilled materials.

Source	DF	Sum of Squares	Mean Square	F Ratio
Model	9	3597922	399769	1.83
Error	34	7445073	218973	**Prob > F**
C. Total	43	11042996		0.0994

Table 50. Effect Tests of Wear Resistance for tested unfilled materials.

Source	Nparm	DF	Sum of Squares	F Ratio	Prob > F
Post-polymerization Method	4	4	1529887.9	1.7467	0.1626
Material	1	1	361832.6	1.6524	0.2073
Post-polymerization Method*Material	4	4	1672221.8	1.9092	0.1314

Table 51. LSMeans Differences Tukey HSD Polymerization Type of Wear Resistance for tested unfilled materials.

Level	Least Sq Mean (Ht Wear at 1 M Cycle, µm)	Std Error	Mean (Ht Wear at 1 M Cycle, µm)	Std Deviation (Ht Wear at 1 M Cycle, µm)	Significance
Procure	981.12	165.44	981.13	802.65	A
Oven	553.12	165.44	553.12	459.37	A
Nanocure	506.85	165.44	506.85	480.23	A
Otoflash without N2	491.04	137.00	529.78	305.28	A
Otoflash with N2	464.69	165.44	464.69	370.72	A

*Levels not connected by the same letter are significantly different.

Table 52. LSMeans Differences Tukey HSD Material*Polymerization type of Wear Resistance for tested unfilled materials.

Level	Least Sq Mean	Std Error	Significance
Procure, Sprintray Denture Base	1346.0	233.97	A
Otoflash without N2, Sprintray Denture Base	723.5	176.87	A B
Nanocure, Rodin Denture Base 2.0	671.2	233.97	A B
Oven, Rodin Denture Base 2.0	659.0	233.97	A B
Procure, Rodin Denture Base 2.0	616.3	233.97	A B
Otoflash with N2, Sprintray Denture Base	598.0	233.97	A B
Oven, Sprintray Denture Base	447.3	233.97	A B
Nanocure, Sprintray Denture Base	342.5	233.97	A B
Otoflash with N2, Rodin Denture Base 2.0	331.4	233.97	A B
Otoflash without N2, Rodin Denture Base 2.0	258.6	209.27	B

*Levels not connected by the same letter are significantly different.

α=0.050 Q=3.38124

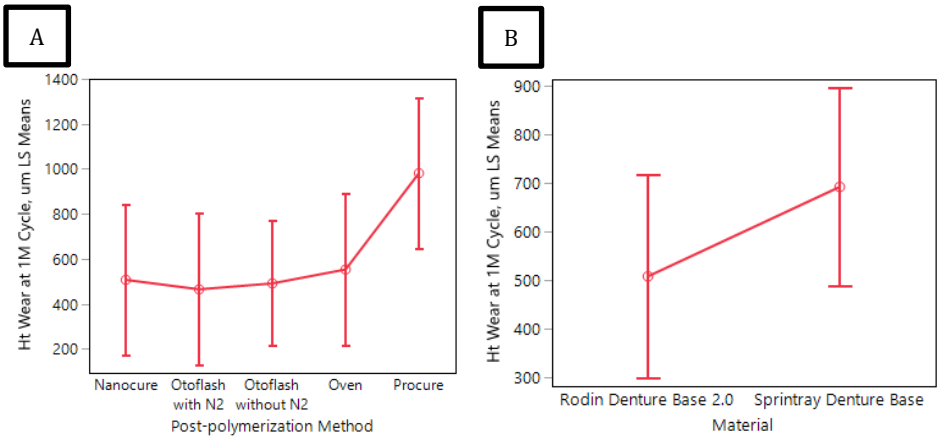

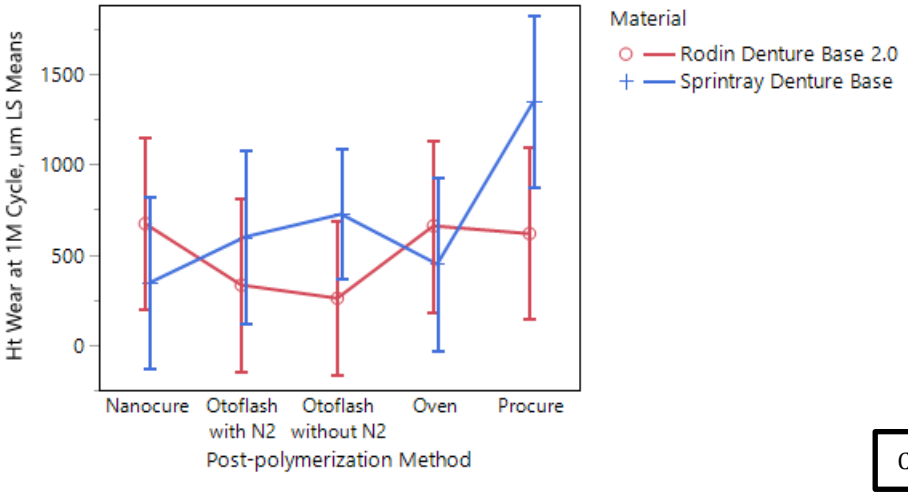

Figure 30. Least Squares means Plot of Height Wear at 1 million cycles by Material (A), Polymerization Type (B), Material*Polymerization Type (C) for unfilled materials.

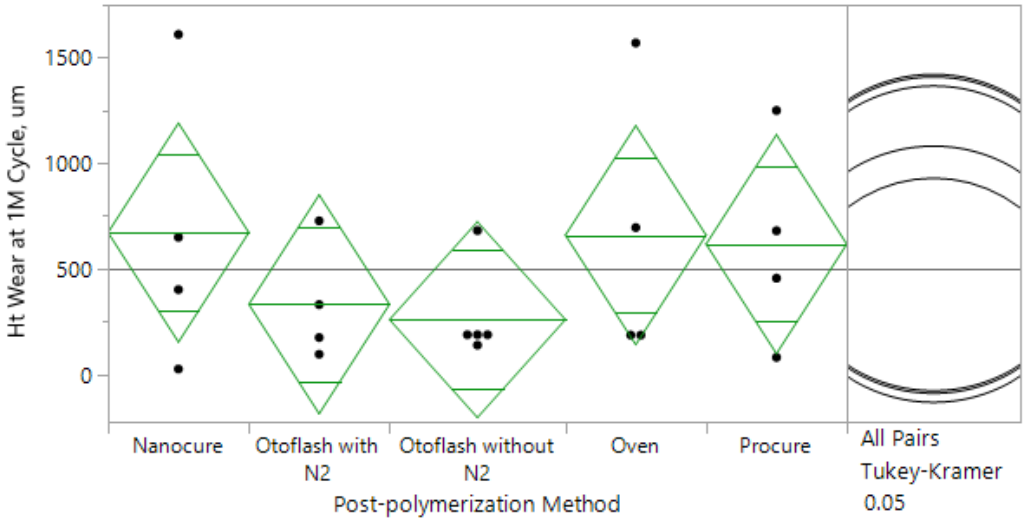

Figure 31. Oneway Analysis of Height Wear at 1 million Cycle by Polymerization Type for RDB2.

Table 53. Analysis of Variance of Height Wear for RDB2.

Source	DF	Sum of Squares	Mean Square	F Ratio	Prob > F
Post-polymerization Method	4	677005.2	169251	0.71	0.5990
Error	16	3832167.4	239510		
C. Total	20	4509172.6			

Table 54. Connecting Letters Report on Height Wear for RDB2.

Level	Mean (Ht Wear at 1 M Cycle, µm)	Std Error	Std Dev (Ht Wear at 1 M Cycle, µm)	Significance
Nanocure	671.20	244.70	676.43	A
Oven	658.99	244.70	653.09	A
Procure	616.25	244.70	489.65	A
Otoflash with N2	331.42	244.70	281.25	A
Otoflash without N2	258.60	218.87	236.29	A

*Levels not connected by the same letter are significantly different.

The one-way ANOVA analysis for height wear at 1M cycle in Rodin Denture Base 2.0 revealed no statistically significant differences among the five post-polymerization methods ($p = 0.5990$) as seen in Table 57. Figure 30 presents the one-way analysis of height wear (µm) at 1 million cycles for Rodin Denture Base 2.0 (RDB2) across different post-polymerization protocols. The highest variability in wear performance was observed in the Nanocure and Oven groups, with individual data points exceeding 1500 µm per million cycle wear, suggesting less predictable surface durability. In contrast, the Otoflash with and without nitrogen groups exhibited more consistent wear resistance, with lower mean values and tighter confidence intervals. Although the mean height wear varied across groups, with Nanocure at 671.20 µm per million cycle wear, oven at 658.99 µm per million cycle wear, and procure at 616.25 µm per million cycle wear showing higher wear values compared to Otoflash with N_2 at 331.43 µm per million cycle wear and Otoflash without N_2 at 258.60 µm per million cycle wear, the overlapping 95% confidence intervals and Tukey HSD results indicate these differences were not statistically significant as seen in Table 58.

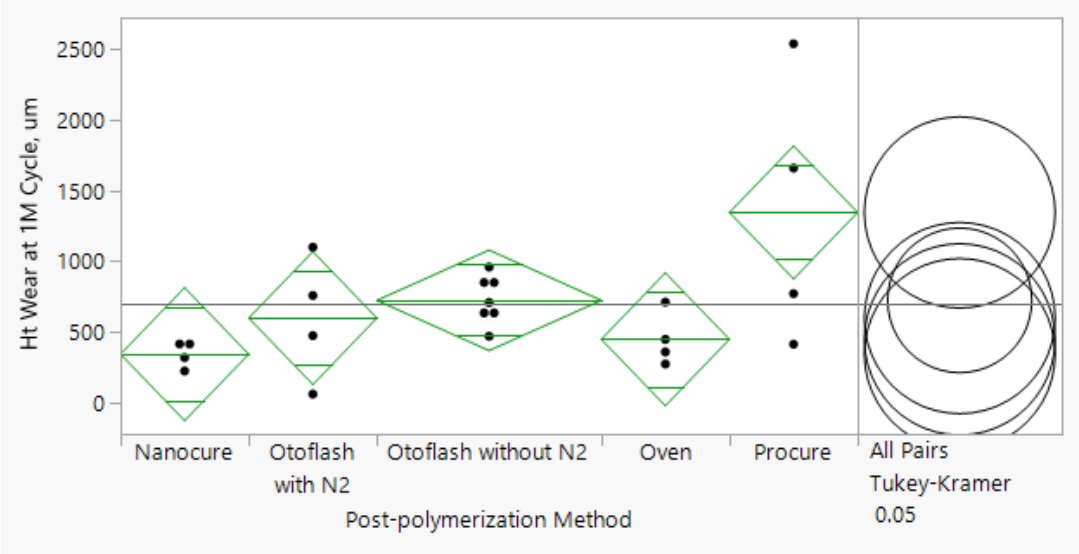

Figure 32. Oneway Analysis of Height Wear at 1 million Cycle by Polymerization Type for SHIDB.

Table 55. Analysis of Variance of Height Wear for SHIDB.

Source	DF	Sum of Squares	Mean Square	F Ratio	Prob > F
Post-polymerization Method	4	2481095.5	620274	3.0903	0.0422*
Error	18	3612905.8	200717		
C. Total	22	6094001.3			

Table 56. Connecting Letters Report on Height Wear for SHIDB.

Level	Mean (Ht Wear at 1 M Cycle, µm)	Std Error	Std Dev (Ht Wear at 1 M Cycle, µm)	Significance
Procure	1346.0	224.01	953.13	A
Otoflash without N2	723.5	169.33	169.05	A B
Otoflash with N2	598.0	224.01	440.7	A B
Oven	447.3	224.01	189.64	A B
Nanocure	342.5	224.01	92.31	B

*Levels not connected by same letter are significantly different.

The one-way ANOVA for height wear at 1M cycle in Sprintray Denture Base revealed a statistically significant difference among the five post-polymerization methods (p = 0.0422) as seen in Table 59. The highest wear was observed with the Procure method at

1346.0 μm, which was significantly greater than Nanocure at 342.5 μm per million cycle wear based on Tukey's HSD post hoc analysis ($p = 0.0375$) as seen in Table 60. Although the mean values for Otoflash without N_2 at 723.5 μm per million cycle wear, Otoflash with N_2 at 598.0 μm per million cycle wear, and Oven at 447.3 μm per million cycle wear were also elevated, the differences among these methods and others were not statistically significant due to overlapping confidence intervals as seen in Figure 31.

3.4 Degree of Conversion

The Degree of Conversion (DC) across the five tested resins demonstrated significant variation depending on both the material type and the post-polymerization method as shown in Table 61. Figure 32 illustrates that RDB2, an unfilled resin, had the lowest overall DC values, with Otoflash without N_2 yielding the lowest DC of 60.78% and Otoflash with N_2 achieving the highest at 68.82%, though all values were accompanied by high variability. RT displayed higher DCs, with values ranging from 88.61% Nanocure to 91.08% Procure, but also showed substantial standard deviations, indicating inconsistent polymerization. SC2 exhibited improved polymerization efficiency, with DCs ranging from 87.41% for Otoflash with N_2 to 93.54% for Oven, and relatively lower variability. SCC showed the most consistent and highest polymerization performance overall, with DCs ranging from 93.87% for Nanocure to a maximum of 98.95% using Otoflash with N_2, and the lowest coefficient of variation, indicating excellent polymerization. SHIDB had DC values between 82.47% for Otoflash without N_2 and 90.66% for Nanocure, with slightly more variability as seen in Figure 32.

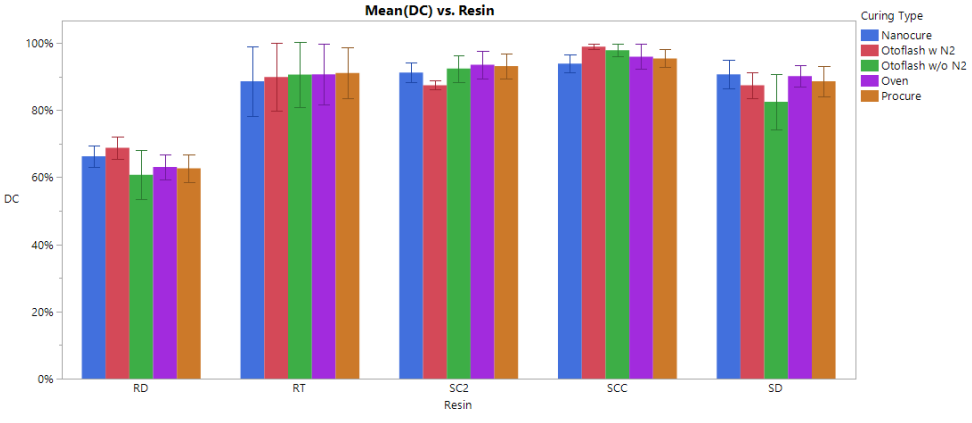

Figure 33. Bar chart of Degree of Conversion for tested materials.

Table 57. Summary of Degree of Conversion.

		DC			
Resin	**Polymerization Type**	**N**	**Mean %**	**Std Dev**	**CV**
RDB2	Nanocure	10	66.25%	3.08%	4.65 %
	Otoflash w N2	10	68.82%	3.33%	4.84 %
	Otoflash w/o N2	10	60.78%	7.29%	12.00 %
	Oven	10	63.09%	3.74%	5.92 %
	Procure	10	62.69%	4.06%	6.48 %
RT	Nanocure	10	88.61%	10.33%	11.66 %
	Otoflash w N2	10	89.90%	10.03%	11.15 %
	Otoflash w/o N2	9	90.64%	9.69%	10.69 %
	Oven	10	90.71%	9.09%	10.02 %
	Procure	10	91.08%	7.61%	8.35 %
SC2	Nanocure	10	91.23%	2.84%	3.11 %
	Otoflash w N2	10	87.41%	1.31%	1.49 %
	Otoflash w/o N2	10	92.38%	4.05%	4.38 %
	Oven	10	93.54%	4.11%	4.39 %
	Procure	10	93.13%	3.74%	4.02 %
SCC	Nanocure	10	93.87%	2.73%	2.91 %
	Otoflash w N2	10	98.95%	0.84%	0.85 %
	Otoflash w/o N2	9	97.88%	1.78%	1.82 %
	Oven	10	95.96%	3.73%	3.88 %
	Procure	10	95.40%	2.64%	2.76 %
SHIDB	Nanocure	10	90.66%	4.24%	4.68 %
	Otoflash w N2	10	87.40%	3.91%	4.47 %
	Otoflash w/o N2	10	82.47%	8.23%	9.98 %
	Oven	10	90.14%	3.16%	3.51 %
	Procure	10	88.59%	4.50%	5.08 %

The Least Squares Means (LSMeans) analysis for Degree of Conversion (DC) across the five resins shows statistically significant differences in polymerization performance ($p < 0.0001$) as seen in Table 62. SCC demonstrated the highest mean DC of 99%, significantly outperforming all other resins as seen in Figure 33. SC2 followed with a mean DC of 91.54%, and RT came next at 90.19%. SHIDB had a slightly lower mean DC of 87.85%, and RDB2 showed the lowest mean DC overall at 64.33%, a statistically significant outlier in performance. As shown in Table 63, the main effect of resin type on the degree of conversion (DC) was highly significant ($p < 0.0001$), indicating substantial differences in polymerization efficiency between materials. The interaction between resin

and polymerization type was also statistically significant ($p = 0.0026$), suggesting that the effectiveness of polymerization protocols varied depending on the resin formulation. However, the effect of polymerization type alone was not significant ($p = 0.5016$), as reflected in the Tukey HSD comparison as shown in Table 64, where all post-polymerization methods yielded statistically similar mean DC values ranging narrowly from 85% to 87%.

Table 58. Analysis of Variance of Degree of Conversion.

Source	DF	Sum of Squares	Mean Square	F Ratio
Model	24	3.26	0.14	44.56
Error	223	0.68	0.003	**Prob > F**
C. Total	247	3.94		<.0001*

Table 59. Effect Tests of Degree of Conversion.

Source	Nparm	DF	Sum of Squares	F Ratio	Prob > F
Resin	4	4	3.14	257.06	<.0001*
Polymerization Type	4	4	0.01	0.84	0.5016
Resin*Polymerization Type	16	16	0.12	2.39	0.0026*

Table 60. LSMeans Differences Tukey HSD Polymerization Type of Degree of Conversion.

Level	Least Sq Mean (%)	Std Error	Mean (%)	Std Dev (%)	Significance
Oven	0.87	0.01	86.68	0.31	A
Otoflash w N2	0.86	0.01	86.5	0.11	A
Procure	0.86	0.01	86.18	0.13	A
Nanocure	0.86	0.01	86.12	0.11	A
Otoflash w/o N2	0.85	0.01	84.44	0.15	A

*Levels not connected by same letter are significantly different.
α=0.050 Q=2.75023

Table 61. LSMeans Differences Tukey HSD Material*Polymerization type of Degree of Conversion.

Level	Least Sq Mean	Std Error	Significance
SCC, Otoflash w N2	0.99	0.02	A
SCC, Otoflash w/o N2	0.98	0.02	A B
SCC, Oven	0.96	0.02	A B C
SCC, Procure	0.95	0.02	A B C
SCC, Nanocure	0.94	0.02	A B C
SC2, Oven	0.94	0.02	A B C
SC2, Procure	0.93	0.02	A B C
SC2, Otoflash w/o N2	0.92	0.02	A B C
SC2, Nanocure	0.91	0.02	A B C D
RT, Procure	0.91	0.02	A B C D
RT, Oven	0.91	0.02	A B C D
SHIDB, Nanocure	0.91	0.02	A B C D
RT, Otoflash w/o N2	0.91	0.02	A B C D
SHIDB, Oven	0.90	0.02	A B C D
RT, Otoflash w N2	0.90	0.02	A B C D
RT, Nanocure	0.89	0.02	B C D
SHIDB, Procure	0.89	0.02	B C D
SC2, Otoflash w N2	0.87	0.02	C D
SHIDB, Otoflash w N2	0.87	0.02	C D
SHIDB, Otoflash w/o N2	0.82	0.02	D
RDB2, Otoflash w N2	0.69	0.02	E
RDB2, Nanocure	0.66	0.02	E
RDB2, Oven	0.63	0.02	E
RDB2, Procure	0.63	0.02	E
RDB2, Otoflash w/o N2	0.61	0.02	E

*Levels not connected by the same letter are significantly different.

α=0.050 Q=3.70504

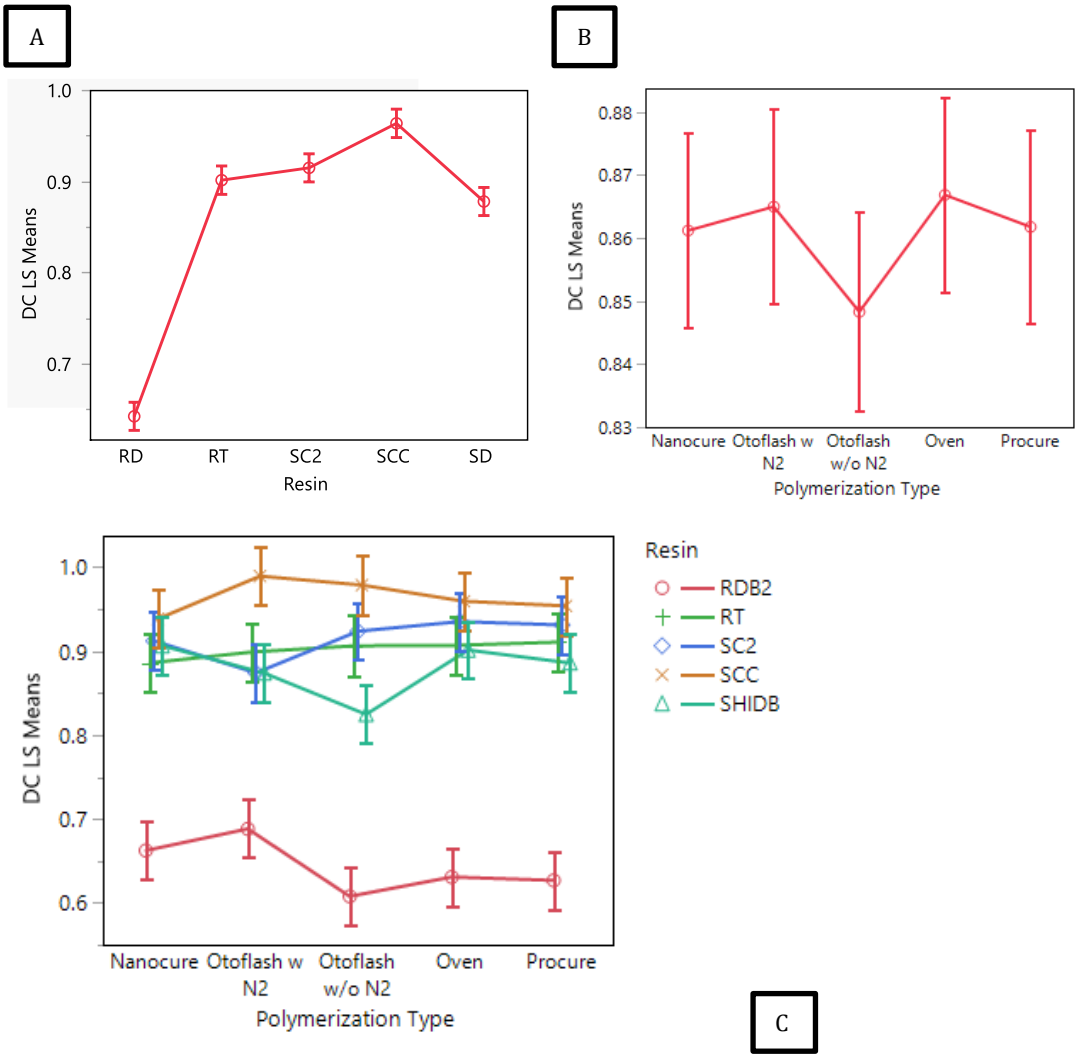

Figure 34. Least Squares means Plot of Degree of Conversion by Resin (A), Polymerization Type (B), Resin*Polymerization Type (C).

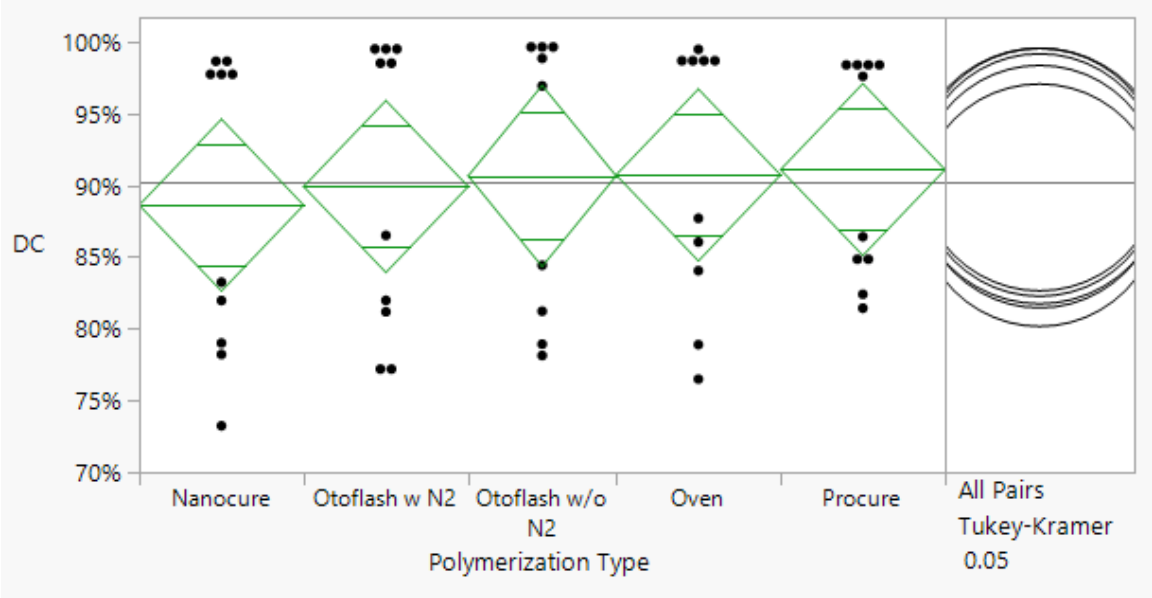

Figure 35. Oneway Analysis of Degree of Conversion by Polymerization Type for RT.

Table 62. Analysis of Variance of Degree of Conversion for RT.

Source	DF	Sum of Squares	Mean Square	F Ratio	Prob > F
Polymerization Type	4	0.003	0.0009	0.11	0.98
Error	44	0.39	0.008		
C. Total	48	0.39			

Table 63. Connecting Letters Report on Degree of Conversion for RT.

Level	Mean (%)	Std Dev (%)	Std Error	Significance
Procure	0.91	0.08	0.03	A
Oven	0.91	0.09	0.03	A
Otoflash w/o N2	0.91	0.1	0.03	A
Otoflash w N2	0.90	0.1	0.03	A
Nanocure	0.89	0.1	0.03	A

*Levels not connected by same letter are significantly different.

For RT, the one-way ANOVA comparing the effect of different post-polymerization methods on DC showed no statistically significant difference among the five

polymerization protocols (p = 0.9789) as seen in Table 67. Figure 34 presents the one-way analysis of the DC across different polymerization methods for RT. The results demonstrate relatively consistent mean DC values among all post-polymerization protocols, with the majority of samples clustering around 90%. Table 68 presents that the mean DC values ranged narrowly from 88.61% for Nanocure which is the lowest to 91.08% for Procure which is the highest, with all standard errors approximately 0.0297–0.0313. Despite minor numerical differences, Tukey's HSD test confirmed that all groups belonged to the same statistical subset, indicating that polymerization method had no meaningful impact on the polymerization efficacy of RT.

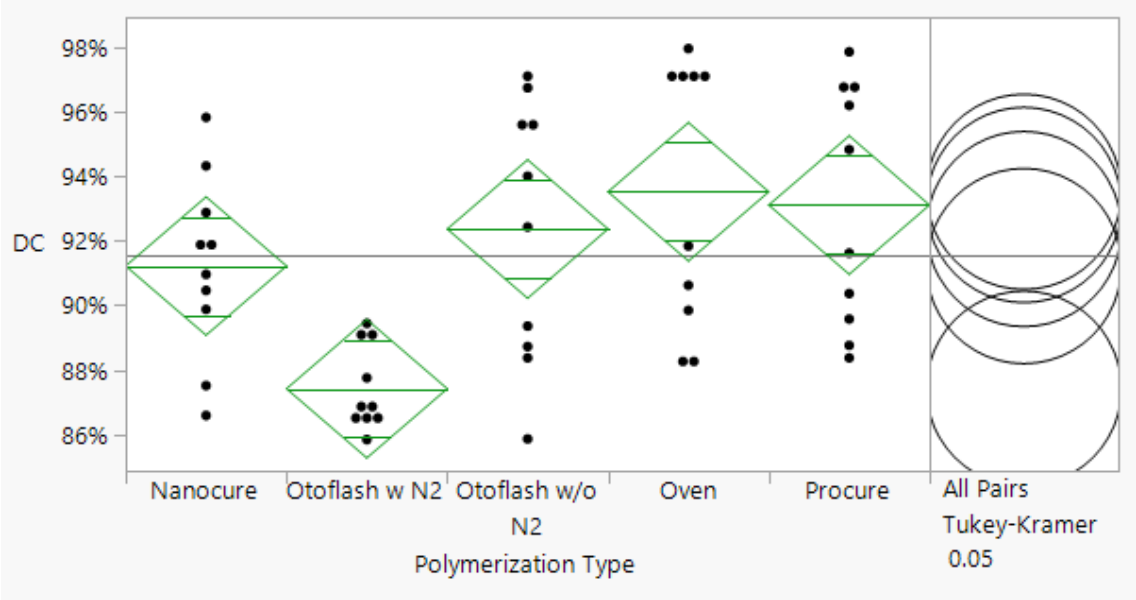

Figure 36. Oneway Analysis of Degree of Conversion by Polymerization Type for SC2

Table 64. Analysis of Variance of Degree of Conversion for SC2.

Source	DF	Sum of Squares	Mean Square	F Ratio	Prob > F
Polymerization Type	4	0.02	0.01	5.33	0.0013*
Error	45	0.05	0.001		

Source	DF	Sum of Squares	Mean Square	F Ratio	Prob > F
C. Total	49	0.08			

Table 65. Connecting Letters Report on Degree of Conversion for SC2.

Level	Mean (%)	Std Dev (%)	Std Error	Significance
Oven	0.94	0.04	0.01	A
Procure	0.93	0.04	0.01	A
Otoflash w/o N2	0.92	0.04	0.01	A
Nanocure	0.91	0.03	0.01	A B
Otoflash w N2	0.87	0.01	0.01	B

*Levels not connected by the same letter are significantly different.

For SC2, the one-way ANOVA revealed a statistically significant effect of post-polymerization method on the DC ($p = 0.0013$) as seen in Table 69. Figure 35 displays the degree of conversion (DC) values for the SC2 resin under different post-polymerization protocols. The spread in data points for each group highlights varying degrees of intra-group variability, particularly for the Otoflash with nitrogen condition. Table 70 presents that the highest mean DC was observed with the Oven method at 93.54%, followed closely by Procure at 93.13% and Otoflash without N2 at 92.38%, while the lowest mean DC was seen with Otoflash with N2 at 87.41%. Tukey's HSD test confirmed that Otoflash with N2 had a significantly lower DC compared to Oven ($p = 0.0018$), Procure ($p = 0.0040$), and Otoflash without N2 ($p = 0.0161$). Although Nanocure showed an intermediate DC value of 91.23%, it was not statistically different from the other groups.

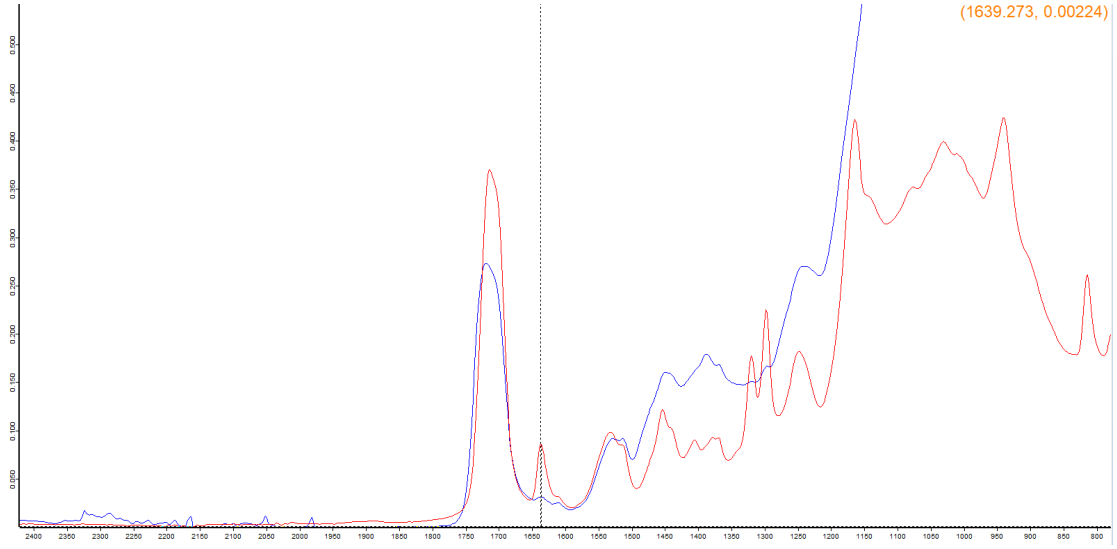

Figure 37. FTIR spectra for Rodin Sculpture 2.0 Uncured (red) vs Otoflash with N2 (blue).

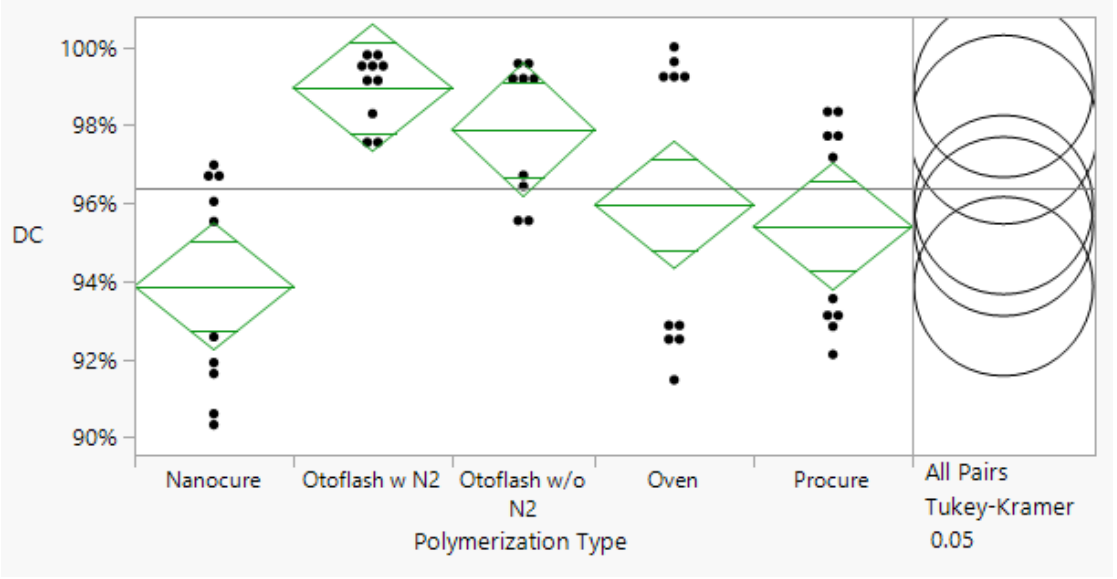

Figure 38. Oneway Analysis of Degree of Conversion by Polymerization Type for SCC.

Table 66. Analysis of Variance of Degree of Conversion for SCC.

Source	DF	Sum of Squares	Mean Square	F Ratio	Prob > F
Polymerization Type	4	0.02	0.004	6.19	0.0005*
Error	44	0.03	0.0006		

Source	DF	Sum of Squares	Mean Square	F Ratio	Prob > F
C. Total	48	0.04			

Table 67. Connecting Letters Report on Degree of Conversion for SCC.

Level	Mean (%)	Std Dev (%)	Std Error	Significance
Otoflash w N2	0.99	0.01	0.01	A
Otoflash w/o N2	0.98	0.02	0.01	A B
Oven	0.96	0.04	0.01	A B C
Procure	0.95	0.03	0.01	B C
Nanocure	0.94	0.03	0.01	C

*Levels not connected by the same letter are significantly different.

For SCC, the one-way ANOVA showed a statistically significant effect of post-polymerization method on the DC ($p = 0.0005$) as seen in Table 71. The highest mean DC was obtained with Otoflash with N2 at 98.95%, while the lowest was observed with Nanocure at 93.87% as seen in Table 72. Tukey's HSD analysis confirmed that Otoflash with N2 resulted in significantly higher DC than Nanocure ($p = 0.0005$), and also significantly higher than Procure ($p = 0.0255$). Similarly, Otoflash without N2 at 97.88% showed significantly better DC than Nanocure ($p = 0.0111$).

Figure 36 illustrates the one-way analysis of the degree of conversion (DC) by polymerization type for SCC. Although minor variations were observed across polymerization methods, all groups demonstrated consistently high conversion rates, generally exceeding 95%. Otoflash with nitrogen yielded the highest DC values with minimal variability, while Nanocure exhibited the lowest mean and greater dispersion. However, no significant differences were found among Otoflash with N2, Otoflash without N2, Oven at 95.96%, and Procure at 95.40%.

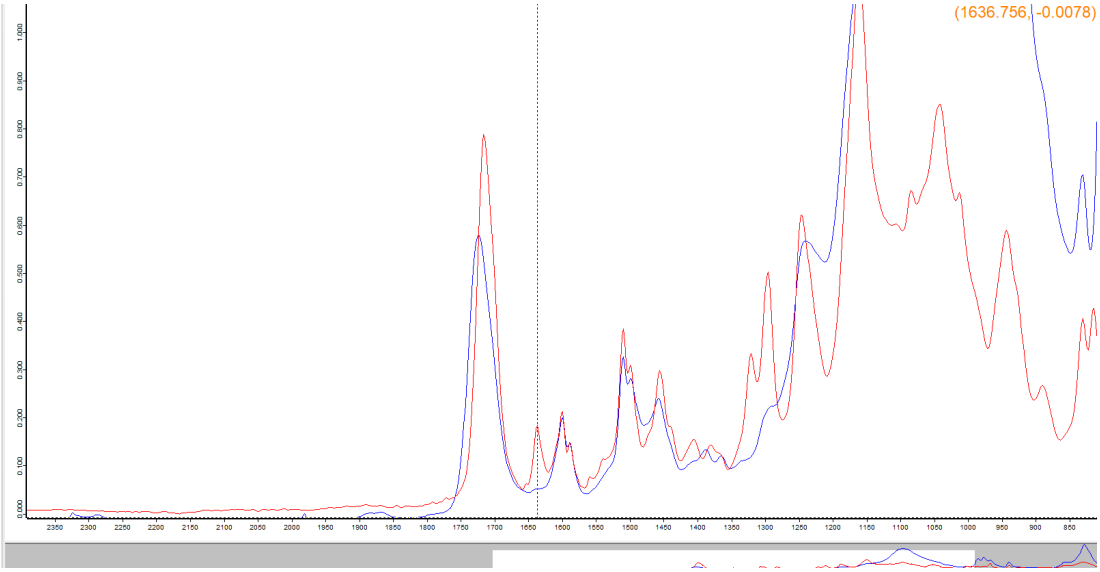

Figure 39. Sprintray Ceramic Crown Uncured (red) vs Otoflash with N2 (blue).

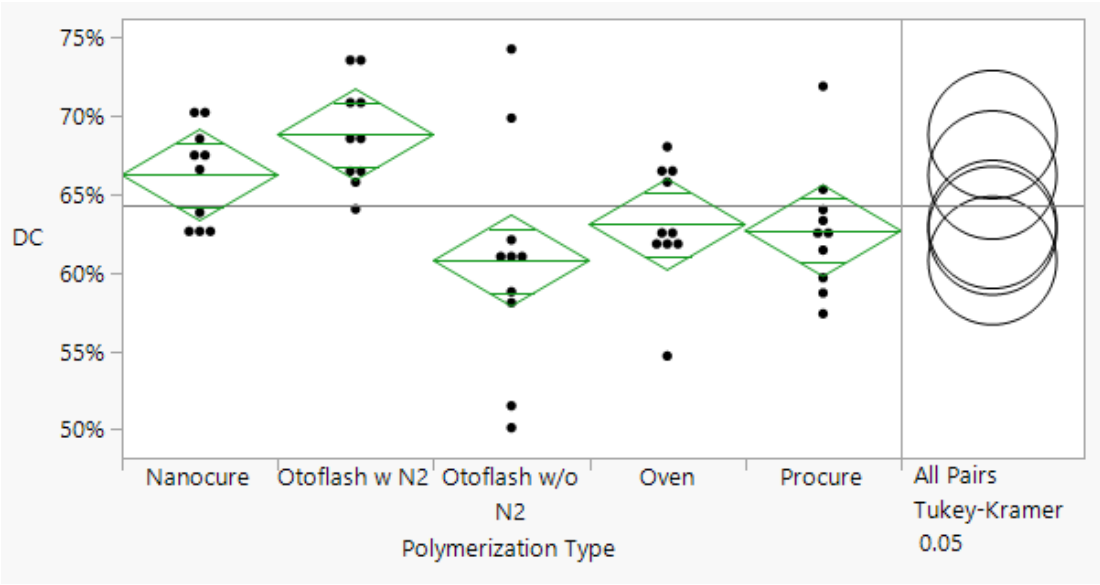

Figure 40. Oneway Analysis of Degree of Conversion by Polymerization Type for RDB2.

Table 68. Analysis of Variance of Degree of Conversion for RDB2.

Source	DF	Sum of Squares	Mean Square	F Ratio	Prob > F
Polymerization Type	4	0.04	0.01	4.88	0.0023*
Error	45	0.09	0.002		

Source	DF	Sum of Squares	Mean Square	F Ratio	Prob > F
C. Total	49	0.13			

Table 69. Connecting Letters Report on Degree of Conversion for RDB2.

Level	Mean (%)	Std Dev (%)	Std Error	Significance
Otoflash w N2	0.69	0.03	0.01	A
Nanocure	0.66	0.03	0.01	A B
Oven	0.63	0.04	0.01	A B
Procure	0.63	0.04	0.01	B
Otoflash w/o N2	0.61	0.07	0.01	B

*Levels not connected by the same letter are significantly different.

For Rodin RDB2, Table 73 presents the one-way ANOVA revealed a significant effect of polymerization method on the DC ($p = 0.0023$). The highest mean DC was achieved with Otoflash with N2 at 68.82%, followed by Nanocure at 66.25%, while the lowest was observed with Otoflash without N2 at 60.78% as seen in Table 74. Figure 37 illustrates the degree of conversion (DC) of the unfilled resin RDB2 across different post-polymerization protocols. Among all methods, Otoflash with nitrogen exhibited the highest mean DC, followed closely by Nanocure, while Otoflash without nitrogen showed the lowest mean values, indicating a potential negative impact of oxygen exposure during polymerization. Tukey's HSD test showed that Otoflash with N2 significantly outperformed Otoflash without N2 ($p = 0.0025$) and Procure ($p = 0.0334$). Although Otoflash with N2 also showed higher DC compared to Oven ($p = 0.0540$), this was only marginally significant.

Figure 41. Oneway Analysis of Degree of Conversion by Polymerization Type for SHIDB.

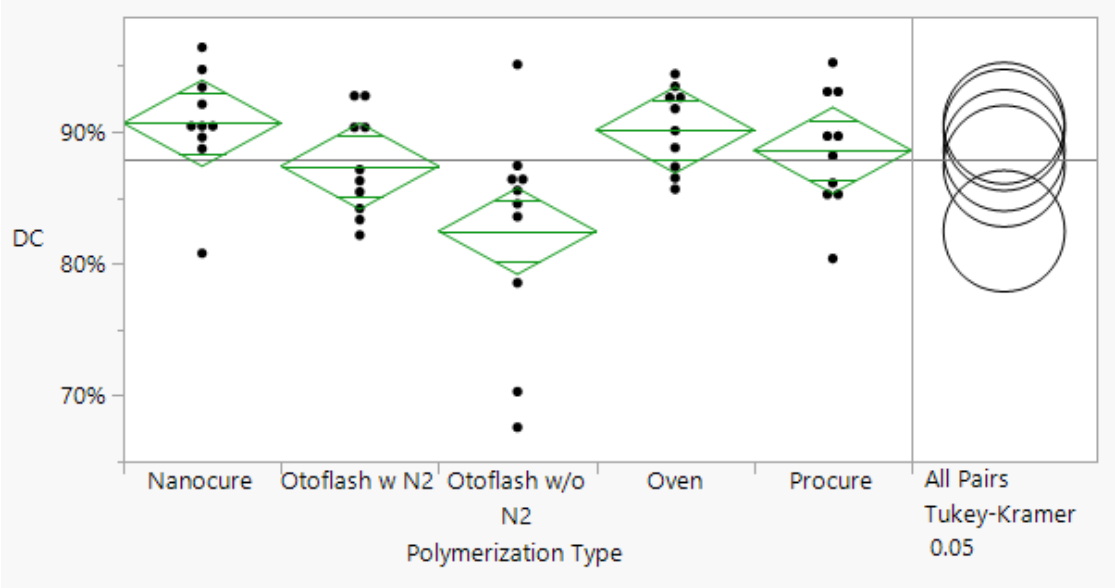

Table 70. Analysis of Variance on Degree of Conversion for SHIDB.

Source	DF	Sum of Squares	Mean Square	F Ratio	Prob > F
Polymerization Type	4	0.04	0.01	4.08	0.0066*
Error	45	0.12	0.002		
C. Total	49	0.16			

Table 71. Connecting Letters Report.

Level	Mean (%)	Std Dev (%)	Std Error	Significance
Nanocure	0.91	0.04	0.02	A
Oven	0.90	0.03	0.02	A
Procure	0.89	0.05	0.02	A B
Otoflash w N2	0.87	0.04	0.02	A B
Otoflash w/o N2	0.82	0.08	0.02	B

*Levels not connected by same letter are significantly different.

For SHIDB, Table 75 presents the one-way ANOVA that showed a statistically significant effect of polymerization method on DC with $p = 0.0066$. Among the groups,

Nanocure yielded the highest mean DC at 90.66%, followed closely by Oven at 90.14%, whereas Otoflash without N2 had the lowest DC at 82.47% as seen in Table76. Tukey's HSD post-hoc comparisons revealed that Nanocure and Oven had significantly higher DC than Otoflash without N2, with p-values of 0.0072 and 0.0136, respectively. No other pairwise differences were statistically significant.

3.5 Microstructure analysis (SEM)

To evaluate the surface and internal morphological characteristics of 3D-printed dental resins, selected specimens were subjected to scanning electron microscopy (SEM). The materials examined included Rodin Titan with Nitrogen (RTN2 #1 and #2) and Sprintray High Impact Denture Base polymerized with Nanocure (SDNC #2 and #4). RTN2 #1 and SDNC #4 demonstrated high mechanical performance based on testing, while RTN2 #2 and SDNC #2 demonstrated lower mechanical properties. SEM imaging was conducted to investigate whether microstructural differences could explain the observed performance outcomes. Both surface and cross-sectional areas were analyzed under magnifications ranging from ×100 to ×5000, allowing for detailed observation of filler morphology, distribution, surface topography, and signs of interfacial defects such as cracks, voids, or delamination. This qualitative assessment aimed to correlate morphological integrity with mechanical behavior and to identify microstructural indicators of successful or deficient post-polymerization.

Table 72. SEM Report Table.

Sample ID	Surface Description	SEM Inspection Result	Explanation
RTN2 #2	Polished bars from 3-point bend test have irregular surface with non-uniformly strewn filler particles. Both the surface and cross section were observed. Multiple voids, pits, and surface defects observed as seen in Figure 40. Particle agglomeration and partial delamination present. Cross-sectional images reveal poor interfacial integrity.	SEM at 2000× and 5000× shows poorly integrated, angular filler particles with inconsistent distribution. Lower magnifications reveal dark voids, coarse pits, and filler pull-outs. Cross-sections show weak filler-matrix bonding and internal discontinuities.	The strewn particle morphology appears loose and disorganized, suggesting inadequate polymerization and poor dispersion. These surface and internal defects compromise the structural integrity and explain the specimen's lower mechanical performance and higher wear.

Sample ID	Surface Description	SEM Inspection Result	Explanation
RTN2 #1	Polished bars from 3-point bend test have smooth, homogenous surface with tightly bound uniformly strewn filler particles. Both the surface and cross section were observed. Minimal surface irregularities or porosities observed across scales from 20 μm to 500 μm as seen in Figure 39. No significant voids or cracks noted.	Filler particles are well embedded in the matrix with consistent dispersion. High magnification (2000×) shows compact, angular fillers with no delamination. Lower magnifications (100×–1000×) confirm dense topography and structural continuity.	The strewn filler particles appear fully integrated into the polymerized resin matrix. This suggests effective light penetration and polymerization through the depth of the material. The smooth and dense appearance supports superior mechanical strength and wear resistance, explaining its high performance.
SDNC #2	Polished surface and cross section of bars from 3-point bend test were observed. At low magnifications, the surface appears macroscopically smooth. However, higher-resolution SEM shows a speckled, porous appearance with many spherical or globular filler particles as seen in Figure 41. There is no tight integration into the matrix, and some areas show exposed filler aggregates and particulate detachment. Figure 42 displayed cross-sectional images revealing poor interfacial integrity. Multiple cracks propagate through the matrix, and delamination is noted at the filler-matrix interface.	SEM at 2000× and 5000× shows poorly integrated, angular filler particles with inconsistent distribution. Lower magnifications reveal dark voids, coarse pits, and filler pull-outs. Cross-sections show weak filler-matrix bonding and internal discontinuities.	The strewn particle morphology appears loose and disorganized, suggesting inadequate polymerization and poor dispersion. These surface and internal defects compromise the structural integrity and explain the specimen's lower mechanical performance and higher wear.
SDNC #4	Polished surface and cross section of bars from 3-point bend test were observed. At low magnification, the surface appears clean and macroscopically smooth. Figure 43 displayed higher-	At ×5000 to ×1000, the surface shows tightly packed, uniformly sized spherical fillers embedded well in the matrix with no signs of dislodgement or microcracks.	The highly uniform and bonded filler distribution indicates efficient polymerization and optimal post-polymerization using the Nanocure system. The

Sample ID	Surface Description	SEM Inspection Result	Explanation
	resolution SEM revealing a finely textured surface densely populated with evenly distributed spherical fillers. There is a consistent, integrated appearance of fillers within the resin matrix, with no signs of delamination, detachment, or major voids.	At ×500 to ×100, cross-sections reveal a smooth fracture surface with minimal porosity and strong continuity between matrix and fillers. No major cracks, voids, or filler pull-outs observed across multiple fields.	intact filler-matrix interface and lack of surface or internal defects correlate with higher mechanical strength and wear resistance. The SEM morphology supports the strong performance observed in hardness and flexural strength testing.

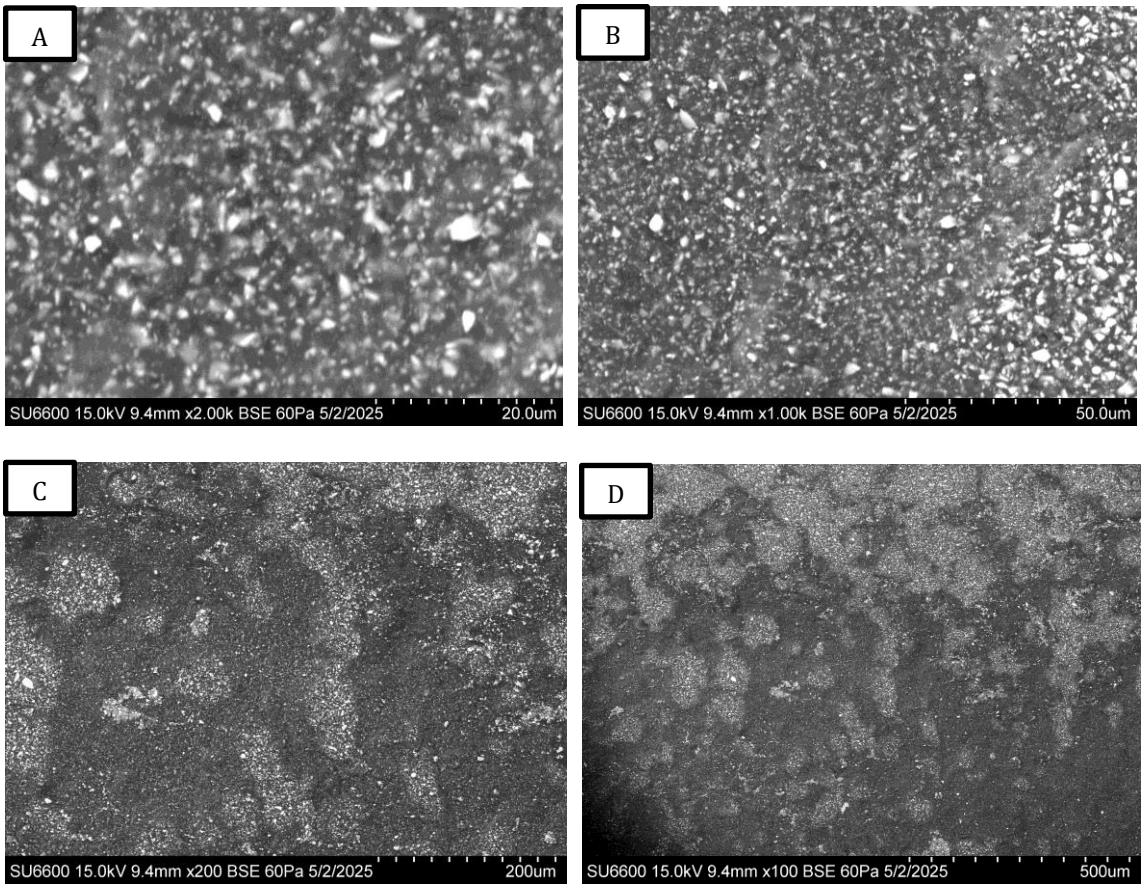

Figure 42. SEM image of RT polymerized with Otoflash with N2 Specimen #1 at varying magnifications A, B C and D.

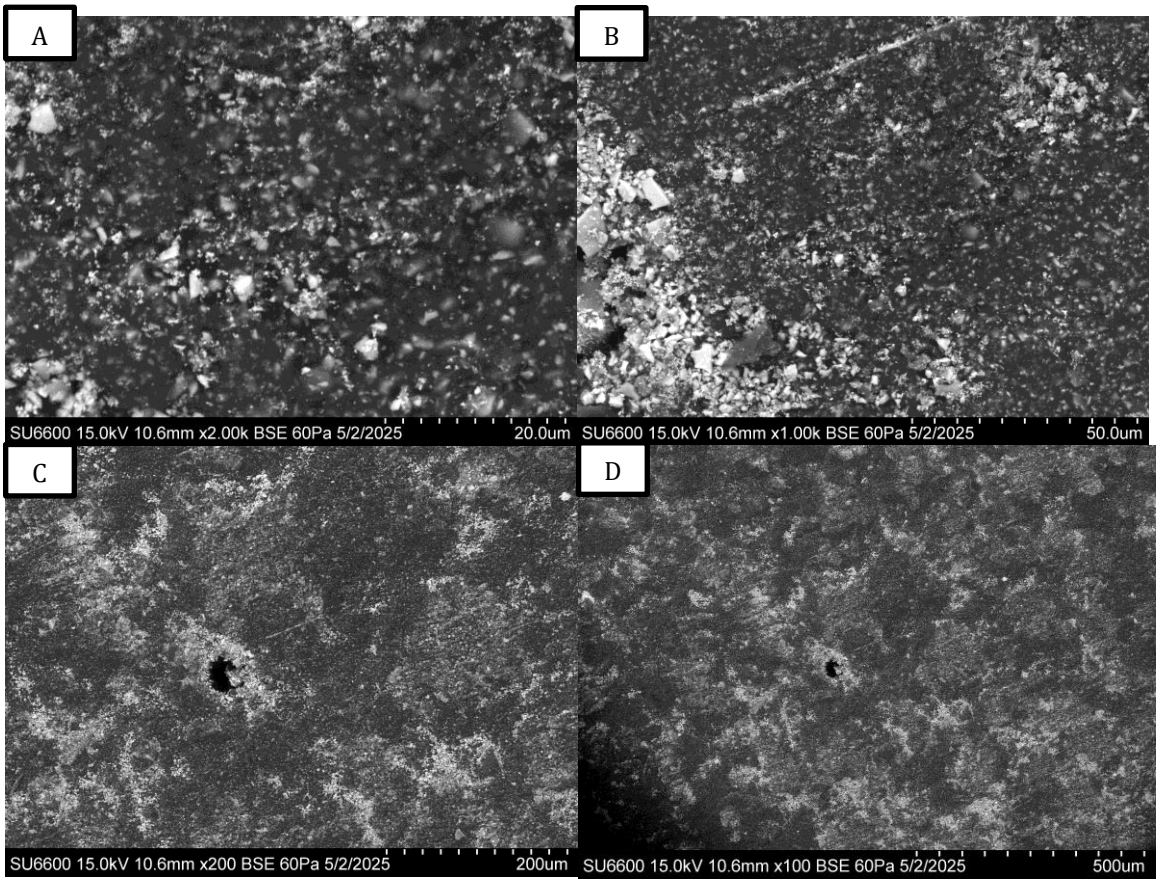

Figure 43. SEM image of RT polymerized with Otoflash with N2 Specimen #2 at varying magnifications A, B C and D.

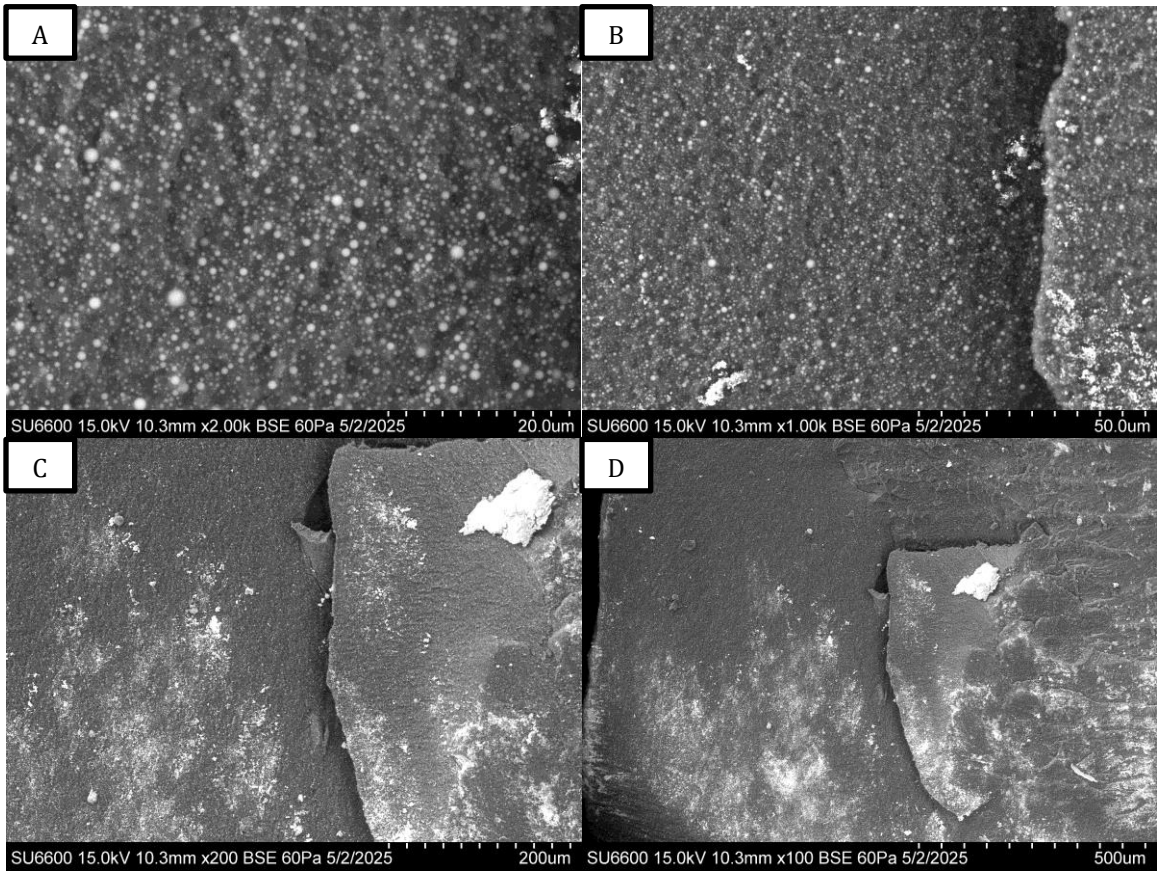

Figure 44. SEM image of SHIDB polymerized with Nanocure Specimen #2 Polished Surface at varying magnifications A, B C and D.

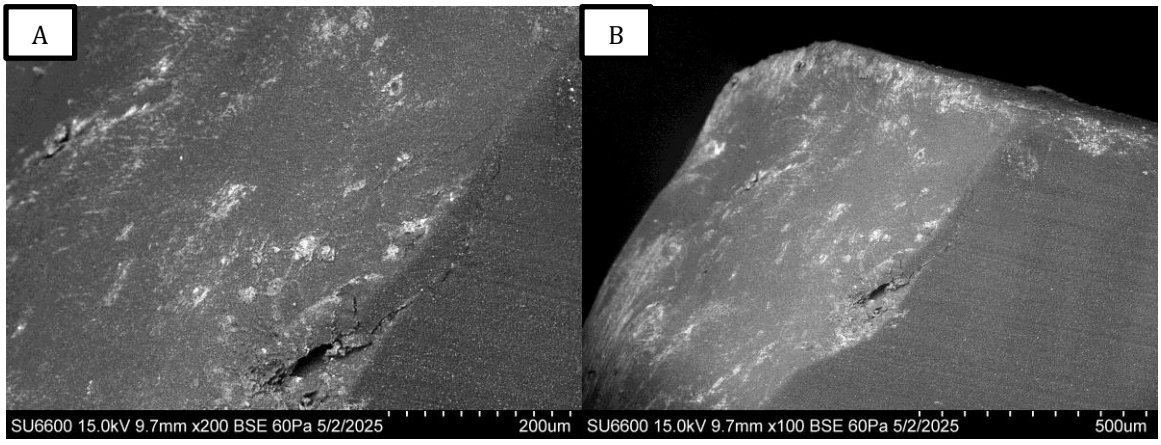

Figure 45. SEM image of SHIDB polymerized with Nanocure Specimen #2 Cross-Section at varying magnifications A and B.

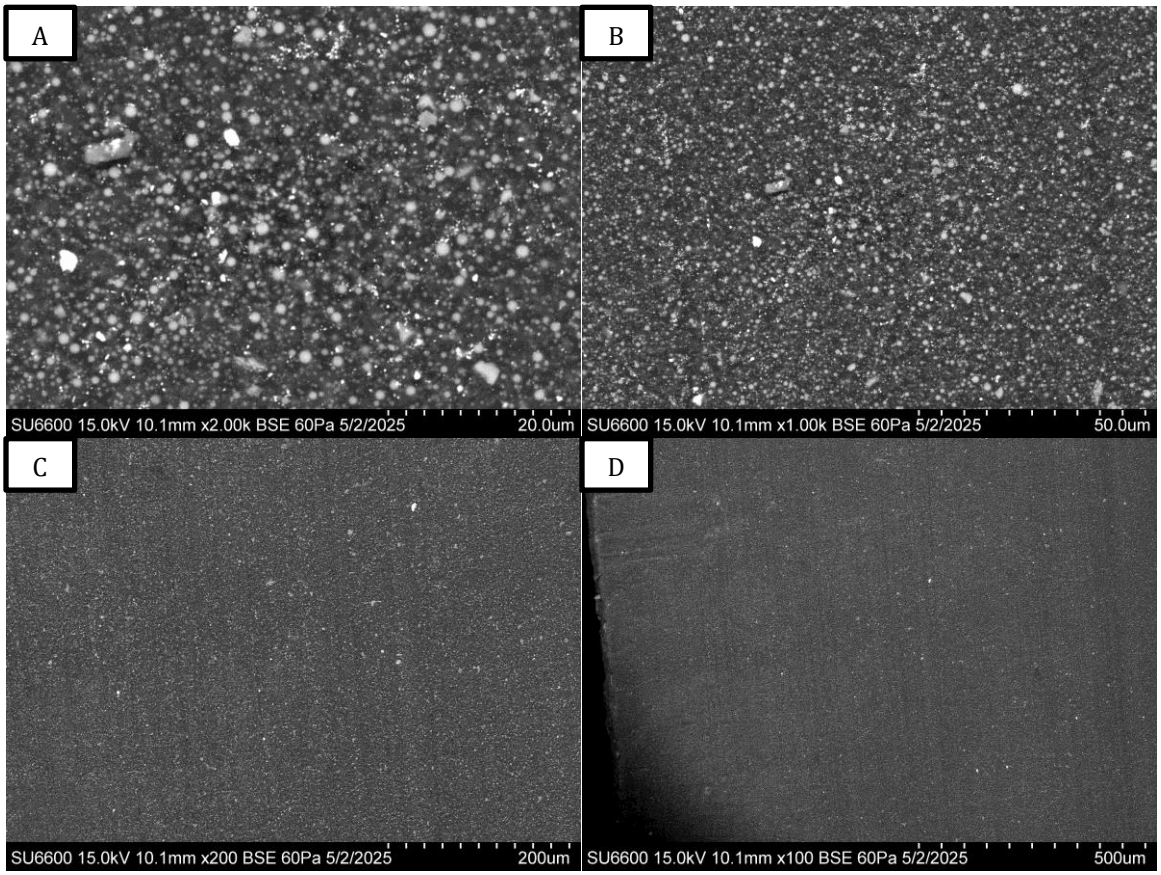

Figure 46. SEM image of SHIDB polymerized with Nanocure Specimen #4 at varying magnifications A, B C and D.

3.6 Microstructure Analysis (EDS)

To elucidate the relationship between elemental composition and mechanical performance of 3D-printed dental resins, SEM coupled with Energy-Dispersive X-ray Spectroscopy (EDS) was conducted on selected specimens. The analyzed materials included Sprintray High Impact Denture Base polymerized with Nanocure (SDNC #2 and #4) and Rodin Titan with nitrogen post-polymerization (RTN2 #1 and #2). For each material, both surface and cross-sectional analyses were performed, with particular focus on comparing high- and low-performing specimens as determined by prior mechanical testing. RTN2 #1 and SDNC #4 demonstrated high mechanical performance, while RTN2 #2 and SDNC #2 demonstrated lower mechanical properties.

The most consistently detected element across all specimens was oxygen, indicating the presence of oxide-based filler systems. Silicon was a dominant component in both SDNC and RTN2 specimens, indicative of silica-based fillers.

Figures 41–52 illustrate the elemental composition of the specimens as determined by Energy-Dispersive X-ray Spectroscopy (EDS).

Table 73 shows the mean elements weight % of SDNC and RTN2 Specimens by EDS.

Table 73. Summary of mean content weight% of SDNC and RTN2 Specimens by EDS.

		Element Mean wt %								
Spectrum Label	Sample ID	O	Al	Si	K	Ti	Br	Zr	Ba	Total
Spectrum 4	SDNC #2 Site 3	53.2	0.9	45.9						100
Spectrum 7	SDNC #2 Site 2	51.3	0.9	42.8				4.94		100
Spectrum 8	SDNC #2 Site 2	50.9	1.1	41.9				6.06		100

Spectrum 9	SDNC #2 Cross Section	51.7	1.5	43.1				3.78		100
Spectrum 10	SDNC #2 Cross Section	52.1		44.8				3.09		100
Spectrum 15	SDNC #4 Cross section	50.1	0.7	40.6		0.7		7.84		100
Spectrum 16	SDNC #4 Cross section	52.5		45.8	1.7					100
Spectrum 17	SDNC #4 Surface	52.1		45.7			2.2			100
Spectrum 18	SDNC #4 Surface	53.3		46.7						100
Spectrum 11	RTN2 #1 Surface	40.4	6.6	27.8					25.2	100
Spectrum 12	RTN2 #1 Surface	40.6	6	28.4					25	100
Spectrum 13	RTN2 #2 Cross section	38	4.8	25.1				5.95	26.1	100
Spectrum 14	RTN2 #2 Cross section	37.3	4.7	24.3				6.4	27.3	100
Spectrum 19	RTN2 #2 Surface	36.6	4	22.5				13.4	23.5	100
Spectrum 20	RTN2 #2 Surface	37.1	4.2	23.7				9.88	25.2	100

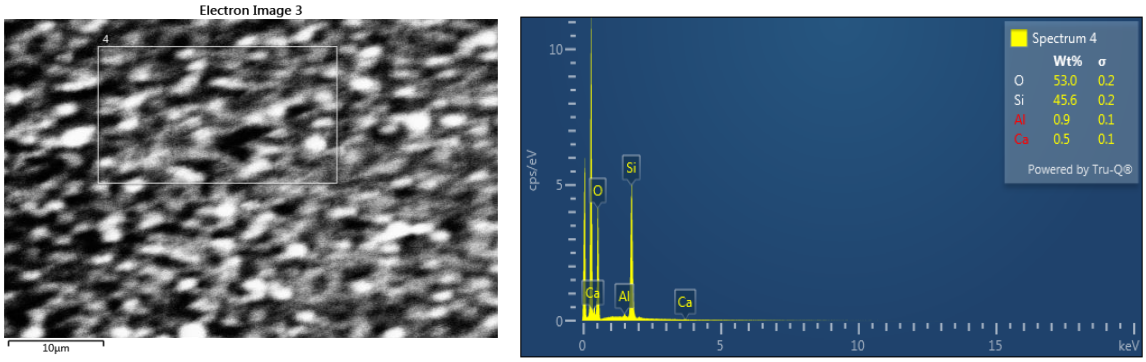

Figure 47. Chemical composition of SDNC #2 site 3

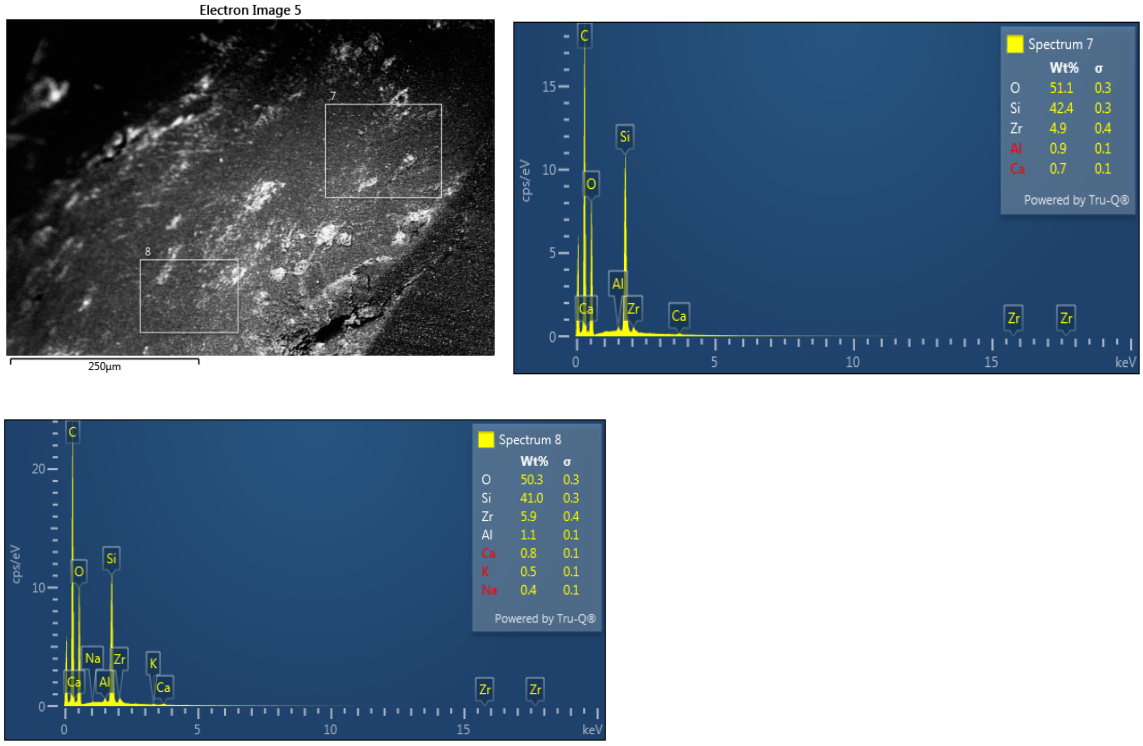

Figure 48. Chemical composition of SDNC #2 Site 2

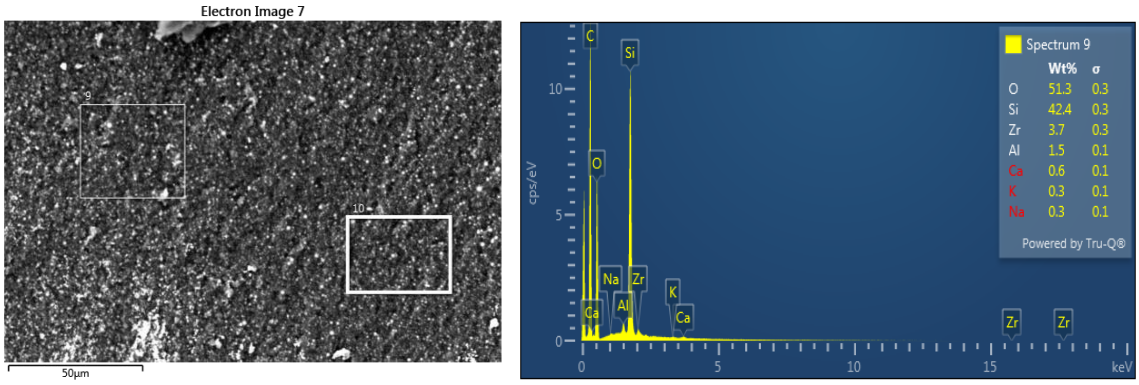

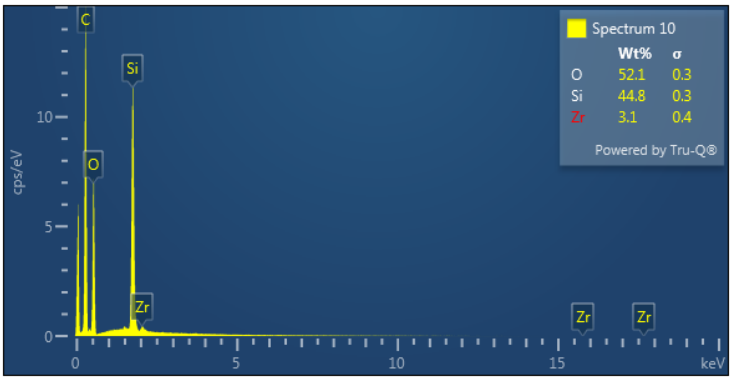

Figure 49. Chemical composition of SDNC #2 Cross Section.

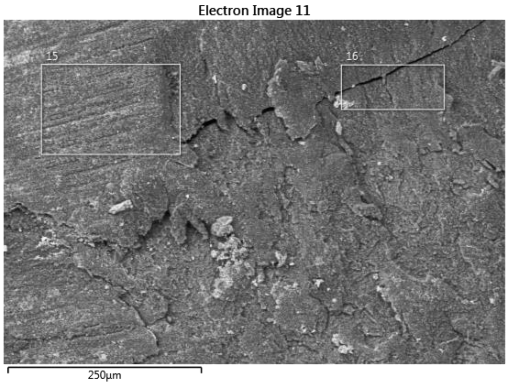

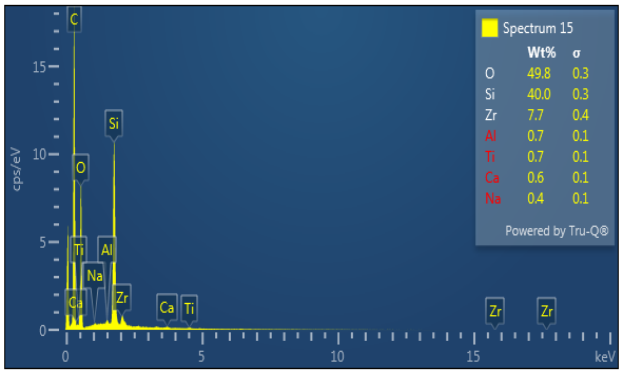

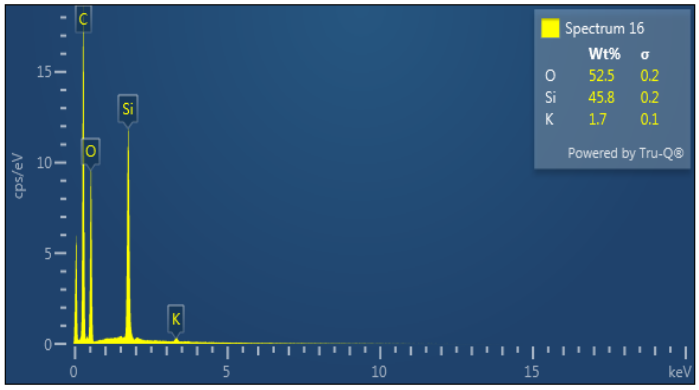

Figure 50. Chemical composition of SDNC #4 Cross Section.

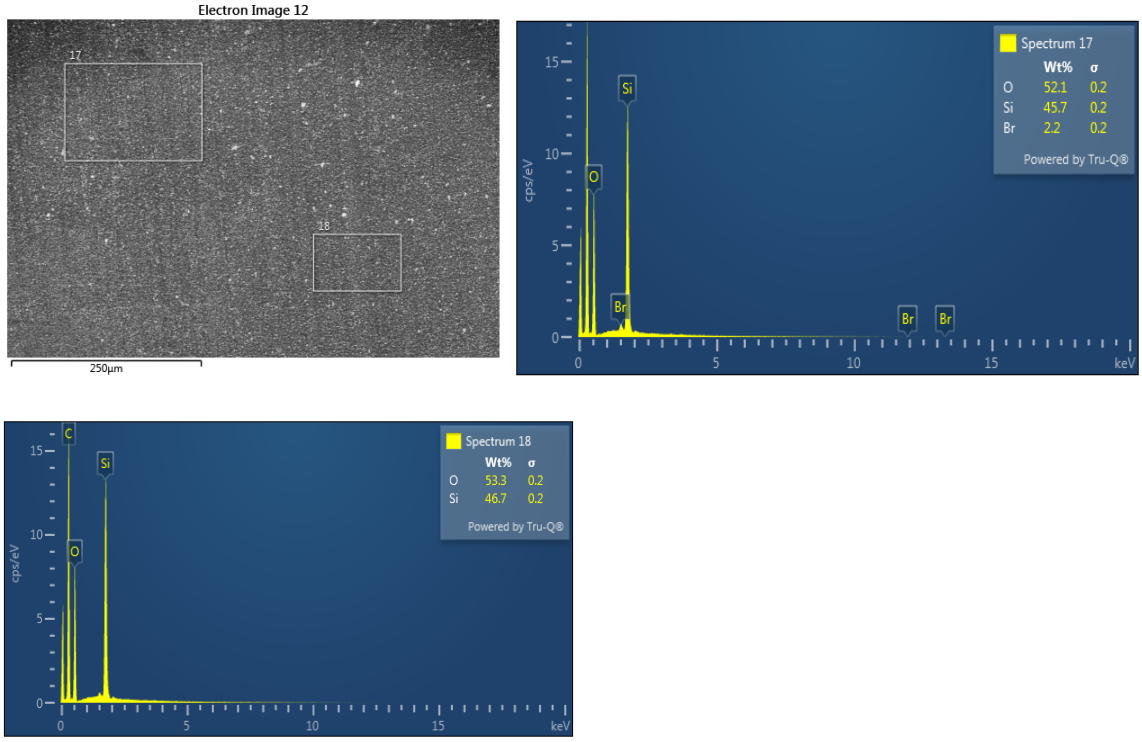

Figure 51. Chemical Composition of SDNC #4 Surface

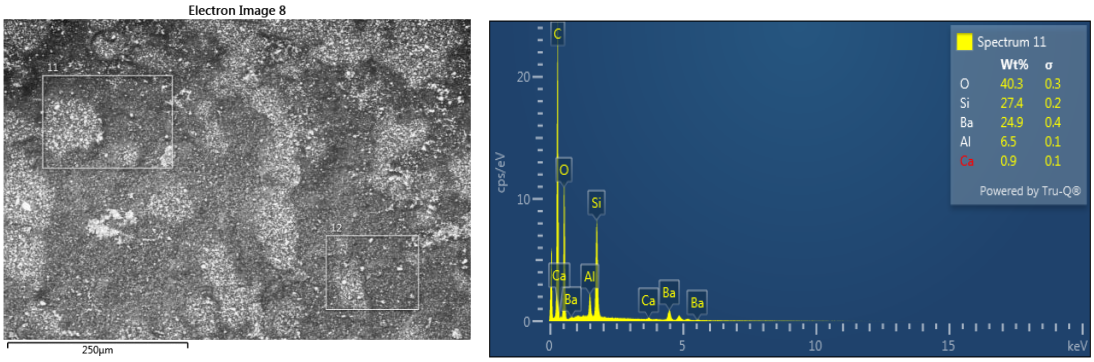

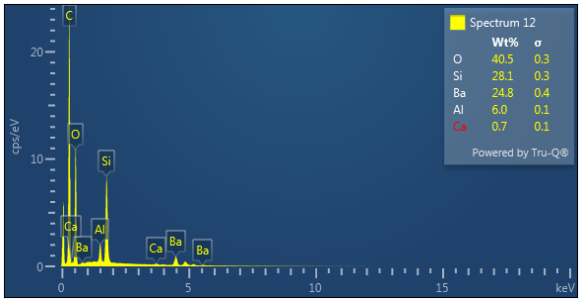

Figure 52. Chemical Composition of RTN2 #1 Surface

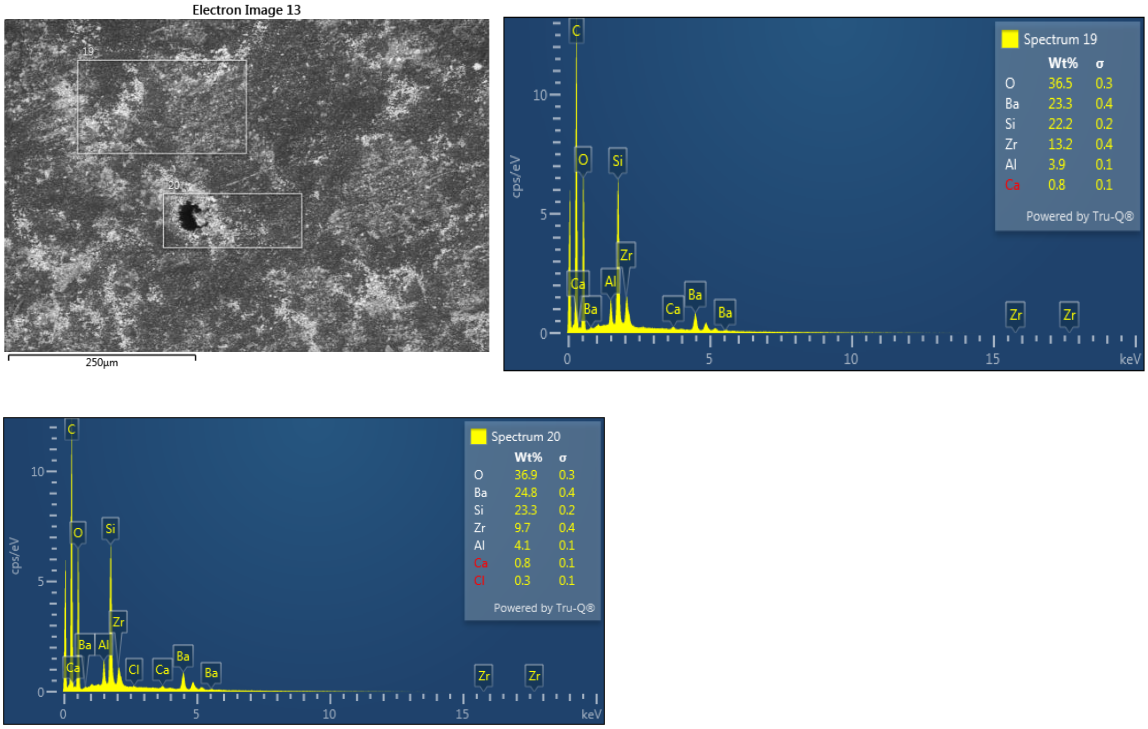

Figure 53. Chemical Composition of RTN2 #2 Surface

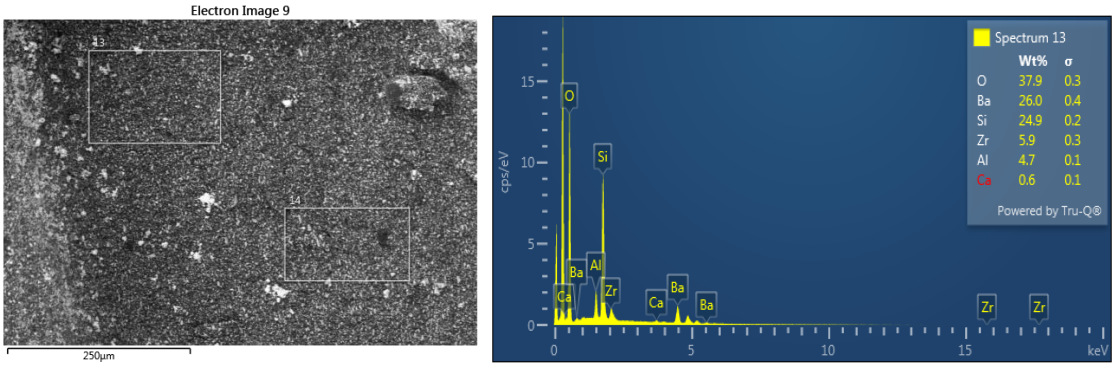

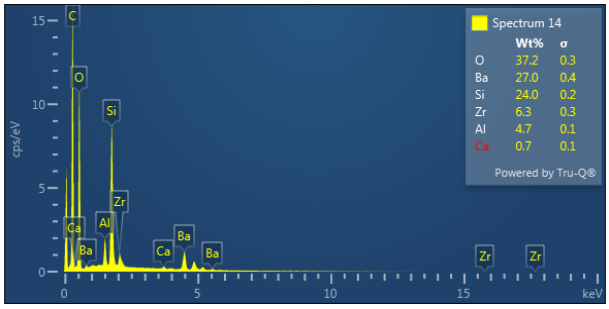

Figure 54. Chemical Composition of RTN2 #2 Cross Section.

3.6.1 Elemental Composition of Sprintray High Impact Denture Base (SDNC)

The SDNC samples (surface, and cross-sectional regions) primarily comprised oxygen (50–53%), silicon (41–45%), and potassium (approximately 43–47%). Trace amounts of aluminum (0.88–1.48%) and zirconium (up to 6.06%) were detected in some regions. The presence of silicon and zirconium indicates a silica-based filler phase with potential zirconia reinforcement.

Notably, SDNC #2 exhibited relatively lower silicon (41.94%), and aluminum (1.11%) levels compared to the corresponding high-performing samples, while demonstrating elevated zirconium content (6.06%). This specimen also displayed inferior mechanical behavior, potentially due to incomplete or non-uniform filler distribution and suboptimal polymerization. In contrast, SDNC #4 samples demonstrated more consistent filler dispersion and slightly higher silicon content, which may have contributed to improved filler-matrix integration and superior mechanical outcomes.

3.6.2 Elemental Composition of Rodin Titan with Nitrogen Polymerization (RTN2)

RTN2 specimens exhibited greater compositional complexity, with the surface of RTN2 #1 containing significant amounts of oxygen (40.4%), silicon (27.78%), aluminum

(6.59%), and barium (25.19%). These elements suggest a densely filled resin matrix containing aluminosilicate and barium-based fillers. RTN2 #2, the low-performing counterpart, demonstrated lower silicon (22.5–23.7%) and oxygen (36.6–37.09%) with slightly higher zirconium (13.41%) and barium (23.54–25.18%) content.

These discrepancies may explain the variance in mechanical performance, with RTN2 #1 showing more homogeneous filler distribution and higher silicate-based reinforcement. The decrease in silicon content and increased heavy metal oxides (Ba, Zr) in RTN2 #2 could have contributed to stress concentration, poor filler-matrix bonding, or greater internal voids, factors that compromise mechanical strength.

3.7 Correlation of the Mechanical Properties

Table 74. Correlation of the Mechanical Properties

Correlations

	Mean(Flexural Strength (MPa))	Mean(Ht Wear at 1M Cycle, um)	Mean(Wt Wear at 1M Cycle, mg)	Mean(Hardness (VHN))	Mean (DC)
Mean(Flexural Strength (MPa))	1.0000	-0.5967	-0.4001	0.7091	0.6526
Mean(Ht Wear at 1M Cycle, um)	-0.5967	1.0000	0.3154	-0.4936	-0.3855
Mean(Wt Wear at 1M Cycle, mg)	-0.4001	0.3154	1.0000	-0.2720	-0.2846
Mean(Hardness (VHN))	0.7091	-0.4936	-0.2720	1.0000	0.7551
Mean (DC)	0.6526	-0.3855	-0.2846	0.7551	1.0000

The correlations are estimated by Row-wise method.

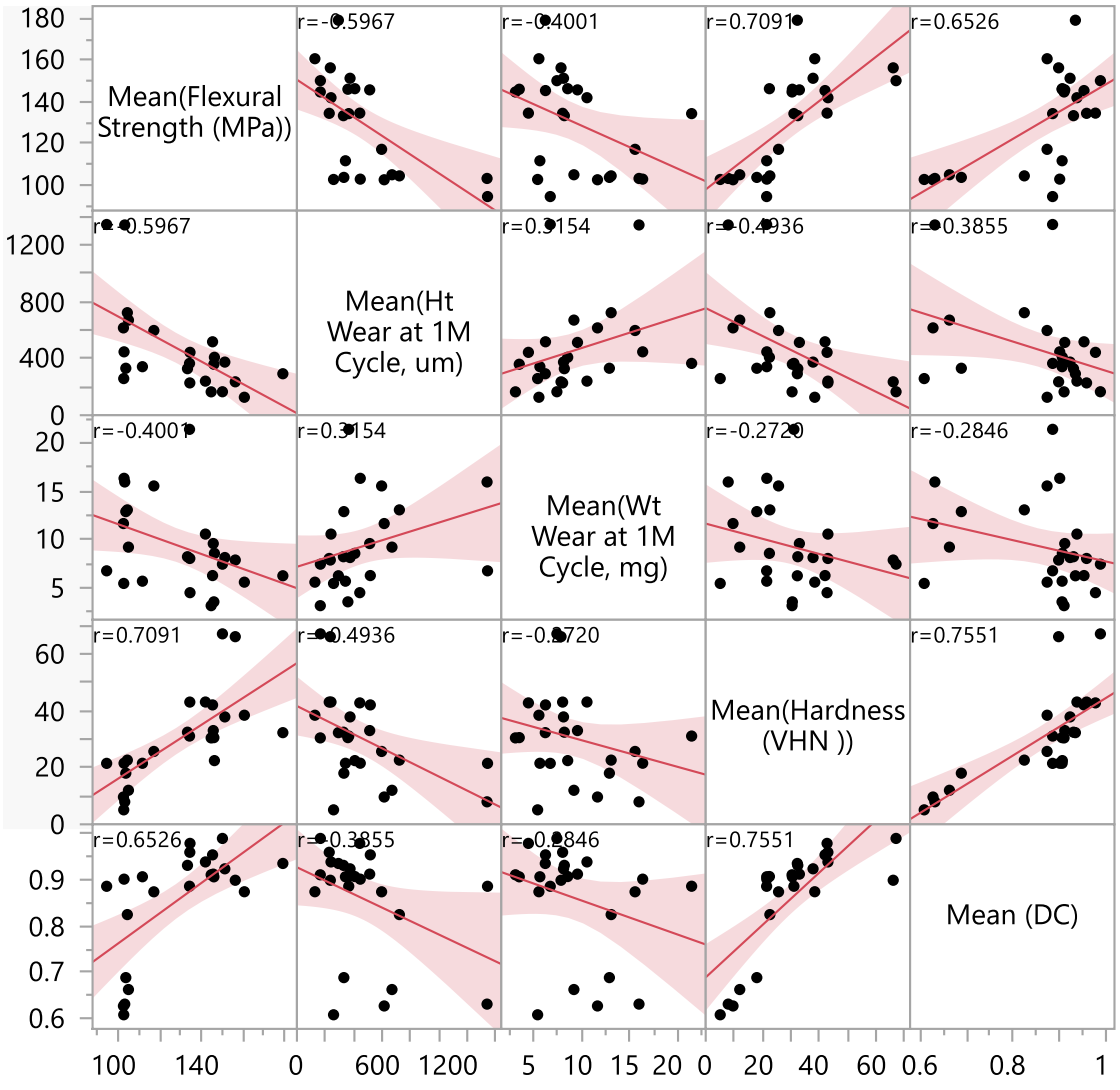

Figure 55. Scatterplot Matrix of correlation mechanical properties with wear resistance and Degree of Conversion.

Chapter 4. DISCUSSION

4.1 Key Findings and Interpretations

This study evaluated the influence of five different post-polymerization protocols such as Nanocure, Otoflash with Nitrogen, Otoflash without Nitrogen, Oven, and Procure, on the mechanical properties and polymerization efficiency of five 3D printed dental resins. The properties assessed included flexural strength, Vickers hardness, wear resistance, and degree of conversion (DC). Statistically significant differences among the post-polymerization methods were observed in three experimental tests: flexural strength, Vickers hardness and degree of conversion, leading to the rejection of the null hypotheses. These findings reinforce the importance of selecting appropriate post-polymerization protocols to optimize the physical and chemical performance of 3D printed dental materials.

4.1.1 Flexural Strength

The three-point bending test revealed material-dependent sensitivity to post-polymerization methods. Among SHIDB specimens, post-polymerization protocol significantly influenced flexural strength, with Otoflash with N2 and Procure producing numerically higher mean values than Nanocure or oven polymerization. While these differences were not always statistically significant across all comparisons, they suggest that more intense or oxygen-shielded photopolymerization may contribute to enhanced cross-linking and improved structural integrity of denture base resins.

These findings align with previous studies reporting that polymerization atmosphere and energy intensity significantly impact polymer matrix rigidity and the completeness of polymerization (Wada et al., 2023; Alharbi et al., 2016). The lack of significant differences in some groups (e.g., RT) may be attributed to intrinsic material properties or high initial polymer conversion, rendering post-polymerization effects less pronounced. These results are clinically relevant as they suggest that careful selection of post-polymerization methods can optimize strength in load-bearing prostheses fabricated from 3D printed resins.

4.1.2 Vickers Hardness

Microhardness values, measured via the Vickers method, showed a clear trend across several materials: polymerization protocols that used high-energy light sources or oxygen-free environments (e.g., Otoflash with N2) yielded the highest hardness values, particularly in SCC and SC2 specimens. For instance, SCC specimens polymerized with Otoflash with N2 showed the highest VHN (98.95 ± 0.84), significantly surpassing Nanocure and oven groups.

This outcome supports the hypothesis that a higher degree of surface polymer cross-linking, facilitated by higher energy densities or oxygen inhibition mitigation, enhances surface hardness (Sultan et al., 2025). Materials polymerized without nitrogen (e.g., Otoflash w/o N2) showed consistently lower hardness values, likely due to the formation of an oxygen-inhibited layer, which compromises the polymer network at the surface (de Melo-Soares et al., 2025).

4.1.3 Wear Resistance

The analysis of vertical wear (height loss) revealed clear differences in performance based on post-polymerization protocol. Specimens polymerized with Procure and Nanocure exhibited the highest mean height loss after 1 million cycles, indicating greater surface degradation and insufficient polymer network integrity. In contrast, resins subjected to post-polymerization, especially with thermal or nitrogen-assisted protocols, showed markedly reduced vertical wear. Otoflash with nitrogen and oven polymerization consistently produced the lowest height loss, demonstrating the positive correlation between enhanced degree of conversion and surface durability.

These findings are in agreement with earlier work showing that increased cross-link density correlates with improved wear resistance (Lingon, 2013). Poorly polymerized or heterogeneously polymerized materials tend to undergo micro-fatigue, leading to increased surface degradation under cyclic loading. Moreover, polymerization protocols with insufficient light penetration or inadequate exposure times may leave residual monomers, which act as plasticizers and reduce the wear stability of the printed matrix (Stansbury & Idacavage, 2016).

4.1.4 Degree of Conversion

Degree of conversion was quantified via FTIR by measuring residual C=C bonds. Results demonstrated a significant material-dependent response to polymerization protocol. For instance, SCC showed the highest DC (98.95%) when polymerized with Otoflash with N2, while RDB2 showed the lowest values overall (as low as 60.78% with Otoflash w/o

N2). This variation can be attributed to both material formulation and polymerization methods, with oxygen inhibition and insufficient energy delivery being primary factors for low DC.

High variability, particularly in RT and SHIDB specimens, underscores the complex interplay between resin chemistry and post-polymerization conditions. Otoflash with N2 consistently delivered high DC values across all materials, reinforcing findings from prior research indicating that inert gas shielding enhances radical polymerization by eliminating the oxygen-inhibited layer (Rueggeberg, 2002).

The degree of conversion is crucial not only for mechanical strength but also for biocompatibility, as unreacted monomers may leach into the oral environment and affect cytotoxicity (Furuse, 2011). Materials failing to achieve high conversion may pose risks in long-term intraoral use.

4.1.5 Microstructural Analysis

The microstructural evaluation of 3D-printed dental resins using SEM and EDS provided critical insights into the relationship between filler dispersion, elemental composition, and the resultant mechanical performance of the materials tested. SEM analysis revealed notable differences in surface and internal morphologies among specimens with high versus low mechanical performance.

SEM Analysis

Specimens with higher mechanical performance, namely RTN2 #1 and SDNC #4, exhibited dense, homogenous microstructures with well-integrated filler particles and

minimal surface porosities. At higher magnifications, filler particles appeared to be uniformly embedded within the resin matrix, suggesting efficient polymer-filler interaction and good interfacial bonding. These features contribute to improved flexural strength and wear resistance, aligning with prior findings that emphasize the importance of microstructural continuity and filler dispersion in enhancing the mechanical integrity of resin composites (Alshamrani et al., 2023).

In contrast, specimens with lower performance, RTN2 #2 and SDNC #2, showed microstructural defects such as micro-voids, loosely bound filler clusters, and evidence of delamination at the filler-matrix interface. These observations are consistent with previous literature reporting that poor filler integration results in stress concentration zones, which reduce the material's ability to resist flexural and compressive forces (Arora et al., 2024). Additionally, non-uniform filler distribution may stem from resin sedimentation or insufficient post-curing, both of which negatively affect polymer crosslinking and homogeneity (Mangoush et al., 2024).

EDS Analysis

EDS results supported the SEM findings by quantifying the elemental composition of the tested resins. Oxygen and silicon were the predominant elements detected across all specimens, indicating the presence of silica-based fillers in most materials. High-performing materials such as RTN2 #1 and SDNC #4 exhibited substantial barium (25.18–27.3 wt%) and zirconia content (6.4–13.41 wt%), which contribute to radiopacity, increased hardness, and improved wear resistance. These results align with studies

reporting that zirconia (ZrO_2) and barium glass fillers enhance the structural integrity and durability of dental composites (Alshamrani et al., 2023; Sonmez et al., 2018). Conversely, low-performing specimens like SDNC #2 contained a lower concentration of zirconia (≤6.06 wt%) and displayed a more heterogeneous elemental profile. Titanium and bromine were only sporadically present and were not uniformly dispersed, suggesting poor filler incorporation or uneven resin formulation. The correlation between elemental uniformity and mechanical behavior supports prior observations that a well-balanced filler-to-resin ratio, verified through EDS, directly contributes to improved material strength and resilience (Sonmez et al., 2018; Wada et al., 2022).

Influence of Post-Polymerization on Microstructure

Post-polymerization methods played a critical role in shaping the observed microstructures. Specimens cured under a nitrogen atmosphere (e.g., RTN2 #1) demonstrated better filler retention at the surface, reduced oxygen-inhibited layers, and smoother topographies compared to those cured in ambient air. This is consistent with findings by Wada et al. (2022), who reported that nitrogen-assisted post-curing enhances surface polymerization and reduces defects by eliminating oxygen inhibition, thereby increasing the degree of conversion (DC) and mechanical performance.

Additionally, high-performance specimens subjected to dual-phase post-curing (light and thermal) displayed fewer micro-voids and tighter polymer-filler integration, corroborating findings from Mangoush et al. (2024) and Hartley et al. (2022), which emphasized that prolonged or multi-stage curing protocols improve crosslinking and material strength.

4.2 Implications

4.2.1 Material and Polymerization Protocol Implications

This study highlights the critical influence of post-polymerization protocols on the mechanical performance and degree of polymer conversion of 3D-printed dental resins. Though all specimens were printed and allowed to reach an initial polymerized state after light exposure from the 3D printer (i.e., not in a “green state”), the subsequent polymerization methods significantly modulated the material behavior. The variability observed across groups subjected to different curing units, including ProCure 2, Nanocure, Oven Polymerization, and Otoflash with and without nitrogen, indicates that polymerization is not a mere formality but a defining process step for final material quality.

The highest degree of conversion (DC) was achieved using Otoflash with nitrogen and oven polymerization, across nearly all tested resin systems. This indicates that photopolymerization enhanced with inert gas shielding, as well as thermal polymerization, are both highly effective in maximizing monomer-to-polymer conversion. Otoflash with Nitrogen minimizes the oxygen inhibition layer and enhances surface and near-surface polymerization, while oven polymerization likely facilitates deeper network mobility and crosslinking due to sustained thermal energy. These observations are consistent with literature demonstrating that post-cure heating can promote secondary polymerization and increase overall crosslink density, particularly in deeper layers and highly filled systems (Bayarsaikhan, 2021).

In contrast, Nanocure and Otoflash without nitrogen demonstrated relatively lower DC, flexural strength, and hardness, likely due to suboptimal energy delivery or oxygen interference during polymerization. Specimens polymerized with ProCure 2 showed moderate performance, adequate for clinical use, but often fell short of the strength and hardness observed in oven-polymerized specimens, particularly for resins designed for definitive prostheses.

Collectively, these findings emphasize that post-polymerization is not a one-size-fits-all process. Matching resin chemistry with appropriate light source characteristics (e.g., wavelength, intensity, exposure duration, atmosphere) is essential to optimize physical properties and clinical reliability. Manufacturers must provide specific polymerization recommendations and invest in validating these across multiple devices.

4.2.2 Clinical implications

The outcomes of this study offer clinically relevant insights regarding the choice of polymerization protocols for 3D printed dental resins used in restorative and prosthetic applications. All tested materials achieved minimum flexural strength thresholds established by ISO 6872-2015 Ceramic materials (ISO 6872:2015 DentistryCeramic materials, 2023) (≥50 MPa), validating their fundamental mechanical suitability. However, significant variations were observed depending on the polymerization method, highlighting the importance of protocol optimization to enhance long-term performance. Notably, oven polymerization and Otoflash with nitrogen produced consistently higher flexural strength and superior wear resistance in multiple resin systems, particularly in

Rodin Titan (RT), Sprintray Ceramic Crown (SCC), and Rodin Denture Base 2.0 (RDB2). These results suggest that extended thermal polymerization at controlled temperatures may allow deeper polymer chain mobility and crosslinking, improving bulk mechanical stability and surface durability. This also supports prior findings that thermal energy can enhance post-cure polymerization in light-activated systems, especially for deeper layers or resins with delayed conversion kinetics (Lümkemann et al., 2020).

In contrast, Nanocure and ProCure 2, despite being proprietary or widely used devices, showed inferior performance in several key areas, particularly in Sprintray High Impact Denture Base and RDB2. This indicates that device configuration, light intensity, and spectral range may not be fully compatible with certain resin chemistries, potentially leading to incomplete polymerization, suboptimal mechanical properties, and lower clinical durability.

The clinical implications are significant. Materials with lower DC and hardness values may show reduced wear resistance, leading to early occlusal degradation, increased surface roughness, or staining, particularly concerning for denture bases and provisional restorations in high-function areas. Additionally, incomplete polymerization can increase monomer elution, posing biocompatibility risks and reducing the longevity of the restoration.

From a clinical standpoint, this suggests that oven-polymerization units, though more time-intensive, may be preferable when strength and durability are critical, such as in definitive removable prostheses or high-load-bearing posterior restorations. In contrast, faster polymerization systems like PC2 or Otoflash (with or without N_2) might be suited

for chairside temporaries or situations prioritizing workflow efficiency, provided the resin is validated for such devices.

Importantly, clinicians and technicians must not assume interchangeability between units. Even FDA-approved 3D printed materials can underperform if not polymerized under validated or optimized conditions, leading to compromised prosthesis longevity, reduced patient satisfaction, and increased clinical failures. Selection of polymerization equipment should therefore be made in coordination with manufacturer guidance and material-specific data, such as those provided by this study.

In conclusion, Otoflash with nitrogen and oven polymerization protocols demonstrated the most favorable overall performance in this investigation and should be seriously considered for clinical use when mechanical strength and wear resistance are primary goals. Workflow decisions must balance clinical demands, equipment accessibility, and resin-specific performance characteristics to achieve optimal patient outcomes.

4.3 Limitations

This in vitro study does not simulate intraoral conditions, where thermal cycling, salivary enzymes, and pH fluctuations can impact resin behavior. Furthermore, the use of bar and disc specimens limits the extrapolation of results to complex tooth- or crown-shaped restorations. The variability in printer types and layer thickness, although controlled, may still influence polymerization kinetics. Some resins (e.g., SCC, SHIDB) are closed-system materials and may behave differently when printed and polymerized outside

manufacturer-specified workflows. Degree of conversion was measured only via FTIR and not validated with Raman spectroscopy or cross-link density assessment.

4.4 Future Research Recommendation

Future work should explore the impact of polymerization duration, energy dose (mW/cm^2), and photoinitiator systems on polymerization depth and homogeneity. Clinical simulation studies, including thermocycling and water sorption/desorption aging, will help contextualize in vitro findings. While this study standardized the printing orientation and placement as much as possible, variation in placement on the build platform, including proximity to the center, edges, or Z-axis height, may lead to inconsistencies in light exposure, polymerization gradients, and mechanical properties. Future studies should systematically investigate how placement on the build platform affects flexural strength, hardness, and degree of conversion, especially for large build platforms and high-volume production. As finishing and polishing steps can alter surface roughness and potentially improve or impair wear resistance and hardness, studies should assess how post-processing techniques interact with different polymerization protocols to influence clinical performance.

Additionally, the effect of post-polymerization on marginal adaptation and bond strength to various cements or adhesives could be investigated to bridge laboratory findings with clinical applicability. Future work should address how different polymerization methods affect translucency, shade stability, and surface gloss, particularly for anterior esthetic restorations and veneer applications. Lastly, studies incorporating 3D printed tooth-

shaped restorations will better elucidate stress distribution and failure modes under masticatory load.

Chapter 5. CONCLUSION

Within the limitations of this in vitro study, the results demonstrate that post-polymerization methods significantly influence the mechanical performance and degree of conversion of 3D-printed dental resins. The following conclusions can be drawn:

1. Flexural strength was significantly influenced by the polymerization protocol for filled resins, with Otoflash with nitrogen yielding consistently higher values across most resins. Nanocure and Procure showed significantly lower flexural strength, suggesting insufficient post-polymerization under their standard settings. For unfilled resins Otoflash with nitrogen provided superior results and procure displayed reduced strength but there was no significance found.
2. Filled resins demonstrated significantly higher surface hardness when polymerized with Otoflash with N_2. Nanocure, procure and oven showed lower values in comparison. For unfilled resins Otoflash with nitrogen yielded the highest surface hardness, demonstrating a statistically significant improvement over all other methods ($p < 0.05$). In contrast, Nanocure (16.774) and Procure (15.574) produced significantly lower hardness values and were grouped in a statistically inferior category. Oven polymerization (14.752) and Otoflash without N_2 (13.884) resulted in the lowest hardness levels, with Otoflash without N_2 performing the worst overall.
3. In filled resins, although no statistically significant differences were found (all grouped under A), Otoflash with N_2 demonstrated the best wear resistance with the lowest height loss of 176.04 μm, while Otoflash without N_2 at 392.83 μm and

Nanocure at 373.33 μm showed substantially higher wear, indicating lower resistance. In unfilled resins, Otoflash with N_2 at 464.69 μm and Otoflash without N_2 at 491.04 μm exhibited better wear resistance, whereas Procure at 981.12 μm had the highest height loss, indicating the least resistance to wear. Interaction analysis further emphasized the trend that Rodin Denture Base 2.0 polymerized with Otoflash without N_2 had the lowest height loss at 258.6 μm, suggesting best wear resistance, while Procure-polymerized Sprintray Denture Base had the highest wear at 1346.0 μm and this pair comparison was statistically significant.

4. The Degree of Conversion analysis revealed statistically significant differences among resin-polymerization protocol combinations. While overall differences among the five polymerization methods were not statistically significant at the global level (all grouped under "A" in Table 63), specific material-cure combinations exhibited meaningful variability. SCC polymerized with Otoflash with N_2 achieved the highest DC value at 98.95%, indicating the most efficient polymerization, followed closely by SCC polymerized with Otoflash without N_2 and Oven. In contrast, RDB2, an unfilled resin, consistently showed the lowest DC values across all polymerization protocols, with Otoflash without N_2 at 60.78% being the lowest.
5. While resin composition played a dominant role, a significant interaction was also observed between resin and polymerization protocol, highlighting that optimal outcomes are both material- and device-dependent.

6. Strong positive correlations were observed between Degree of Conversion and Vickers Hardness r = 0.7551, Degree of Conversion and Flexural Strength r = 0.6526, and Flexural Strength and Vickers Hardness r = 0.7091 as seen in Table 78. These findings align with literature that reports strong relationships between cross-link density and both strength and hardness (Alharbi, 2025).
7. Moderate negative correlation was observed between Height Wear and Flexural Strength r = –0.5967, Height Wear and Vickers Hardness r = –0.4936, and Degree of Conversion and Height Wear r = –0.3855 as displayed in Figure 44.

BIBLIOGRAPHY

Abduo, J. (2014). Accuracy of CAD/CAM prosthodontic complete dentures. Journal of Prosthodontics, 23(3), 179–187.

ADA. (2023). Code on Dental Procedures and Nomenclature (CDT). American Dental Association.

Alharbi, S., Alshabib, A., Algamaiah, H., Aldosari, M., & Alayad, A. (2025). Influence of Post-Printing Polymerization Time on Flexural Strength and Microhardness of 3D Printed Resin Composite. *Coatings*, *15*(2), 230. https://doi.org/10.3390/coatings15020230

Alshamrani A, Alhotan A, Kelly E, Ellakwa A. Mechanical and Biocompatibility Properties of 3D-Printed Dental Resin Reinforced with Glass Silica and Zirconia Nanoparticles: In Vitro Study. Polymers (Basel). 2023 May 30;15(11):2523. doi: 10.3390/polym15112523. PMID: 37299322; PMCID: PMC10255304.

Arora, N., Dua, S., Singh, V. K., Singh, S. K., & Senthilkumar, T. (2024). A comprehensive review on fillers and mechanical properties of 3D printed polymer composites. *Materials Today Communications*, *40*, 109617.
Bagheri, A., & Jin, J. (2019). Photopolymerization in 3D printing. *ACS Applied Polymer Materials*, *1*(4), 593-611.

Bayarsaikhan, E., Lim, J.-H., Shin, S.-H., Park, K.-H., Park, Y.-B., Lee, J.-H., & Kim, J.-E. (2021). Effects of Postpolymerization Temperature on the Mechanical Properties and Biocompatibility of Three-Dimensional Printed Dental Resin Material. *Polymers*, *13*(8), 1180. https://doi.org/10.3390/polym13081180

Çakmak, G., Kose, E., & Unver, S. (2022). Evaluation of the mechanical properties of 3D printed restorative materials: A systematic review. Materials, 15(1), 205.

Chen, H., Wang, Y., & Yu, H. (2021). Advances in photopolymerizable resins for 3D printing. Polymers, 13(1), 102.

Chrószcz, M. W., Barszczewska-Rybarek, I. M., & Wori, P. (2021). The Relationship between the Degree of Conversion in Dental Dimethacrylate Polymers Determined by Infrared Spectroscopy and Polymerization Shrinkage. *Engineering Proceedings*, *11*(1), 52. https://doi.org/10.3390/ASEC2021-11151

Davidowitz, G., & Kotick, P. G. (2011). The use of CAD/CAM in dentistry. Dental Clinics of North America, 55(3), 559–570.

Garoushi, S., Mangoush, E., Vallittu, M., Lassila, L. (2013). Short fiber reinforced composite: a new alternative for direct onlay restorations. The Open Dentistry Journal, 7, 181–185.

Hartley, P., Eder, J., & Schnieders, J. (2022). The role of light exposure and thermal polymerization on dental composite conversion and mechanical behavior. Dental Materials Journal, 41(1), 25–32.

Huang, S. H., Liu, P., Mokasdar, A., & Hou, L. (2013). Additive manufacturing and its societal impact: A literature review. The International Journal of Advanced Manufacturing Technology, 67, 1191–1203.

Ilie, N., & Hickel, R. (2009). Investigations on mechanical behavior of dental composites. Clinical Oral Investigations, 13(4), 427–438.

ISO 6872:2015 Dentistry- Ceramic materials. (2023, 05 09). Retrieved from ISO (the International Organization for Standarization): https://www.iso.org/obp/ui#iso:std:iso:6872:ed-4:v1:en

Javaid, M., & Haleem, A. (2019). Current status and applications of additive manufacturing in dentistry: A literature-based review. Journal of Oral Biology and Craniofacial Research, 9(3), 179–185.

Jockusch, J., & Özcan, M. (2020). Additive manufacturing of dental polymers: An overview on processes, materials and applications. Dental Materials Journal, 39(3), 345–354.

Ko, S., Park, J., & Lee, J. (2021). Optimization of 3D printing post-polymerization process for mechanical property enhancement. Journal of Advanced Prosthodontics, 13(2), 75–85.

Lassila, L., Mangoush, E., He, J., Vallittu, P. K., & Garoushi, S. (2024). Effect of post-printing conditions on the mechanical and optical properties of 3D-printed dental resin. *Polymers*, *16*(12), 1713.

Mirică, I., & Boariu, O. (2020). Evaluation of filler size and content in dental composite materials. Romanian Journal of Oral Rehabilitation, 12(1), 72–76.

Nulty, A. B., Raffaelli, L., & Schweiger, J. (2022). Accuracy of 3D printing technologies for dental applications: A systematic review. Journal of Prosthodontic Research, 66(1), 11–23.

Quan, H., Zhang, T., & Xu, H. (2020). Masked stereolithography (MSLA) and its application in bioprinting: An emerging method for biofabrication. Biofabrication, 12(3), 032001.

Revilla-León, M., & Özcan, M. (2019). Additive manufacturing technologies used for processing polymers: Current status and potential application in prosthetic dentistry. Journal of Prosthodontics, 28(2), 146–158.

Schweiger, J., Edelhoff, D., & Güth, J. F. (2021). 3D printing in digital prosthetic dentistry: An overview of materials and technologies. International Journal of Computerized Dentistry, 24(1), 55–68.

Sonmez, N., Gultekin, P., Turp, V., Akgungor, G., Sen, D., & Mijiritsky, E. (2018). Evaluation of five CAD/CAM materials by microstructural characterization and mechanical tests: a comparative in vitro study. *BMC oral health*, *18*(1), 5. https://doi.org/10.1186/s12903-017-0458-2

Stansbury, J. W., & Idacavage, M. J. (2016). 3D printing with polymers: Challenges among expanding options and opportunities. Dental Materials, 32(1), 54–64.

Strub, J. R., Rekow, E. D., & Witkowski, S. (2006). Computer-aided design and fabrication of dental restorations: Current systems and future possibilities. The Journal of the American Dental Association, 137(9), 1289–1296.

Tian, Y. C., Zhu, M., & Zhang, Y. (2021). Impact of post-polymerization on the mechanical properties of 3D printed dental resins. Journal of Prosthetic Dentistry, 126(4), 592–598.

Turkyilmaz, I. (2021). Advances in digital dental technology. Journal of the Turkish Dental Association, 72(1), 40–47.

Wada, J., Wada, K., Gibreel, M., Wakabayashi, N., Iwamoto, T., Vallittu, P. K., & Lassila, L. (2023). Effect of Nitrogen post-polymerization on surface conditions of 3D-printed splint. *Dental Materials*, *39*, e78-e79.

Wang, X., Song, S., Chen, L., Stafford, C. M., & Sun, J. (2018). Short-time dental resin biostability and kinetics of enzymatic degradation. *Acta Biomaterialia*, *74*, 326-333.

Zhu, Y., Sun, J., & Pan, Y. (2022). An overview of LCD-based vat photopolymerization 3D printing technology. Micromachines, 13(2), 258.

CURRICULUM VITAE